5-2015

Targeting An Ancient Retrovirus During Melanoma Using Adoptive T Cells Therapy

janani Krishnamurthy

TARGETING AN ANCIENT RETROVIRUS DURING MELANOMA USING ADOPTIVE T CELLS THERAPY

by

Janani Krishnamurthy, B.Pharm, M.S.

APPROVED:

_____
Supervisory Professor: Laurence J.N. Cooper, Ph.D., M.D.

_____
Dean Lee, Ph.D., M.D.

_____
Willem Overwijk, PhD.

_____
Samir Hanash, PhD.

_____
Michelle Barton, PhD.

APPROVED:

_____

Dean, The University of Texas

Graduate School of Biomedical Sciences at Houston

TARGETING AN ANCIENT RETROVIRUS DURING MELANOMA USING ADOPTIVE T CELLS THERAPY

A

DISSERTATION

Presented to the Faculty of

The University of Texas

Health Science Center at Houston

and

The University of Texas

M. D. Anderson Cancer Center

Graduate School of Biomedical Sciences

in Partial Fulfillment of the Requirements

for the Degree of

DOCTOR OF PHILOSOPHY

by

Janani Krishnamurthy, B.Pharm, M.S.

Houston, Texas

May, 2015

DEDICATION

I dedicate my dissertation work to my family and friends. A special gratitude to my loving mom, Jaya Krishnamurthy whose words of encouragement and “threats” helped me push through tough phases of my life. My brother Vinodh, who never stopped reminding me that PhD is a training for bigger things in life and not just science and to take things easy. My aunt Lakshmi, for being super supportive and hearing me out during my low phases. My uncle Mani and Jayanthy family for sending me sweets every single year during Diwali so I don’t miss my family. Vishwanathan family and Gopu mama for initially supporting my dream to travel to USA for higher education. My grandparents for all their love and blessings. Uncle Shankar and family for their love and affection from Bombay. My best friends Pearl, Jaymie, Neha, Dora, Lettie, Meenu, Anu, Uma, Sridevi, Lalit, Harjeet, Krina, Sanchaika, Charuta, Rachyata, Ninad, Radhika, Mansi, Wendy, Chris, Victor, Aakash and Harinder for being there for me when I most needed them, and, supporting me tremendously through this journey. A special thanks to my Father for watching me from heaven, Raja uncle, Chakku bhai, Navin and Sai Ram for their blessings and meditative prayers.

ACKNOWLEDGEMENTS

I would like to thank Dr. Cooper first and foremost for giving me an opportunity and full freedom to learn and grow in this lab. I thoroughly admire his penmanship and I thank him for helping me to apply various grants and submit my manuscript. I learnt and share his value that science is for all and also that science is part management. I was fortunate enough to experience first-hand to manage, work as a team with greater than 40 people in the lab and handle difficult situations. These experiences have definitely shaped me and changed my outlook to a more positive one about science and world outside.

I would like to thank my past and current committee members: Dr. Feng Wang-Johanning (for introducing HERV-K to Cooper lab, providing reagents and recommendation letters), Dr. Renata Pascalini (supporting me during candidacy), Dr. Bradley McIntyre (for his consults with cross-linking membrane protein), Dr. Lazlo Radvanyi (for supporting me during my switch from breast cancer model to melanoma model), Dr. Qing Yi (for developing the hypothesis for my initial K562 project), Dr. Willem Overwijk (for supporting me during the immunology retreat and for my thesis defense).

I would like thank Dr. Vickey Knutson and Dr. Michelle Barton for checking in on me supporting me immensely with my manuscript publication and thesis defense.

I would to thanks to Dr. Dean Lee specifically for taking time out and organizing manuscript writing club and helping me better analyze my data and use appropriate statistical measures.

I thank him also for inviting graduate students to his home to watch fireworks and organizing beer-fest during our manuscript writing club.

I am grateful to Dr. Samir Hanash and Dr. Satyendra Tripati for believing in this project and running a very expensive unbiased mass spectrometric analysis for tumor cell lines to determine the presence of HERVs. I would like to thank Dr. Bar-Eli and Dr. Fidler for providing me metastatic melanoma cell line for my *in vivo* model and Dr. Bar-Eli for trouble shooting the model when the metastasis failed to happen during my first try.

This project would not have reached this level if not for the kind guidance and encouragement of Dr. Brian Rabinovich. I thank him for his generous help in understanding the structure of HERV-K env on cell surface and developing variations of membrane bound-IL12 (mb IL-12). Brian also helped me identify the shedding of HERV-K antigen despite being not able to detect through conventional techniques such as ELISA. I like to thank Dr. Ana Korngold and Gary for all their technical support during preparing huge batches of electrocompetant bacteria. I like to thank Simon Olivares for helping me design constructs for HERV-K env-specific CAR, mb-IL-12, and HERV-K env antigen for my knock-in model.

I would like to thank Helen Huls for putting up with me (literally). There have been times I have used expired po numbers for product purchase by mistake and Helen dealt with all the paper work. She would send in request for my item even in the middle of the night and never complained about it. Her organizational skill is something I will never forget and aspire to

include in my life. I like to thank Natalya for bringing orderliness into my work and help me work as a team with purchasing items for the lab every week.

I like to thank Harjeet Singh for being one of the best support I got during my PhD years in lab. He was always available during anytime of the day to help me in understanding my data, design experiments and controls, and more importantly identify unnecessary experiments and focus on manuscript publication and graduation. I definitely improved my people skills by talking to him and learn that it is ok to be wrong and not to take failed experiments so personal.

I would like to thank Colleen O Connor for helping me to prepare my documents for candidacy, manuscript, presentation for job interviews. She has been incredibly patient and understanding my short-comings and coached me towards better writing and presentation skills. I would like to thank Dr. Judy Moyes for painstakingly editing my entire thesis and for her valuable edits.

I thank Dr. Bipulendu Jena for his support in designing my ELISA experiment with CAR maxibody and providing control antibodies, Dr. Sourindra Maiti for his support with n-string data and real time PCR. Dr. Maiti was also involved in mir-155 project with me and it was great experience learning about isolation of these micro RNAs. I like to thank Dr. Pappa Kumaresan for his help with cross-linking membrane protein and immune-precipitation experiments. Sincere gratitude to Dr. Kumar and Dr. Jena help me get educated in the proteomics field. I like to thank Dr. Hiroki Torikai for his consults with Cas9 project to

knock out HERV-K. I like to thank Dr. Jae Chen for scoring my IHC tissues and Fabion for purifying CAR maxibody.

Heartfelt gratitude to Tiejuan and Dr. Kirsten Switzer for all their support with my *in vivo* work. I like to thank Tiejuan specifically for making me feel absolutely welcomed when I first entered the lab and Kirsten for being a wonderful inspiration for healthy living. I like to thank Ling, Sam for providing me AaPCs and other reagents exactly when I need them. Radhika, Chetan and me were part of the T-reg group. I thank them for sharing their excitement in science and it was always refreshing to discuss various aspects of the project. I thank Drew for his help in analyzing n-string data and Lenka for coaching me in performing my very first manual MACs sort. I like to thank Hillary and Denise in helping me chose my committee members and edit my candidacy work. I like to thank David for his helpful scientific discussions and providing me chocolate cookies whenever my experiments failed.

I like to thank our clinical team Matthew and Ping for teaching me to ficol blood samples, electroporation and growing CAR T cells. I like to thank Alexandria (Ola) , Alan, Tamara and Krina for their friendly support, Sonny for his support with flow cytometry, Alvaro for his help in setting up biostation imager, Amer for his assistance with hydrodynamic infusion of IL-15 and *in vivo* sample analysis.

Finally I would like to thank GSBS, DOD BCRP and Joanna M melanoma foundation for their financial support.

TARGETING AN ANCIENT RETROVIRUS DURING MELANOMA USING ADOPTIVE T CELLS THERAPY

Janani Krishnamurthy, B.Pharm, M.S.

Supervisory Professor: Laurence J.N. Cooper, Ph.D., M.D.

Patients with metastatic melanoma have a poor prognosis due to resistance to conventional therapies. Thus, new targeted treatment strategies are required to improve therapeutic outcome. One prospective approach is to infuse T cells that are rendered specific for tumor-associated antigens (TAAs) preferentially expressed on melanoma cells. Recognition of cell-surface TAAs independent of major histocompatibility complex can be achieved by introducing a TAA-specific chimeric antigen receptor (CAR) on T cells using gene therapy. This approach is being used in clinical trials to adoptively transfer CD19-specific CAR^+ T cells in patients with B-lineage malignancies. To generate T-cell therapy for melanoma we targeted a TAA derived from human endogenous retroviruses (HERV), whose genome stably integrated into humans millions of years ago. During oncogenesis, biologically active variants of HERV, such as the envelope (env) protein of HERV-K, are expressed on the surface of melanoma, but not normal cells. To target HERV-K, T cells were engineered to express a CAR specific for this env protein, by replacing the antigen-binding exodomain of CD19-specific CAR with the single chain antibody (scFv) sequence of an anti-HERV-K env specific monoclonal antibody. This new CAR was cloned as a transposon into our *Sleeping Beauty* (SB) system that we have adapted for human application. DNA plasmids coding for the HERV-K env-specific CAR and SB transposase were electro-transferred into primary

human T cells, and genetically modified CAR^+ T cells were selectively propagated on irradiated artificial activating and propagating cells (AaPC) expressing HERV-K env and the desired T-cell co-stimulatory molecules. After co-culture on γ-irradiated AaPC, 95% of $CD3^+$ T cells expressed the CAR and these HERV-K env-specific CAR^+ T cells were able to specifically kill HERV-K env^+, but not HERV-K env^-, melanoma targets *in vitro* in contrast to control (no DNA) T cells. Specificity of these CAR^+ T cells was proved by over-expressing HERV-K env protein in antigen negative EL4 mouse cells that were preferentially killed compared to HERV-K env^- EL4 parental cells. HERV-K env knockdown by shRNA on A888 cells resulted in reduced killing compared to parental A888 melanoma cells. A novel observation was that the antigen is not a type 1 transmembrane protein and that it is shed from its surface which is recognized by HERV-K env-specific CAR^+ T cells. The CAR^+ T cells were also successful in reducing tumor growth and metastasis of A375-super metastatic (SM) tumor cells from lungs to liver *in vivo*. The tumor-bearing mice receiving the CAR^+T cells lived longer and appeared healthier than the control tumor-bearing mice who received no CAR^+ T cells. In aggregate, these data demonstrate for the first time that T cells targeting an active ancient retrovirus can be used as an immunotherapy for melanoma, using an approach that has translational appeal for clinical trials.

TABLE OF CONTENTS

LIST OF ILLUSTRATIONS

LIST OF TABLES

ABBREVIATIONS

AaPC artificial activating and presenting cell

ACT adoptive cell therapy

APOBEC3G apolipoprotein B mRNA editing enzyme

Ag antigen

AML acute myelogenous leukemia

ANOVA analysis of variance

AP-1 activator protein 1

APC antigen presenting cell

BLI bioluminescent imaging

bZIP basic leucine zipper domain

CAR chimeric Antigen receptor

CD cluster of differentiation

CDK4 cyclin-dependent kinase 4

CML chronic myelogenous leukemia

CTL	cytolytic T lymphocyte
CTLA-4	cytotoxic T lymphocyte-associated antigen
CRA	chromium release assay
CREB	cAMP response element-binding protein
DAPI	4',6-diamidino-2-phenyindole
EBV	Epstein-Barr virus
ELISA	enzyme-linked immunosorbent assay
env	envelope
ERBB2	receptor tyrosine-protein kinase
FACS	fluorescence-activated cell sorting
FBS	fetal bovine serum
FcR	Fc receptor
FDA	Food and Drug Administration
ffLuc	firefly luciferase
gag	group-specific antigen

GD2/3	disialoganglioside
HA	hemagglutinin
HERV-K	human endogenous retrovirus K
HLA	human leukocyte antigen
HML2	human mouse mammary tumor-like type 2
Id	idiotypic
IgG	immunoglobulin G
IFN-γ	interferon gamma
IFS	immunofluorescence staining
IHC	immunohistochemistry
IL	interleukin
IP	intraperitoneal
IV	intravenous
kDa	kilodalton
LINE	long interspersed nuclear elements

LFA-3	lymphocyte function-associated antigen-3
LTR	long terminal repeat
mAb	monoclonal antibody
MAGE	melanoma-associated antigen
MART-1	melanoma antigen recognized by T cells 1
mAx	maxibody
MHC	major histocompatibility complex
MITF-M	microphthalmia-associated transcription factor
mKate	monomeric version of Katushka
MMTV	mouse mammary tumor virus MUM1
NAHR	non-allelic homologous recombination
NK	natural killer cell
NOG	NOD/Shi-scid/IL-2Rγ^{null}
OCT	optimum cutting temperature
ORF	open reading frame

PBMC	peripheral blood mononuclear cell
PBS	phosphate buffered saline
PMA	phorbol 12 myristate 13 acetate
pol	polymerase
pro	protease
RLVP	retro-virus like particles
rLuc	Renilla luciferase
RT	reverse transcriptase
RT-PCR	reverse transcription-polymerase chain reaction
SB	sleeping beauty
scFv	single-chain variable fragment
SCID	severe combined immunodeficiency
shRNA	short hairpin ribonucleic acid
SINE	short interspersed nuclear elements
SP	signal peptide

SU	surface
SV40	simian vacuolating virus 40
TAA	tumor associated antigen
TCR	T cell receptor
TIL	tumor-infiltrating lymphocyte
TM	transmembrane
TNF-a	tumor necrosis factor- alpha
t-RNA	transfer RNA
TRP-2-1NT2	tyrosinase-related protein
VH	variable heavy chain
VL	variable light chain
YY1	yin yang 1

Chapter 1: Introduction

1.1 Melanoma: Melanoma, a cancer of melanocytes, which are melanin pigment-producing cells in the skin, is the most serious form of skin cancer. The incidence of melanoma has increased over the years faster than other cancers [1]. It is the second and third most commonly diagnosed cancer in women and men respectively. In the USA, nearly 55,560 individuals were diagnosed with melanoma in the year 2012 alone with the incidence rate of melanoma steadily rising over the last 30 years [2,3]. In the United States, there is a 1 in 30 chance in risk of developing melanoma [4]. Though the median age of diagnosis for male and female has been 60 years, recently more patients under 30 years are being diagnosed with melanoma. 20% of all primary melanoma lesions will metastasize depending upon the primary tumor size, age, gender, anatomical sites, infiltration of lymphocytes and ulceration [3]. One of the most aggressive forms of skin cancer is metastatic melanoma and accounts for up to 46,000 deaths annually worldwide [1].

The National Cancer Institute describes the different stages of melanoma as follows: Stage 0 or melanoma in situ includes abnormal melanocytes found on the epidermal layer of the skin. These melanocytes have a propensity to become cancerous and spread; Stage I: the tumor is about 1-2 millimeter thick with or without ulceration; Stage II: the tumor is 2-4 millimeter thick with or without ulceration; Stage III: the primary tumor can be any thickness with or without ulceration but has spread to lymph nodes and smaller tumors are found approximately 2 centimeters from the primary site; Stage IV: the cancer has metastasized to other organs such as the lung, liver, gastrointestinal tract, bone and other soft tissues.

The survival of patients diagnosed at various stages of disease progression drops from 95% at stage I to 10% at stage IV. Treatment of melanoma is dependent on the stage of disease progression. Routine therapy for stage 1 and 2 melanoma includes surgical excision. About half the patient population with advanced disease receives either chemotherapy or immunotherapy along with radiation and surgery. Adjuvant therapy such as Interferon-α (IFN-α) is administered to patients with increased risk of disease recurrence [5,6]. Until 2011, the only two US FDA approved therapies for metastatic melanoma were chemotherapy with dacarbazine and high-dose IL-2 [7,8]. Widespread multiorgan toxicity was reported with high-dose IL-2 and low response rates of about 10-15% were reported with dacarbazine [9-11]. Newer therapeutic interventions such as ipilimumab, which targets cytotoxic T-lymphocyte-associated antigen 4 (CTLA-4) and vemurafenib, a BRAF inhibitor are now FDA-approved after showing efficacy in clinical studies targeting metastatic melanoma [12-14].

Despite the development of these therapeutic options, the incidence and frequency of complete or partial regression of melanoma has not improved over the years [15]. Melanoma with micrometastases to secondary sites is in general not a candidate for treatment due to three factors namely (a) inadequate detection using current tomographic procedures [16,17] (b) persistence of micrometastases in a dormant stage [18] and, (c) resistance of micrometastases to chemo- and radiation therapy [19-21].

1.2 Immune landscape in the melanoma microenvironment

Previous clinical studies on tumor environment of melanoma strongly suggest that the immune system can be naturally harnessed to target and clear melanoma cells [22]. In primary melanoma, about 14-50% of the tumor spontaneously disappears without treatment. It has been suggested this is due to the robust activity and infiltration of $CD4^+$ and $CD8^+$ T cells at the tumor site [23]. Thus, immune-based targeted therapy where the immune cells are manipulated to enhance its response can be a potential therapy for overcoming the toxicity and low response rate associated with the current treatment protocols for metastatic melanoma. Melanoma cells that express tumor-associated antigen (TAA) can be recognized by antigen-specific autologous antibody and T cells resulting in a targeted tumor clearance. TAAs on melanoma cells were categorized as [24-28]

- Differentiation antigens – expressed on malignant and normal malanocytes - gp100, tyrosinase, melan-A and the retained intron in tyrosinase-related protein (TRP-2-INT2)
- Cancer testis antigens – expressed on malignant tumor and not on normal tissues (except testis and placenta) - melanoma antigen 1 (MAGE1), Ny-ESO-1, PRAME, mutated CDK4 and MUM1.

The above mentioned TAAs can be used as potential targets for immunotherapies.

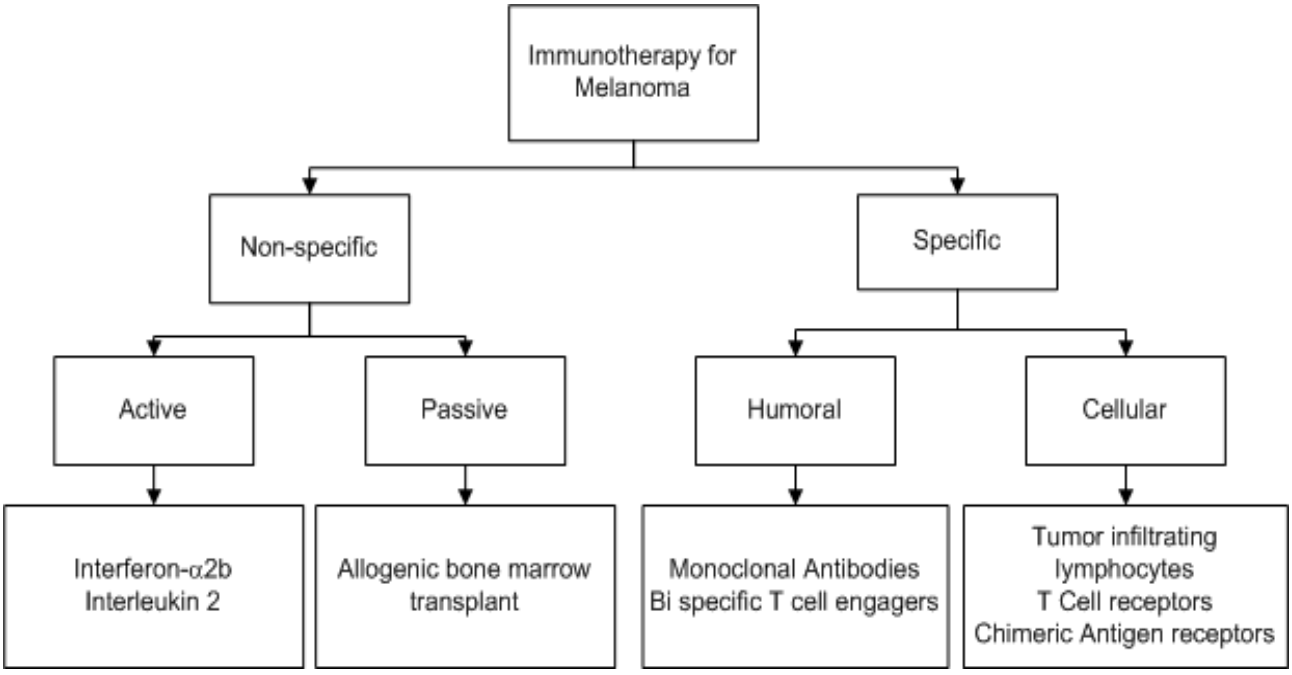

Figure. 1: Melanoma as a model tumor for immuno-oncology. Adopted from reference with permission from Maio M 2012. Melanoma as a model tumour for immuno-oncology. Ann Oncol 23 Suppl 8:viii10-14.

1.3 Immunotherapy for melanoma: Before 2011, the treatment strategy for metastatic melanoma included chemotherapy and IL-2. Over the years, many immune therapies have been tested against melanoma. These therapies fall in three different strategies:

- Therapeutic vaccination includes anti-idiotypic (anti-Id) antibodies as "surrogate" TAA to induce or potentiate a systemic TAA-specific immune response
- Passive immunization where antibodies or their derived molecules directly target tumor-associated antigens (TAA) expressed on malignant cells.
- Adoptive T cell therapy includes transfusion of autologous or allogeneic T cells to control tumor growth in patients. This therapy is based on the inherent cytolytic activity of T cells in killing tumor cells. The strategies for adoptive T cell therapy include tumor infiltrating lymphocytes (TILs) and Engineered T cells

Many immune therapies have been tested against melanoma with varying results. There are two broad classifications of immune therapy: specific and non specific (**Figure. 1**). Non-specific immunotherapy which includes infusion of large doses of IL-2 and IFN-a2b or allogenic bone marrow transplant involve toxicity associated with dosage and restriction in the population of patient eligible for such therapy[29]. In contrast, specific immunotherapy which includes antibody and T cell- derived therapy are lesser off-target toxicity compared to non-specific treatment options.

Monoclonal antibody based therapy for melanoma:

The generation of the first murine monoclonal antibody was possible with the development of hybridoma technology and mice breeding. In the 1980s a range of antibodies were

introduced in clinical trials for the treatment of various solid tumors [30]. The development of toxicity to these murine antibodies accelerated the production of engineered humanized monoclonal antibody which revolutionized cancer treatment strategy [31]. For melanoma treatment, the development of a clinically relevant antibody-based therapeutic approach has been the focus of interest for considerable time. Treatment of melanoma with anti-GD3 murine R24 monoclonal antibody alone or in combination with chemotherapy showed poor clinical response [32]. Therapeutic vaccination with a melanoma associated TAA resulting in production of idiotypic (Id) antibody was also explored [33].

T cell therapy:

In the past decade adoptive T cell therapy (ACT) has emerged as an optimistic therapeutic strategy for tumor elimination. ACT involves isolation and ex vivo expansion of autologous T cells in an antigen non-specific manner. These expanded T cells are later infused into the patient and have been shown to result in successful regression of melanoma [34].

Tumor infiltrating lymphocytes (TILs)

Melanoma is considered a highly immunogenic tumor due to the presence of TILs at the tumor site [35]. The concept of TILs has evolved from a cancer inducing immune cell to cancer ablating immune cells [35,36]. In the early days, TILs also served as a prognostic marker, with an increase in lymphocyte infiltration predicting improved prognosis of 3-5 years in patients with metastatic melanoma [37]. These TILs can recognize melanoma associated tumor antigen and lyse tumor cells in a major histocompatibility complex (MHC) dependent manner [38]. TILs are isolated from the tumor site and pulsed with melanoma specific peptides along with

antigen presenting cells, such as dendritic cells, with the addition of IL-2, resulting in several fold expansion of TILs *ex vivo* [39,40]. Though TIL therapy has successfully reduced melanoma progression, the effectiveness of the therapy may be reduced due to several reasons including (i) TILs sometimes include exhausted and/or senescent functionally anergic memory T cells [41] (ii) though the peptides used for the ex vivo expansion of TILs have anchor residue for HLA molecules, they might not elicit the expansion of tumor-specific T cells [42]., e.g. in a panel of 10 MART-1 peptides used only one successfully induced the TILs for melanoma recognition [43] (iii) as melanoma progresses, the tumor cells modulate the expression of TAA on their surface and alter their phenotype in a process known as immunosculpting, which enables avoidance of immuno-surveillance by the host immune system and leads to failed spontaneous or therapy-induced regression of metastatic tumor [44,45]. To circumvent these shortcomings, there is a need to develop engineered T cell therapy that can recognize tumor targets and bring about active tumor regression.

Engineered T cell therapy:

There are two approaches for engineering re-directed T cell specificity (**Figure. 2**) [46]:

1. Gene modification with tumor specific T-cell receptors (TCRs) in which the α and β chains of the TCR are cloned from TAA-specific T cell clones.

2. Introduction of chimeric antigen receptor (CAR) that recognizes TAAs through the single chain variable region (scFv) that is derived from the corresponding monoclonal antibody.

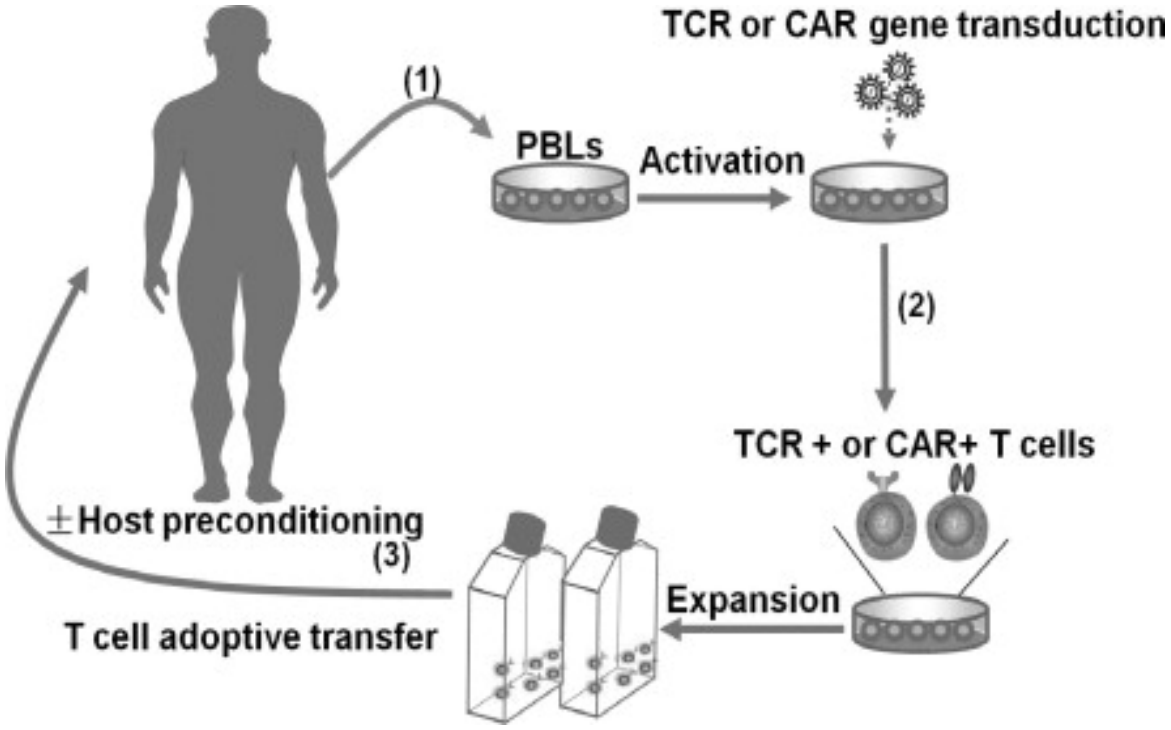

Figure. 2: Schematic representation of patients receiving T cells with T-cell receptor (TCR) or chimeric antigen receptor (CAR) T cells. (1) Patient peripheral blood T cells isolation. (2) T cells are engineered to express antigen-specific TCR or CAR genes (3) Expansion and adoptive transfer of antigen-specific T cells with prior lymphodepleting conditioning. Adopted from reference with permission from Shi H, Liu L, Wang Z 2013. Improving the efficacy and safety of engineered T cell therapy for cancer. Cancer Lett 328(2):191-197.

TCR-based therapy:

TCRs are found on the T cell surface as heterodimers of α and β chain that are rendered specific to an antigen presented by MHC on an antigen presenting cells (APC). Genes of tumor antigen specific TCR are isolated from patients and engineered into T cells using a viral or non-viral based vector system [47,48]. These T cells are expanded ex vivo to generate large numbers for infusion. Improvements in vector design, avidity of TCR by amino acid substitution in its complementarity determining region (CDR3) and introduction of cysteines to form disulphide bonds thereby preventing α and β chain mispairs has increased the efficacy of this therapy [49-51 52].

Though the TCR driven ACT is effective in reducing tumor [53], increased incidence of toxicity was reported especially with high avidity TCRs [54]. Patients with epithelial cancer infused with T cells bearing TCR specific to carcinoembryonic antigen (CEA) developed inflammatory colitis [54]. Also TCR specific therapy is MHC restricted hence tumor cells can lose antigen expression by down regulating MHC thereby evading the T cells [55]. Hence the application of TCR-specific T cell recognition is restricted to a single type of MHC molecule presenting the antigen [56]. In order to circumvent this problem CAR-based therapy was developed where the tumor recognition of the TCR will be non-MHC dependent [57,58].

CAR based therapy:

The CAR based therapy involves genetically engineered fusion of variable light (VL) and variable heavy chain (VH) specific for the antigen with a cell surface molecule which is tailored to produce an activating signal to the host immune cell upon antigen engagement [59]. These CARs are generally delivered to the peripheral blood T cells using a mammalian-

based Sleeping Beauty (SB) vector or nonmammalian-based retroviral system. The CAR identifies the tumor target in a human leukocyte antigen (HLA) independent manner unlike the αβ TCR receptors. Key advantages of this therapy include

- CAR based approach can be used in all tumor conditions expressing the antigen and is not MHC restricted.
- varied range of tumor antigens can be targeted using this system including glycoproteins and lipids [60-62].

The overall structure of the CAR consists of four elements namely the antigen targeting domain, an extracellular linker/spacer, a membrane spanning domain and intracellular signaling domain. The CAR has gone through successive generations with fine structural refinement (**Figure. 3**) [63]. The antigen specific domain is generally derived from the scFv portion of the monoclonal antibody (mAb) targeting the antigen. The linker is required to make the CAR flexible to reach the antigen. A mutated IgG derived Fc sequence that does not activate the innate immune cells is commonly used due to its stability in expressing the CAR on cell surface [64]. The transmembrane transitioned from CD4 or CD8 (first generation CARs) to CD28 (second generation CARS) [65]. The signaling endodomain of second generation CARs had CD3ζ along with the co-stimulatory signaling domain CD28 [66]. Improved tumor clearance and persistence has been observed in second and third generation CAR^+ T cells compare to the first generation CARs [64-70].

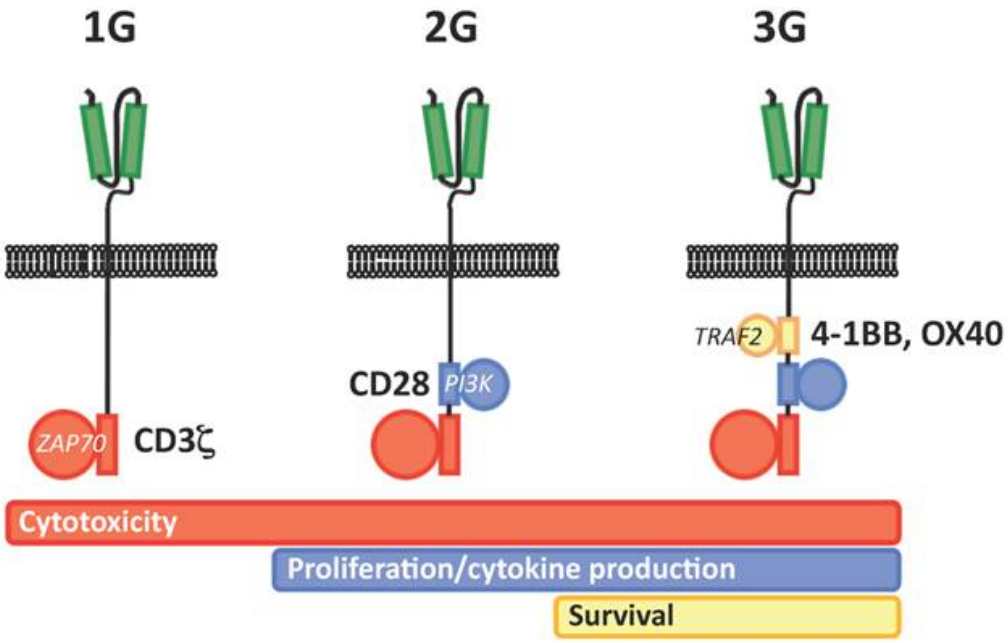

Figure. 3: Schematic representation of first (1G), second (2G) and third (3G) generation CAR molecules. Adopted from reference with permission from Casucci M, Bondanza A 2011. Suicide gene therapy to increase the safety of chimeric antigen receptor-redirected T lymphocytes. J Cancer 2:378-382.

Introduction of CAR into T cells:

Multiple vector systems have been developed to introduce the CAR into T cells. Of these, mammalian transposon/transposase based vectors can produce robust integration with low immunogenicity and more ease for plasmid manipulation [71]. Multiple mammalian vectors have been studied including *Sleeping Beauty* (SB) transposon (derived from *fish Tanichthys albonubes), piggyBac* element (moth *Trichoplusia ni)*, *Frog Prince (*frog *Rana pipiens), Himar1* (hornfly *Haematobia irritans), Tol2* (fish *Oryzias latipes)*, and *Passport* (flatfish *Pleuronectes platessa)* [72]. Among all element with activity in mammalian cell, SB transposon is one of the most widely studied for gene-transfer purpose [73]. A typical SB vector consists of the target gene sequence flanked by 230 bps long inverted and direct repeats (IR/DR) [73]. These IR/DR sites are involved in binding with SB transposase to transfer the target gene to host genome. The SB transposase was derived by combining inactive transposase sequences from the genome of salmonid fish followed by reversing termination codon to activate the transposase activity [71]. Components of SB transposase include IR/DR sequence, DNA recognition site, nuclear localization signal (NLS) and catalytic domain.

Gene transfer using SB transposon/transposase involves cut and paste mechanism [74]. The SB transposase protein is translated and accumulated in the cytoplasm which is then imported into the nucleus using NLS. The SB transposase protein binds to the IR/DR sequence of the transposon causing DNA breaks flanking the gene of interest.

Integration site of gene cut from the SB transposon into the T cell genome depend on the presence of dinucleotide TA site, DNA flexibility and proximity of the donor and receiver (local hopping) [75-77]. More than 25% of integrations happen within 200 bp between the donor

and receiver sites of the gene and more than 75% of integration happen in a single chromosome.

1.4 CAR based immune therapy for melanoma

Despite the success of CAR T cell therapy in treating patients with conditions including chronic and acute myeloid leukemia (CML, AML) and colon cancer, there are no successful clinical studies using CAR T cell therapy for melanoma [78]. Pre-clinical studies on mouse models such as SCID and NOG using CARs specific for melanoma antigens such as GD2, GD3 and MAGE-A1 have suggested the feasibility of this therapy in the clinic [60,79,80].

One of the major concerns of CAR therapy is the toxicity profile. These $CAR^{+}T$ cells are highly specific to the tumor associated antigen which can also be expressed on normal cells. A clinical study on patients with metastatic colon cancer using CAR specific against ERBB2 tumor antigen resulted in respiratory distress within fifteen minutes of infusion due to influx of infiltrates into the lungs [81].

Hence in summary, CAR T cell therapy can be a potential strategy to bring about immune cell mediated tumor antigen recognition, generate memory lymphocytes and prevent immune suppression [82]. Toxicity issues during available immunotherapy necessitate the need to identify new antigens that are specifically expressed on metastatic melanoma cells and not on normal tissue.

1.5 Oncogenesis of retrovirus:

An estimated one in five cancers is associated with viral infection[83]. The discovery of retrovirus involvement in cancer involved the transformation of tumor free chicken cell to

acquire erythro myeloblastic leukemia in 1908. The factor involved in this transformation was later identified as avian myeloblastosis virus [83]. Later research in mice led to the discovery of mouse mammary tumor virus [84]. Discovery and invention of quantitative focus forming assays, and of reverse transcriptase, helped in further understanding the mechanism of tumorigenesis of these viruses [85,86]. Several biomolecular studies were performed to illustrate the mechanism of oncogene activation leading to pathogen-induced/related cancer. These include (a) introduction of exogenic viral oncogenes (b) activation of endogenous retrovirus (c) inactivation of suppressor genes [87].

Oncogenic retroviruses are classified into two subgroups depending on their pathogeneses. The first group, the acute transforming retroviruses, are defective in replicating and induce cancer via their viral oncogenes. The second group, the non-acute retroviruses, are competent in replication but are devoid of oncogenes and they cause cancer by inserting the proviral DNA around the genes encoding proto-oncogenes [88].

A retrovirus typically consists of a single-stranded RNA genome ranging from 7 to 13 kb. This genome encodes the structural proteins gag, pro, pol and env (**Figure. 4**). In addition to this, a wide array of accessory proteins such as viral capsid proteins, viral proteases, viral enzymes (reverse transcriptase and integrase) are encoded. Retroviral infection involves formation of provirus by cleaving the gal-pro-pol polyprotein precursor. The viral RNA is reverse transcribed (RT) into viral DNA in the host cell. The RT-viral DNA consists of long terminal repeats (LTR) which are classified into three regions, U3, R and U5 regions, based on their functionality. The U3 LTR which includes the promoter and enhancer sequence is responsible for initiation of transcription. The U3-R region involves the transcription of

provirus by RNA polymerase II, and the RNA cleavage and polyadenylation occurs at the R-U5 downstream region [88].

In general retroviruses target the somatic cells for their ability to replicate and do not lyse the target cells resulting in a long term association of the somatic cell with the virus. However, when these retroviruses target the gamete cells the provirus becomes permanently embedded in the host genome and passed on through successive generations during the course of evolution. These inherited provirus are termed "endogenous retroviruses" and some these elements have been recorded in fossils dating back 40 million years [89]. Phylogenetic analysis reveals that there are about 31 groups of ERV variants integrated into the human genome [90]. These ERVs typically consists of 2LTRS separated by approximately 300 to 1000 nucleotides in length that encode for the structural proteins of the virus [91]. The chromosomal location of each ERV is unique due to random integrations [89]. Though the ERVs initially colonized the human germline, over the period of time the ERV coding sequence accumulated a multitude of random mutations making them noninfectious to the host cells [92]. Alternatively the ERV transcription is silenced in differentiated tissues by epigenetic silencing such as DNA methylation, histone modifications and RNA interference [93,94].

The present method of classification of HERVs is based on the first letter amino acid code involved in t-RNA complimentary to the primer binding site used for reverse transcription. Thus HERV-K has lysine as the starting amino acid in its tRNA primer [95]. This classification however, does not take into account the fact that the different pro-viruses can have the same primer binding site sequence. The frequency of ERV integration in various species has been helpful in indicating the evolutionary significance.

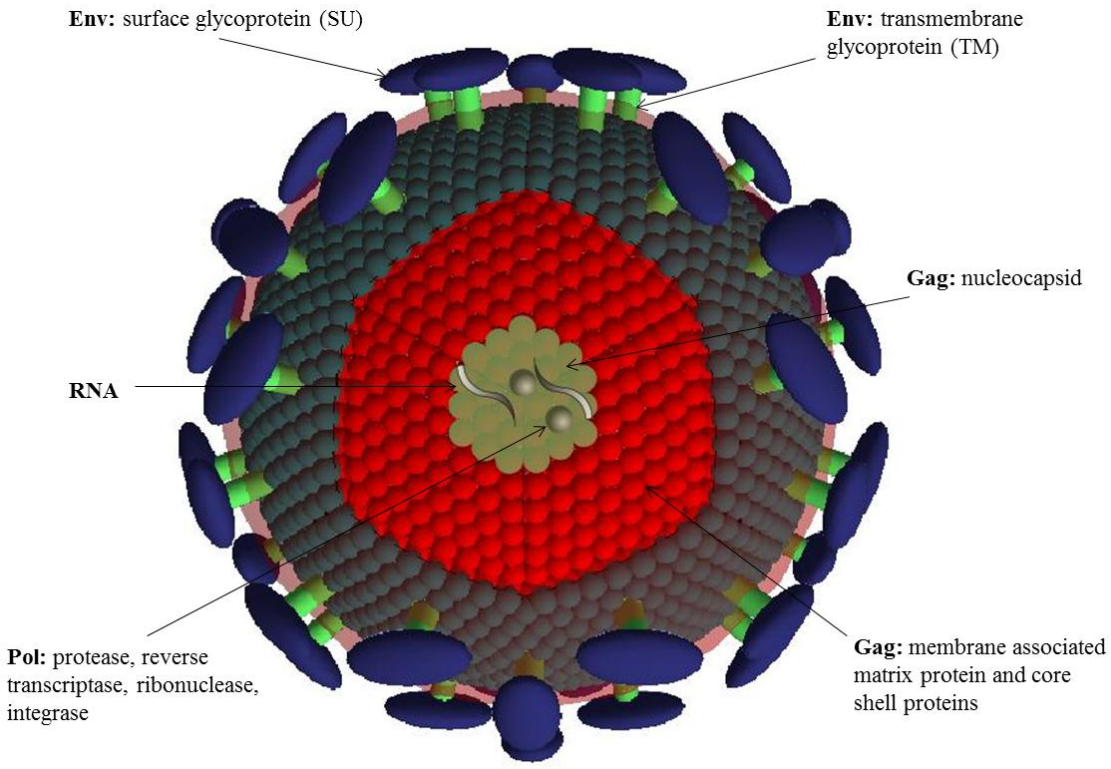

Figure. 4: Schematic structure of a retrovirus. Adopted from reference with permission from Dr. Rycaj.

In silico analysis has shown evidence for relative distribution of LTR elements in the host genome are generally found in the intergenic regions than the introns and are generally underrepresented [96,97]. The LTR sequences found in the introns are generally in the opposite transcriptional orientation from that of the host gene emphasizing the deleterious effect of viral gene expression [97].

The provirus content in humans exhibits reduced polymorphism compared to other mammals since most of the proviral element locations are the same as in chimpanzees. In contrast to this observation is the active member of HERV, mouse mammary tumor virus (MMTV) related HERV-K (HML-2), which was discovered only in the humans [98].

1.6 Evolutionary significance of HERVs:

Immunity: When a retrovirus is endogenously integrated with the germ cell of a species its expression may interfere with other exogenous retroviruses infecting the host. This might provide a selective advantage in the survival and propagation of the host causing extinction of the exogenous counterpart (**Figure. 5**) [99]. Transmission of the virus within and between species may alter the pathogenicity and virulence of the virus. HERV-W has been shown to protect the host from superinfection by exogenous retrovirus in vitro [100].

Development: In addition to providing protection against exogenous infections, some ERVs have been adapted in the host genome to provide additional physiological advantages. One such example is the HERV-W and HERV-FRD mediated syncytins-1 and syncytin-2 proteins that are involved in the placental membrane development by protein cell fusion and syncytium formation [101]. Syncytin-2 is also known to be involved in immune suppression which may be involved in protecting the fetus from host rejection or cancer

progression in humans [102,103]. The env protein of HERV-R is found to be expressed in several fetal tissues including the adrenal gland and is suggested to contribute to cellular differentiation and placental development [104].

Promoters: The function of a genome can be altered by the retroviral sequence integrated nearby to the corresponding gene [91]. Retroviral LTRs are in general found in antisense direction upstream and in sense direction downstream to a host gene [84]. For example, integration of HERV-E LTR in antisense direction upstream of the amylase gene promotes its expression from the parathyroid glad and its release into saliva [105]. Strong bidirectional promoter activity has been observed with several LTRs of HERV-H group [106]. HERV-E LTRs are involved in promoting the transcription of apolipoprotein C-1 which in turn regulates other genes in the genome [107].

Regulatory elements and anti-cancer properties: About 30% of all p53 binding sites are HERV LTR sequence and regulate the expression of p53 genome-wide contributing to the anti-oncogenic functions [108]. Renal cancer cells with increased protein expression of HERV-E were shown to recruit T-cells from allogeneic transplant donors and led to tumor regression in patients undergoing immunotherapy suggesting the HERVs are dormant and re-activation is not well tolerated by the host cells [109].

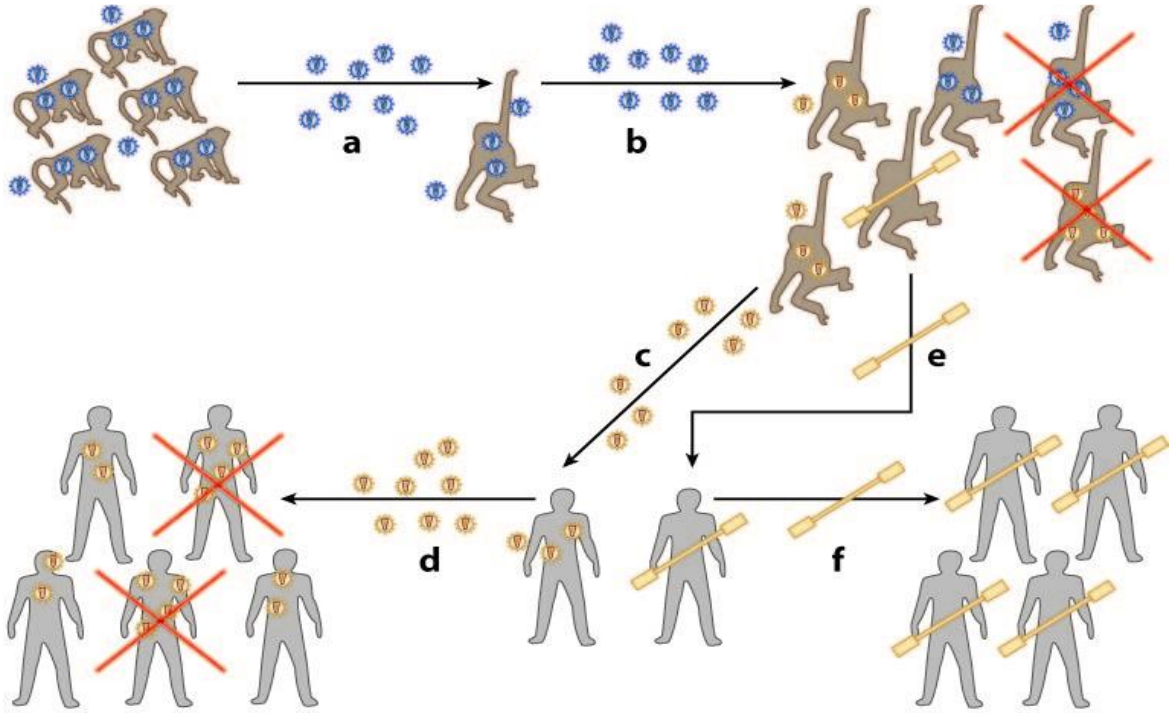

Jern P, Coffin JM. 2008.
Annu. Rev. Genet. 42:709–32

Figure. 5: Schematic representation of transmission of HERV-K virus between species and persistent survival of species due to presence of viral genes in their genome. Adopted from reference with permission from Jern P, Coffin JM 2008. Effects of retroviruses on host genome function. Annu Rev Genet 42:709-732.

1.7 HERV-K

Among all the HERVs studied, HERV-K is one the youngest and the most active provirus found in the host genome [110]. One such example is HERV-K 113 located on chromosome 19 and possesses all open reading frames for genes encoding Gag, Pol, Env and a protease flanked by two non-coding LTRs. Apart from these structural proteins, two accessory proteins Rec and Np9 proteins are also encoded specific to the HERV-K family [111]. Rec protein is responsible for nuclear transport of spliced mRNA into the cytoplasm and Np9 is known to be involved in transcriptional regulation of myc- related proto oncogenes [112,113]. The Rec and Np9 protein is suggested to be involved in pro-oncogenesis by increased levels of myc and its downstream products such as p53 resulting in reduced apoptosis and increased proliferation [113,114].

Non-allelic homologous recombination (NAHR) of different isoforms of HERV-K at the same or a different chromosomal location can lead to human genomic rearrangement. In about 40 haploid copies of HERV-K, one-tenth of these subfamily members have undergone NAHR after insertion into the human genome [115]. Though most of the HERVs deposited in the human genome are silent, they can be activated by external or internal triggers such as environmental factors including diet, infection from exogenous virus or cancer [116-119]. For instance, Epstein-Barr virus (EBV) infection mediated interferon-gamma (IFN-γ) production by host T cells leads to transcriptional activation of HERV-K18 at the CD48 locus [120].

Transcriptional activation of HERV-K has been attributed to the epigenetic changes which include CpG methylation of the U3 promoter sequence [121]. Low level of LTR methylation results in increased levels of HERV-K [122]. Apart from methylation, APOBEC3G-mediated cytidine deamination is also involved in suppressing HERV-K LTR activation [123].

Apart from epigenetic changes, transcriptional regulators also play an important role in regulating HERV-K expression. Ubiquitous regulators belonging to the family of SP, YY1, microphthalmia-associated transcription factor (MITF-M) proteins which are implicated in various pathologies such as cancer are suggested to bind to the GC region (G rich elements), 5'terminus of the U3 promoter of HERV-K proviral LTR and the U3 region of HERV-K6 [124-126]. Indirect activation of HERV-K has been observed by alternative transcriptional regulators such as OCT-1 and bZip family members (AP-1 and CREB) during exogenous infection [127-129]. HERV-K has several NF-κB binding sites which results in upregulation of the proviral expression during inflammation mediated by IFN-γ [130-132], TNF-α [133] or IL-6 [134] which mediate increased NF-κB production thereby inducing HERV-K [135]. Recent HERV genome sequencing has shown that 0.2 to 1% of all cell transcription factors in a cell are derived from HERVs and some have tissue specific transcription activity [136].

1.8 HERV-K involvement in human diseases

Among the HERV family, HERV-K is the only member found to have intact open reading frames and produce retroviral particles [111,137,138]. HERVs are suggested to play a role in tumor development by their immune suppressor function involved in fetal development which can be detrimental for the host during tumor growth (**Table. 1**) [138,139]. Antibodies against the transmembrane portion of HERV-K have been detected in the serum of some tumor patients and pregnant women [140]. The transmembrane proteins of many HERV env proteins have been shown to contribute to this immune suppressor function [103,141].

Table. 1:

HERV-K expressing tumor and infections	**Reference**
Melanoma	1. Muster T, Waltenberger A, Grassauer A, et al. An endogenous retrovirus derived from human melanoma cells. *Cancer Res.* Dec 15 2003;63(24):8735-8741. 2. Buscher K, Trefzer U, Hofmann M, Sterry W, Kurth R, Denner J. Expression of human endogenous retrovirus K in melanomas and melanoma cell lines. *Cancer Res.* May 15 2005;65(10):4172-4180 3. Li Z, Sheng T, Wan X, Liu T, Wu H, Dong J. Expression of HERV-K correlates with status of MEK-ERK and p16INK4A-CDK4 pathways in melanoma cells. *Cancer Invest.* Dec 2010;28(10):1031-1037. 4. Reiche J, Pauli G, Ellerbrok H. Differential expression of human endogenous retrovirus K transcripts in primary human melanocytes and melanoma cell lines after UV irradiation. *Melanoma Res.* Oct 2010;20(5):435-440. 5. Serafino A, Balestrieri E, Pierimarchi P, et al. The activation of human endogenous retrovirus K (HERV-K) is implicated in melanoma cell malignant transformation. *Exp Cell Res.* Mar 10 2009;315(5):849-862
Breast cancer	1. Patience C, Simpson GR, Colletta AA, Welch HM, Weiss RA, Boyd MT. Human endogenous retrovirus expression and reverse transcriptase activity in the T47D mammary carcinoma cell line. *J Virol.* Apr 1996;70(4):2654-2657 2. Wang-Johanning F, Frost AR, Jian B, Epp L, Lu DW, Johanning GL. Quantitation of HERV-K env gene expression and splicing in human breast cancer. *Oncogene.* Mar 13 2003;22(10):1528-1535. 3. Seifarth W, Skladny H, Krieg-Schneider F, Reichert A, Hehlmann R, Leib-MoschC. Retrovirus-like particles released from the human breast cancer cell line T47-D display type B- and C-related endogenous retroviral sequences. *J Virol.*1995;69(10):6408-6416.
Ovarian Cancer	Wang-Johanning F, Liu J, Rycaj K, et al. Expression of multiple human endogenous retrovirus surface envelope proteins in ovarian cancer. *Int J Cancer.* Jan 1 2007;120(1):81-90
Lymphoma	Contreras-Galindo R, Kaplan MH, Leissner P, et al. Human endogenous retrovirus K (HML-2) elements in the plasma of people with lymphoma and breast cancer. *J Virol.* Oct 2008;82(19):9329-9336.
Teratocarcinoma	1. Bieda K, Hoffmann A, Boller K. Phenotypic heterogeneity of human endogenous retrovirus particles produced by teratocarcinoma cell lines. *J Gen Virol.* Mar 2001;82(Pt 3):591-596. 2. Lower R, Lower J, Tondera-Koch C, Kurth R. A general method for the identification of transcribed retrovirus sequences (R-U5 PCR) reveals the expression of the human endogenous retrovirus loci HERV-H and HERV-K in teratocarcinoma cells. *Virology.* Feb 1993;192(2):501-511.
Acquired immunodeficiency syndrome (AIDS)	Jones RB, Garrison KE, Mujib S, et al. HERV-K-specific T cells eliminate diverse HIV-1/2 and SIV primary isolates. *J Clin Invest.* Dec 3 2012;122(12):4473-4489

1.9 HERV-K and melanoma

Since the 1970s numerous reports have suggested the involvement of retrovirus like particles (RVLPs) in melanoma using electron microscopy and biochemical techniques (42). These RVLPs were initially detected in the lymph node of metastatic patients and they resembled the C-type virions and RT activity [142].These RLVPs had a reverse transcriptase activity and sequence homology to HERV-K 108 Gag and Env protein but were defective in replicating themselves and were noninfectious [143]. In early 2000, studies reported that HERV-K antigen on tumor cells presented in the context of HLA-A2 and was detected by the patient CTLs [144]. Pathology slide preparations of melanoma from various sites including lymph node and skin revealed the high copy number of HERV-K 108 via in situ hybridization. Absence of HERV-K 108 was observed in nevi tissues from healthy donors [143]. Metastasis of melanoma was associated with the expression of full length HERV-K gag and env mRNA [145]. Recently, antibody against HERV-K gag and env protein was detected in 16% of patient sera but not in normal controls. The serum HERV-K expression correlates with the reduced prognosis associated with melanoma disease progression [146].

1.10 Targeting HERV-K during melanoma- Project overview

We have shown that HERV-K env is specifically expressed in the 220 melanoma patient samples and absent in 33 normal donor organ tissues, each obtained from three different donors. The antigen expression on the tumor cell surface at any point during cell culture was variable due to shedding of the env protein from the cell surface. This variation was detected by flow cytometry and pseudo-infection of HERV-K^{neg} EL4 cells. Over expression or knockdown of antigen was unstable and did not yield stable clones. Even though there was

no stable antigen expression on these EL4 cells by plasmid encoding HERV-K-env, we predict that the antigen should have a type 2 transmembrane protein structure in contrast to the suggested type 1 membrane based on the detection of both N and C terminal of the protein inside the cell.

Our laboratory has previously designed a CD19-specific CAR for treatment of B-cell malignancies which is currently being evaluated in clinical trial [70,147]. We electroporated PBMCs from a normal donor using a non-viral SB vector, and, the T cells expressing our CD19-specific CARs were selectively propagated on γ-irradiated artificial activating and propagating cells (AaPC) derived from K-562 cells [148], [149], [150]. Based on this approach, we have successfully developed HERV-K-specific CAR^+ T cells using the SB system and their numeric expansion on HERV-K^+ AaPC. These CAR^+T cells were also able to detect HERV-K env shed from the tumor cell surface. *In vivo*, infusion of HERV-K env-specific CAR^+ T cells decreased tumor burden in a mouse model of metastatic melanoma. These data suggest that ACT of HERV-K env-specific T cells are a potential therapeutic strategy for patients with melanoma.

Chapter 2: Materials and Methods

2.1 Study Design: The overall objective of this study is to determine the expression of HERV-K env on primary melanoma cells, but not on normal tissues, and to develop HERV-K env-specific CAR^+ T cells that can recognize and kill melanoma cells *in vitro* and *in vivo* expressing this TAA. The expression of HERV-K env was evaluated by IHC staining of patient samples and normal human tissue array using an H-index. The *in vitro* studies include construction of HERV-K env-specific CAR and evaluation of specificity and effector function (from multiple donors and tumor cells). Variability in tumor cell surface expression of HERV-K-env was apparently linked to shedding of this TAA, and, CAR^+ T cells could recognize shed antigen. The efficacy of HERV-K env-specific CAR^+ T cells was evaluated in a mouse model. All animal experiments were performed after the approval of Institutional Animal Care and Use Committee at MD Anderson Cancer Center (MDACC) in accordance to NIH guidelines for the Care and Use of Laboratory Animals.

2.2 Immunohistochemistry: Tissue microarrays (catalog # ME1004a, ME2082b, FDA998t) obtained from U.S. Biomax (Rockville, MD) were hydrated with distilled water and antigen retrieval using citrate buffer pH 6 without EDTA was performed. Slides were blocked with 3% hydrogen peroxide (Biocare Medical, Concord, CA), avidin (Biocare Medical), biotin (Biocare Medical) and polyclonal whole serum (Biocare Medical). Slides were incubated for 30 minute each with HERV-K mAb (3 μg/mL) followed by biotinylated anti-mouse IgG (Biocare Medical) and strepavidin-HRP (Sigma-Aldrich, St Louis, MO) and visualized with a Mayer's Hematoxylin counterstain (Sigma-Aldrich). Similar staining procedure was

performed on the slides with isotype control mouse IgG2a (3 μg/mL) antibody (BD Pharmingen, Franklin Lakes, NJ). Percentage of HERV-K env antigen staining and expression intensity was quantitated using microscopy and pathology analysis. H-index was calculated as a product of intensity and percentage of HERV-K env expression on tumor tissue.

2.3 Real-time polymerase chain reaction: Quantitative examination of HERV-K mRNA levels in normal tissue cDNA was performed using the StepOnePlus real-time PCR system (Applied Biosystems, Grand Island, NY). Pooled complementary DNA (cDNA; catalog # 636742, 636743) from three different normal donors for each of the 16 different organs analyzed (Clonetech, Mountain View, CA). Five-fold serial dilution of normal donor tissue cDNA was performed to develop standard curves. For TaqMan assay primers (forward primer: 5-GGGTACCTGGCCCCATAGAT-3; reverse primer: 3-CATCATCCCTTCTTCCTCAGGTT-5) and probes (5-ATCGCTGCCCTGCC-3) were obtained from Applied Biosystems. Reaction mixture (20 μL) containing 1 μL of cDNA template, 2 μL each of primer and probe mix, 10 μL TaqMan universal PCR master mix (Applies Biosystems) and water. Amplified was performed as follows: denaturation at 95°C for 10 minutes and 40 cycles at 95°C for 15 seconds, 60°C for 1 minute. Direct detection of PCR products monitored by measuring the fluorescence produced by the result of TaqMan probe hydrolysis after every cycle. Amplification efficiencies were tested for HERV-K env and housekeeping gene (RNaseP). All samples were tested with the reference gene RNaseP for data normalization to correct for variations in cDNA quality and quantity. All samples were performed in triplicate. The parameter threshold cycle (Ct) defined as the cycle number

at which the first detectable fluorescence increase above the threshold observed. For fold-changes in relative gene expression was calculated using the equation ΔCt = Ct (HERV-K env) − Ct (RNaseP). The ΔΔCt is then calculated using ΔCt values of HERV-K env^{+} K-562 parental cell as reference using the equation, ΔΔCt= ΔCt (Normal organ) − ΔCt (K-562). The relative mRNA expression is then calculated using the equation, relative mRNA expression = $2^{-\Delta\Delta Ct}$

2.4 Plasmids: The scFv sequence (from mAb clone 6H5) against HERV-K env protein (Dr. Wang-Johanning, MDACC) was codon optimized (CoOp) (Invitrogen, Carlsbad, CA) and cloned into SB transposon vector under human elongation factor-1α (hEF-1α) promoter, flanked by SB inverted repeats forming $_{CoOp}$ 6H5CD28/pSBSO. HERV-K env was cloned and expressed from SB plasmid containing bidirectional hEF-1α and cytomegalovirus (CMV) promoters. The codon optimized (CoOp) full length HERV-K env antigen sequence with the viral transmembrane domain was cloned under hEF-1α promoter and neomycin gene was transcribed under CMV promoter in a bi-directional vector, HERV-K (CoOp) Neo/pSBSO-Bidirectional. The transposase (SB11) was expressed in *cis* from the plasmid pCMV-SB11 [151]. The 6H5 CAR maxibody specific for the scFv derived from the 6H5 antibody was fused to IgG4Fc domain and poly histidine tag and cloned into lentiviral vector PDC415 under SV40 promoter (**Figure. 11**) and expressed on HEK293 mammalian cells, and the supernatant was collected and purified using polyA columns (Fabion, Seattle, WA). To generate the *in vivo* imaging SB plasmid for T cells, codon optimized firefly luciferase gene was fused to myc tag under control of a CMV promoter. A lentiviral vector encoding

mKate-Renilla luciferase constructed under eEF1α promoter was used as an imaging vector for melanoma tumor cells *in vivo*.

To understand the structure of HERV-K env, two different lentiviral plasmids were constructed modifying the HERV-K env signal peptide and transmembrane sequences. The signal peptide was either switched to IgKL sequence or modified to express FlagM2 and FlagM1 on either side of it. The transmembrane domain was switched to Fc-CD8. In both the plasmids, the furin cleavage site between the SU and TM domain was removed and protein was encoded under a RSV U3 promoter sequence and has a polyhistidine tag and mKate flourescence marker following the transmembrane domain for detection.

2.5 Cell lines and their propagation: A375, A624, and A888 were provided by Dr. Laszlo Radvanyi (MDACC); EL4 parental cell line was obtained from American Type Culture Collection (catalog # TIB-39, Rockville, MD); and A375-SM (super-metastatic melanoma cell line) was received from the Characterized Cell Line Core Facility (CCCF) at MDACC. All cell lines were cultured in RPMI (Thermo Scientific, Rockford, IL) with 10% FBS (Thermo Scientific) and 5% glutamax (Gibco Life technologies, Grand Island, NY). All cell lines were verified by morphology, cell single tandem repeat finger printing and/or flow cytometry. They were routinely tested for *Mycoplasma* and all tests were negative.

2.6 Generation and expansion of HERV-K env-specific CAR$^+$ T cells: Generation and expansion of HERV-K env-specific CAR$^+$ T cells were performed using a protocol previously described [149]. Briefly, the 2x10^7 PBMC cells were washed and rested in complete RPMI supplemented with 10% fetal bovine serum (Thermo Scientific) and 1% glutamax

(Gibco Life technologies) for 2 hrs. On day 0, these cells were then re-suspended in 100 μL of Nucleofector solution (Human T-cell Kit) (Lonza, Allendale, NJ), with supercoiled DNA coding for HERV-K env-specific CAR transposon (15 μg $_{CoOp}$6H5CARCD28/pSBSO) and supercoiled DNA coding for SB transposase (5 μg pCMV-SB11), transferred to a single cuvette, and electroporated using the U-14 program (Lonza). The electroporated T cells were rested for 4 hours at 37°C in complete phenol red-free RPMI (Thermo Scientific) after which a half-media change was performed. The K562-derived clone 4 expresses endogenous HERV-K env (**Figure 11**) and thus serves as AaPC to propagate HERV-K env-specific CAR^+ T cells. The electroporated T cells cultured in RPMI containing 10% FBS were supplemented with γ-irradiated (100 Gy) K562-AaPC at a 1:2 T cell/AaPC ratio on day 1. Irradiated AaPC were re-added at the end of every week for T-cell stimulation at the same ratio. Soluble recombinant IL-21 (eBioscience, San Diego, CA) and IL-2 (Invitrogen) cytokines were supplemented at a concentration of 30 ng/mL and 50 U/mL respectively to complete RPMI media on a Monday, Wednesday, Friday schedule. Mock transfected negative "no DNA" control T cells were propagated in the presence of OKT3-loaded AaPC, IL-2, and IL-21. CD19-specific CAR^+ T cells electroporated with $_{CoOp}$ CD19CARCD28/pSBSO and SB11 transposase and propagated under the same culture conditions as for HERV-K env-specific CAR^+ T cells served as a negative control. The T-cell cultures were monitored weekly for the contaminating presence of $CD3^{neg}CD56^+$ NK cells which were depleted if this population exceeded 10% of the total population. A depletion usually occurred between 10 and 14 days of initial co-culture with AaPC and was carried out using CD56 beads (Miltenyi Biotech Inc, Auburn, CA) on autoMACS (Miltenyi Biotech) using the positive selection "possel" program according to manufacturer's

instruction. T-cell viability was assessed by trypan blue exclusion using a Cellometer automated cell counter (Auto T4 Cell Counter, Nexcelom Bioscience, Lawrence, MA). The fold expansion was calculated (compared to day 1) of total, $CD3^+$, $CD4^+$, $CD8^+$, and CAR^+ cells at the end of 7, 14, 28, and 32 days of co-culture on AaPC with cytokines. The average CAR^+ T-cell growth of 4 donors was compared between the CD19-specific CAR^+ T cells and no DNA control cells using a Student's t-test.

2.7 Generation of HERV-K env-specific CAR^+ $ffLuc^+$ T cells by double transposition: Two SB plasmids encoding (i) HERV-K env-specific CAR and (ii) myc-ffLuc-neomycin (7.5 μg each) along with SB transposase (5 μg pCMV-SB11) were electrotransferred into PBMC and propagated on AaPC similar to HERV-K env-specific CAR^+ T cells. A cytocidal concentration of neomycin (0.8 mg/mL) was added to select CAR^+ffLuc^+ T cells. All T-cell cultures received IL-21 (30 ng/mL) and IL-2 (50 U/mL) three times a week.

2.8 Flow cytometry: One million cells were stained with antibody conjugated with fluorescein isothiocyanate (FITC), phycoerythrin (PE), peridinin chlorophyll protein conjugated to cyanine dye (PerCPCy5.5), or allophycocyanin (APC). All antibodies used are listed in (**Supplement Table 1)**. Blocking of nonspecific antibody binding was achieved with goat IgG and using FACS wash buffer (2% FBS and 0.1% Sodium Azide in PBS). Data acquisition was on a FACS Calibur (BD Biosciences) using CellQuest version 3.3 (BD Biosciences). Analyses and calculation of median fluorescence intensity (MFI) was undertaken using FlowJo version 7.5.5.

2.9 Integration Analysis: Genomic DNA from HERV-K env-specific CAR^+ T cells was isolated using a QIAamp DNA mini kit (Qiagen) and real-time PCR was performed as previously described [152]. Genomic DNA from Jurkat cells (clone 12) bearing a single integration of the CD19-specific CAR copy previously described was used as a positive control. The experiment was undertaken in triplicate with 100 ng of genomic DNA mixed with 10 µL of TaqMan Gene Expression Master Mix (Applied Biosystems, Foster City, CA), 1 µL (1x probe at 250 nM and 1x primer at 900 nM) of 20x FAM labeled CAR-specific TaqMan probe primer set specific for IgG4Fc [forward (5'-GAGGGCAACGTCTTTAGCTG-3') and reverse (5'-GATGATGAAGGCCACTGTCA-3') primers and carboxyfluorescein (FAM)-labeled probe (5'-AGATGTTCTGGGTGCTGGTC-3')] and 1 µL (1x primer at 900 nM and 1x probe at 250 nM) of 20x VIC labeled TaqMan RNaseP Probe Primer set (Applied Biosystems) in a total reaction volume of 20 µL. The primers hybridize at the IgGFc4 portion of the CAR. Amplification cycle included: 2 minutes at 50°C, 10 minutes at 95°C, forty 15-second cycles at 95°C, and 1 minute at 60°C and detection was performed with a StepOnePlus Real-Time PCR System (Applied Biosystems). Autosomal RNaseP gene present at 2 copies per diploid cell, was used as an endogenous reference for normalization. The $\Delta\Delta C_T$ method (Applied Biosystems, CA) was used to calculate the number of integrations with reference to RNaseP and Jurkat clone as normalization controls [152].

2.10 nCounter analysis digital gene expression system: Digital gene expression analyses were performed as previously described [153]. Differences in gene expression between HERV-K env-specific CAR^+ T cells and no DNA control T cells were evaluated using the nCounter

Analysis System (model no. NCT-SYST-120, NanoString Technologies) [153]. Briefly, 10^4 HERV-K env-specific CAR^+ T cells or no DNA T cells were lysed in RNeasy lysis buffer (RLT; 5 μL, Qiagen, Gaithersburg, MD) and the mRNAs were hybridized for 12 hours at 65°C with a reporter probe code set and a capture probe code set (**Appendix Table 2**) custom designed using the nCounter Gene Expression Assay Kit. An nCounter prep station was used for the post-hybridization processes. R-program, tree-view and clustal view were used to output the data with statistical analysis.

2.11 6H5 mAx: In order to measure the HERV-K env expression on the tumor cell surface we developed a 6H5 mAx specific for the HERV-K env antigen. 6H5 mAx represents soluble CAR by swapping the CD28 and CD3ζ endodomain with a polyhistidine tag (**Figure 15A**). This construct was inserted into a DNA plasmid coding for lentiviral vector (**Figure 15B**) which was introduced into 293 METR cells (provided by Dr. Brian Rabinovich) using Lipofectamine 2000 (Life Technologies, Grand Island, NY), and conditioned supernatant was concentrated using 100 kDa cut-off centrifugal filter (catalog # UFC910024, EMD Millipore, Billerica, MA). The 6H5 mAx was then purified using a polyA column (Life Technologies) and analyzed on a SDS-PAGE gel to confirm purity.

2.12 ELISA: To determine the specificity of 6H5 mAx made, we coated the 96-well plates (NUNC) with purified HERV-K env recombinant protein K10 (from Dr. Wang-Johanning) at 0 to 1 μg/well as serially diluted in PBS buffer. Antigen-coated wells were incubated for 1 hour at 37°C followed by washing with PBS containing 0.1% tween (PBST). 10% BSA was used for blocking nonspecific binding for 2 hours at room temperature. 6H5 mAx or 6H5

mAb or unrelated CD19-specifdic antibody (catalog # FMC63, Millipore) was added at 0.25 mg/mL final concentration and incubated for 1 hour at room temperature. In some instances, 10 mg/mL of blocking antibody (either 6H5 mAb or 6H5 mAx) was used followed by washing with PBST buffer and addition of probing antibody (6H5 mAx or 6H5 mAb). A secondary HRP-labeled goat anti mouse- (Pierce, Thermo Scientific) was used to detect 6H5 mAb or unrelated CD19 antibody and HRP-labeled goat anti human (Jackson Laboratories) was used to detect 6H5 max. After the final washing 100 μL of tetramethyl benzidine ELISA substrate (Sigma-Aldrich) was added and incubated for 5 minutes in the dark. 50 μL of 1N sulfuric acid was then added to stop the reaction. The absorbance was measured at 450 nm using a plate reader Victor X5 (Perkin Elmer, Waltham, MA).

2.13 sh-RNA mediated HERVK knockdown in A888-mel cells: HERV-K specific sh-RNA and scrambled sh-RNA lentiparticles were kindly provided by Dr. Wang-Johanning (MDACC, Bastrop, TX). The A888 cells were grown to 90% confluence in a 6-well plate. The media was later replaced using optimum media with sh-RNA lentivirus (titre of 100 μl) and polybrene (5 μg/ml) and transduced for 4 hours at 37^{o}C and then replaced with regular RPMI media. The cells were then sorted based on GFP expression and grown further. Scrambled shRNA transduced A888 cells were used as control.

2.14 Chromium release assay (CRA): The CRA was performed as previously described [149,154]. Briefly, HERV-K^{+} targets were loaded with ^{51}Cr for 2 hours and incubated with HERV-K env-specific CAR^{+} T cells or no DNA control T cells grown for 35 days and the percentage ^{51}Cr release was calculated using the following formula:

$$\%^{51}Cr\ release = \frac{Experimental\ release - Background\ release}{Minimum\ release - Background\ release} \times 100$$

2.15 Video time-lapse microscopy (VTLM): Tumor cells were co-cultured with HERV-K env-specific CAR^+ T cells in Hi-Q4 glass bottom dishes (Ibidi, Verona, WI) with complete RPMI containing 1 ng/mL SYTOX (Invitrogen). Tumor cell death was recorded as the time when the tumor cell membrane was permeabilized and the cells produced green fluorescence using a BiostationIM cell-S1-P system (Nikon, Melville, NY). The camera captured at 7 frames/min. The intensity of fluorescence in each tumor cell was recorded using live cell imaging software (Nikon) over a period of 15 hours.

2.16 Intracellular IFN-γ assay: HERV-K env-specific CAR^+ T cells were co-cultured with tumor cells at 10: 1 ratio in a round bottom 96 well plate with 200 μL of complete RPMI culture medium. Protein transport inhibitor (BD Golgi Plug containing Brefeldin A) was added to trap IFN-γ inside the cell. The co-culture was incubated for 4 hours at 37°C and then stained for HERV-K env-specific CAR expression for 20 minutes at 4°C. The cells were then washed, fixed, and permeabilized with 100 μL of Cytofix/Cytoperm buffer (catalog # 555028, BD Biosciences) for 20 minutes at 4°C. The permeabilized cells were then stained for the cytokine with anti-IFN-γ APC conjugated mAb. The cells were washed and analyzed by FACSCalibur (BD Biosciences). PMA (phorbol 12 myristate 13 acetate) and ionomycin (BD Biosciences) treated T cells were used as positive control. A similar assay was performed with no DNA control T cells.

2.17 Immunoprecipitation: 10 billion cells were grown and lysed using RIPA buffer containing protease inhibitor (Roche Applied Science, San Francisco, CA) and pre-cleared overnight with protein A beads at 4°C. The beads were then removed and the supernatant was incubated for 3 hours with HA-tag antibody at 4°C. At the end of incubation, 40 µl of protein A beads were added and incubated again for 1 hour at 4°C. The beads were then spun down at very low speed for 1 minute and washed two times with cold PBS. These beads with the antibody-antigen complex were boiled with SDS and ran on 4-20% SDS PAGE. The gel was stained with commasie blue and submitted for mass spectrometric analysis.

2.18 Confocal microscopy: Ten million cells were stained for intracellular expression of HERV-K env using 6h5 mAx and IgG4 Fc-FITC antibodies. The cell membrane was perforated using Cytofix/Cytoperm buffer for 20 minutes at 4°C followed by a 30 minutes block with goat IgG. The cells were spun on to the positive side of a microscope slide at 1000g for 1 minute. The stained sample was then visualized using OMX microscope (Applied Biosystems) using an oil immersion 100X/1.4NA objective lens magnification. The images were captured as z-stacks spanning 12 µm of the cell above and below the mid-point using Photometrics EMCCD.

2.19 Concentration of HERV-K env from conditioned tumor cell culture supernatant: 10 million cells were plated in two T-75 flasks (if adherent) or one T-75 (if cells are in suspension) in RPMI media without FBS or glutamax for 32 hours. The supernatant was then harvested and passed through a 0.45 µm cell filter to remove debris and concentrated at

1000g for 10 minutes using 100 kDa cutoff centrifugation filter (EMD Millipore, Billerica, MA).

2.20 Spinfection: 150 μL of concentrated tumor cell culture supernatant was plated with 10^6 EL4 parental cells in a 48 well plate. The plate was then subjected to centrifugation at 1000g for 90 minutes at room temperature.

2.21 Western blot analysis: All immunoblot assays were performed with 6H5 mAb instead of 6H5 mAx since the latter could not recognize denatured antigen. Ten million tumor cells were lysed with RIPA buffer containing protease inhibitor (Roche Applied Science, San Francisco, CA). Alternatively, concentrated cell culture supernatant from A888, A375, A375-SM, AaPC, and EL4 was also performed. Bicinchoninic acid assay (BCA) was used to detect protein concentration (Thermo Scientific Pierce). A 4 to 20% gradient gel (Biorad, Hercules, CA) was used to analyze 10 μg of protein boiled in 1X SDS-sample loading buffer (Bio-Rad). The protein was then transferred to a nitrocellulose membrane and blocked with 5% non-fat dry milk in phosphate buffered saline with 0.1% tween 20 and incubated with 6H5 HERV-K antibody (1 mg/mL). Binding was detected by goat anti-mouse Fc-HRP (catalog # 170-6516, Bio-Rad) and developed using ECL West femto substrate (Thermo Scientific Pierce). The blot was imaged using Versa doc Quantity one software (Bio-Rad).

2.22 *In vivo* CAR$^+$ T cell and tumor cell activity measurement by photon quantification: 5 week old female NOD.Cg-*Prkdc*^{scid}*Il2rg*^{tm1wjl}/SzJ (NSG, Jackson Laboratories, Bar Harbor, ME) mice were intravenously injected with 10^6 A375-SM-RmK cells on Day 0 [155]. Mice in the treatment cohorts (n = 7) received $2x10^7$ HERV-K env-specific CAR$^+$ ffLuc$^+$ T

cells on Days 7, 14 and 21. $6x10^4$ U IL-2 (eBioscience) was injected intraperitonealy (IP) on day of each T-cell infusion and twice on the day after. One cohort of mice (n = 6) bearing the tumor received no treatment while a control group of mice (n = 5) without tumor received a similar number of CAR^+ T cells as in treatment group. Bio luminescence imaging (BLI) on mice in anterior-posterior position was performed weekly using a Xeno IVIS 100 series system (Caliper Life Sciences, Alameda, CA) to reveal the distribution and quantity of tumor and T cells as previously described [156]. Mice were anesthetized and placed in for BLI. To measure the HERV-K env-specific CAR^+ffLuc^+ T-cell activity 150 μL (200 μg /mouse) of D-Luciferin potassium salt (Caliper Life Sciences) was injected IP. Ten minutes after injection emitted photons were quantified using the Living Image 2.50.1 (Caliper Life Sciences) program. To image the tumor cell activity 100 μL (60 μM final concentration) of EnduRen (Promega, Fitchburg, WA) was injected IP. 20 minutes after injection the tumor activity was quantified similar to ffLuc. Unpaired Student's *t*-test was performed to establish statistical significance of the photon flux. The livers from the tumor alone and treatment groups were isolated on day 25 and imaged directly for mKate expression using a Leica M205FA stereo microscope and quantified for the number of metastatic foci present in each liver.

2.23 Genetic modification of cell lines

- **HERV-K env^+ EL4 cells:** Two million mouse T cell lymphoma EL4 parental cells were suspended in the mouse T-cell nucleofector solution (catalog # VPA-1006, Lonza). HERV-K env-expressing SB transposon with bi-directional promoter and SB11 transposase (2 μg of supercoiled DNA) were added to a final volume of 100

μL which was transferred to a single cuvette and electroporated using the C-09 program. The cells were rested for 4 hours at 37°C in electroporation media supplemented with 10% FBS (Thermo Scientific Pierce). The cells were then transferred to DMEM supplemented with 10% FBS (Thermo Scientific Pierce) and 5% glutamax (Gibco Life technologies). Cells were cultured in the presence of 0.8 mg/mL G418, and neomycin-resistant HERV-K env$^+$ EL4 cells were sorted using HERV-K antibody.

- **HERV-K SU-Fc-CD8$^+$ EL4 and IgKL HERV-K SU-Fc-CD8$^+$ EL4:** One million EL4 cells in a 24-well plate were transduced with 100 μL HERV-K SU Fc-CD8 or IgKL HERV-K SU-Fc-CD8 lentiviral particles along with 5 mg/mL polybrene (Sigma-Aldrich). The plate was spun at 1000g for 90 minutes at room temperature and incubated for 4 hours at 37^{o}C. The cells were grown in DMEM, 10% FBS (Thermo Scientific Pierce) and 5% glutamax (Gibco Life technologies). The cells were bulk sorted for 100% pure mKate$^+$ population using a FACS cell sorter (BD Biosciences) to obtain a homogenous population.
- **A375-SM-RmK:** One million A375-SM cells in a 24-well plate were transduced with 100 μL mKate-rRLuc lentiviral particles along with 5 mg/mL polybrene (Sigma-Aldrich). The plate was spun at 1000g for 90 minutes at room temperature and incubated for 4 hours at 37^{o}C. The cells were grown in DMEM, 10% FBS (Thermo Scientific Pierce) and 5% glutamax (Gibco Life technologies). The cells were bulk sorted for 100% pure mKate$^+$ population using a FACS cell sorter (BD Biosciences) to obtain a homogenous population.

Chapter 3: Results

3.1 Tumor-specific expression of HERV-K env on primary melanoma

The 6H5 HERV-K env-specific monoclonal antibody (mAb) [157] was used in immunohistochemistry (IHC) to investigate expression of the HERV-K env protein. Initially, we evaluated melanoma tumor-cell lines A888, A624, A375, A375-super metastatic cells (SM) that are highly metastatic upon passage in mice [155], and K-562 parental cells. The 6H5 mAb revealed the presence of full length HERV-K env represented as a single band on western blot at 66 kDa under reducing conditions which was absent in the mouse parental EL4 T-cell line (**Figure. 6A**) [157]. This mAb was used to interrogate expression of HERV-K env on and in primary and metastatic melanoma and normal skin. Punctate cell surface expression (solid arrow) and diffuse cytoplasmic staining (dotted arrow) were observed in tumor cells in a mutually exclusive manner (**Figure. 6B**). IHC staining (scored from 0 to 3) was graded based on intensity of staining for HERV-K env (**Figure. 6C**). An H-index was calculated by multiplying the percentage of HERV-K env$^+$ cells with the intensity of staining compared to the isotype control [158]. The average H-index for melanoma was 9.2 (n = 220, standard error of mean (SEM) = 2.4) which was 206-fold greater ($p < 0.001$) than normal skin (H-index = 0.045, n = 55, SEM = 0.03; **Figure. 7A**). The average H-index calculated for metastatic tissues (10.65, n = 84, SEM = 3.9) was greater than that for primary tissues (8.4, n = 136, SEM = 3.0) though this did not reach statistical significance ($p = 0.07$) (**Figure. 8A**). HERV-K env was observed on tumor cells originating from multiple anatomical sites (**Figure. 8B**). To determine whether HERV-K env expression was restricted to tumor cells, tissues from 33 types of healthy organs from three different donors were

assessed by IHC. Though we observed HERV-K env mRNA expression in normal human samples (cDNA pooled from three independent donors) (**Figure. 9**) we observed an apparent absence of HERV-K env expression on all of these normal tissues (**Figure. 10**). These data support our contention that HERV-K env is a TAA and that as it is expressed on the cell surface it may be targeted by HERV-K env-specific CAR^+ T cells.

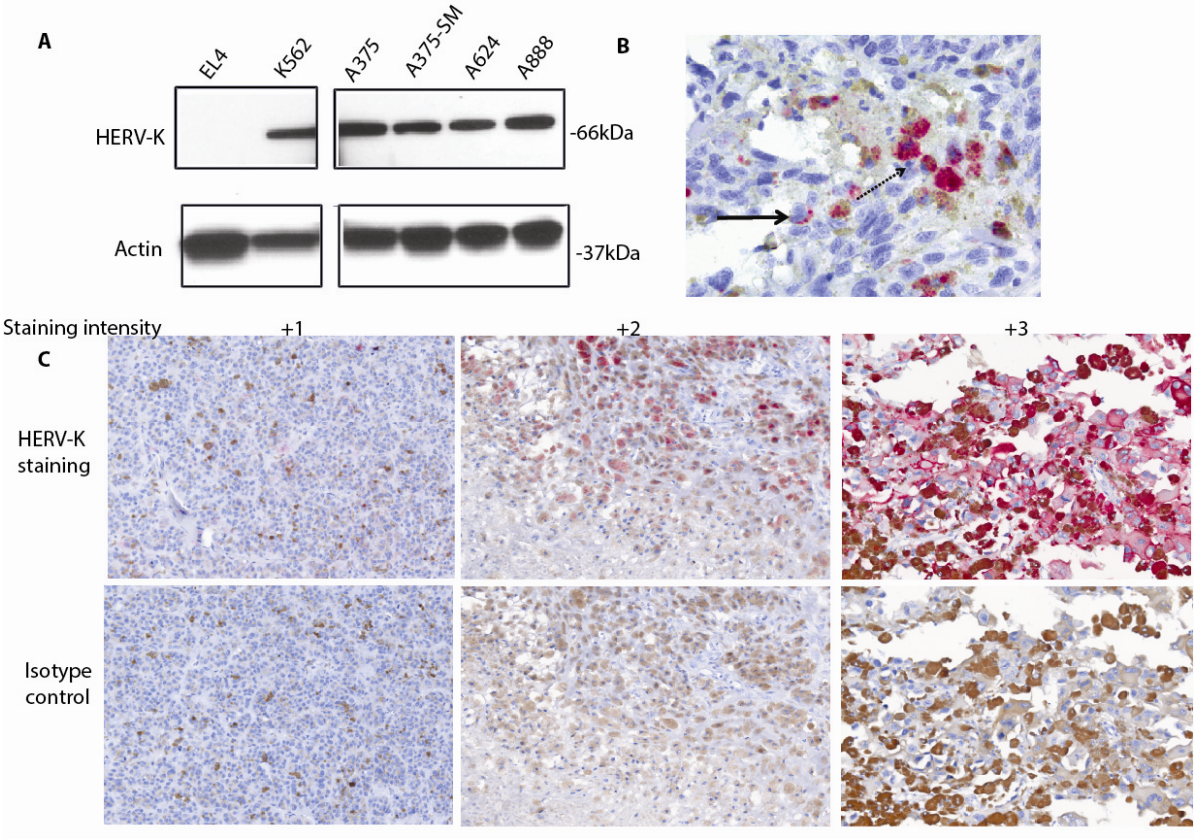

Figure. 6: (**A**) Immunoblot analysis of HERV-K env from K-562 parental, EL4 parental, A375, A375-SM, A624 and A888 cells. Actin protein expression was used as a control for protein loading. A representative blot from three independent assays is shown. (**B**) Tumor cells (400X) showing HERV-K expression on cell membrane (punctate pattern; solid arrow) or cytoplasmic staining (diffuse pattern; dotted arrow). **C**) Representative images of tumor cells (200X) with varying staining intensity (scored 0 to 3) of HERV-K env expression (top panel) when compared to isotype IgG2a control staining (bottom panel).

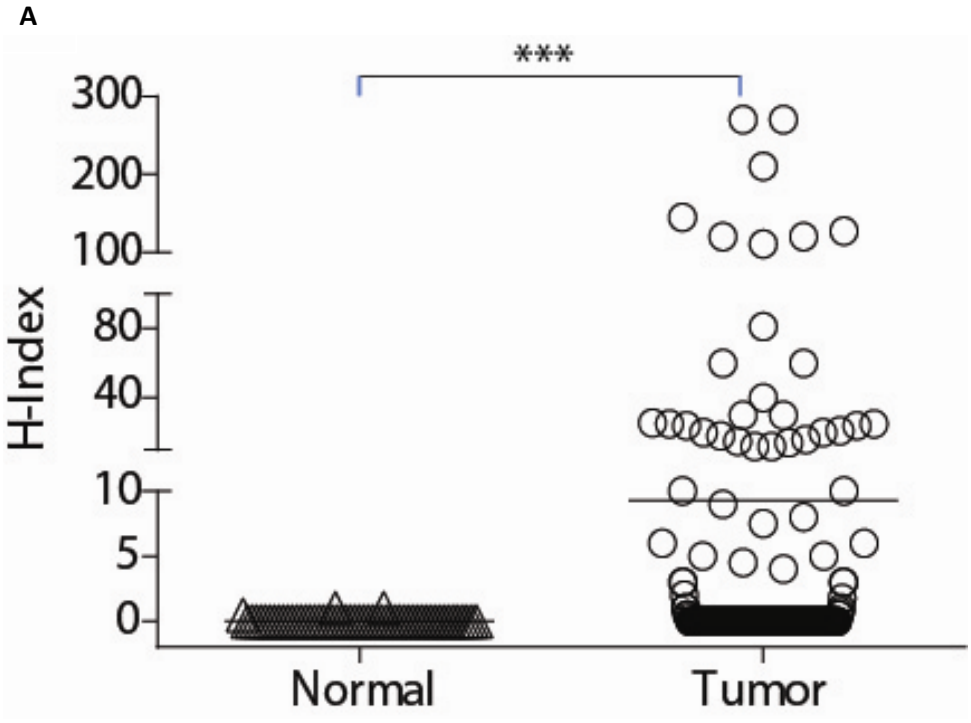

Figure. 7: (**A**) A dot plot representing H-index (measured as product of intensity of staining by percent HERV-K env^{+} tumor cells) of normal tissue (n = 55) and melanoma primary tumor samples (n = 220). Each dot in the dot plot represents an individual donor; unpaired Student's t-test with Mann-Whitney post-test; ***$p < 0.001$.

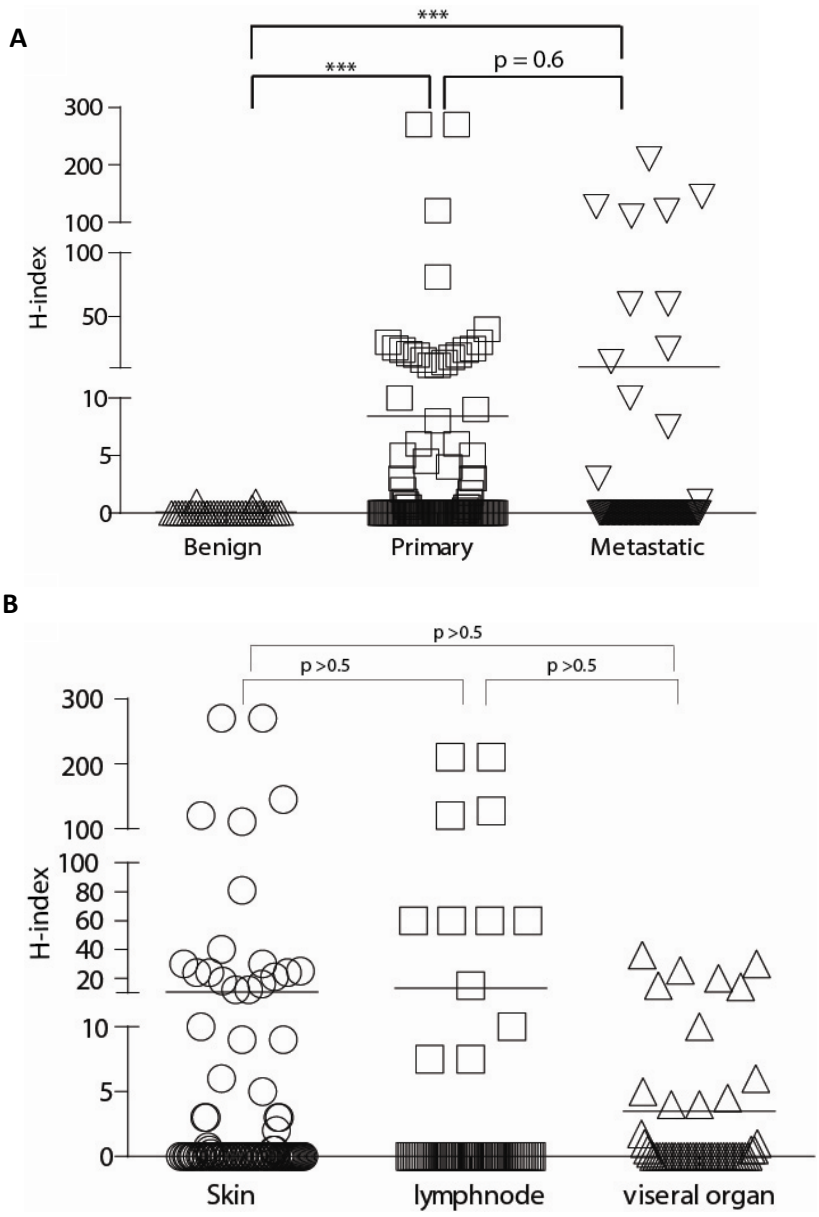

Figure. 8: (**A**) H-index of benign, primary and metastatic tumors. (**B**) H-index of patient-derived malignant tissues are shown. Each symbol in the dot plot represents an individual donor; unpaired Student's t-test was with Mann-Whitney post-test; ***$p < 0.01$.

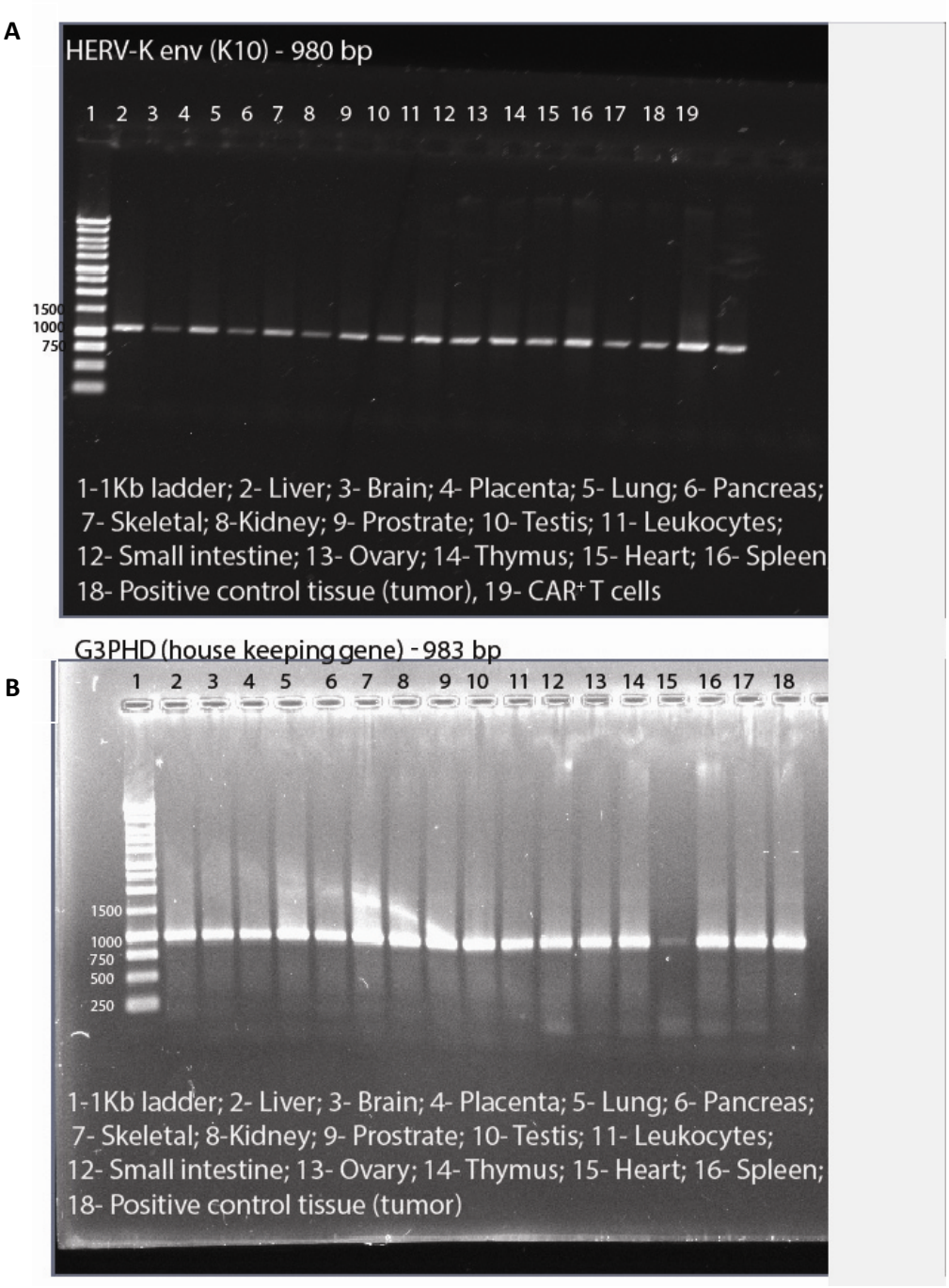

Figure. 9: (**A**) RT- PCR bands representing mRNA expression of HERV-K env 108 in normal human tissues. (**B)** RT- PCR bands representing mRNA expression of housekeeping gene (G3PHD) in normal human cells. All experiments had (cDNA pooled from three independent donors and the experiment was repeated thrice.

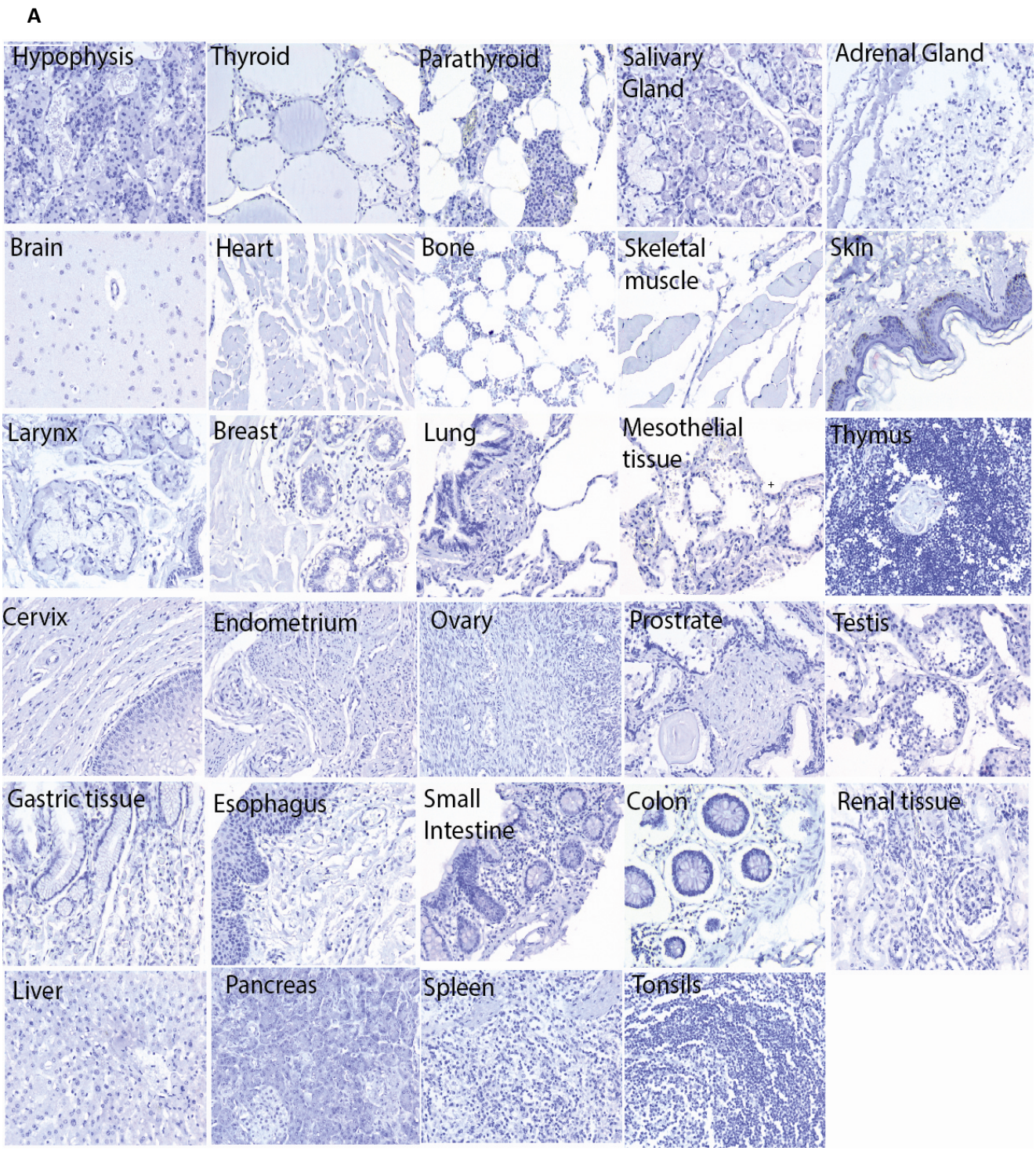

Figure. 10: Representative pictures (200X) of HERV-K env antigen expression on tissues sections from 29 normal organs are seen. The H-index was calculated as zero since no staining was observed in these tissues.

3.2 Generation and characterization of HERV-K env-specific CAR derived from 6H5 mAb

We engineered a CAR with specificity for HERV-K env based upon the V_H (at amino terminus) and V_L domains derived from the 6H5 mAb which were joined via Whitlow linker to form a single chain variable fragment (scFv). This was fused in frame to a modified human IgG4 hinge/Fc [159] stalk, CD28 transmembrane domain, and a combination of CD28 and CD3ζ intracellular domains. This design is similar to our 2nd generation CD19-specific CAR (designated CD19RCD28) currently employed in clinical trials [149]. We stably expressed this CAR on T cells derived from peripheral blood mononuclear cells (PBMC) using the SB transposon/transposase system (**Figure. 11A**). HERV-K env-specific CAR^+ T cells were then selectively propagated on AaPC [160] (designated clone 4) derived from K-562 cells which expresses endogenous HERV-K env and were previously genetically modified by lentivirus transduction to co-express CD64, CD86, CD137L, and a first-generation membrane-bound IL-15 (**Figure. 11B**) [149]. Control T cells from PBMC were (i) mock electroporated without DNA ("no DNA control") and expanded on AaPC clone 4 pre-loaded via transgenic CD64 with a CD3-specific mAb (OKT3) and (ii) CD19-specific CAR^+ T cells generated per published method for our clinical trials [149]. 95% of the electroporated/propagated T cells stably expressed the HERV-K env-specific CAR on their cell surface after 28 days of co-culture with AaPC in the presence of soluble recombinant IL-2 and IL-21 (**Figure. 12A**). Compared with CD19-specific CAR^+ T cells, no appreciable difference was seen in (a) growth kinetics of HERV-K env-specific CAR^+ T cells (**Figure. 12B**), (b) percentage outgrowth of $CD3^+CAR^+$ T cells (**Figure. 12C**), or (c) ratio of CD4 to CD8 T cells (**Figure. 12D**). The average copy number of integrated transposon was 1.6 (n =

3, standard deviation (SD) = 0.03) per T-cell genome (**Figure. 13A**) which is less than that reported after virus-mediated transduction of T cells to express a CAR [161]. We evaluated the therapeutic potential of the T cells (n = 4) using multi-parameter flow cytometry which revealed the percentage of CAR^+ T cells with naive ($CD45RO^{neg}CD45RA^+CD28^+$; mean 7.79 ± SD 2.3), central memory ($CD45RO^+CD45RA^{neg}CD28^+$; 12.02 ± 10.4), effector memory ($CD45RO^+CD45RA^{neg}CD28^+$; 87.9 ± 10.9) and effector memory RA phenotypes ($CD45RO^{neg}CD45RA^+CD28^+$; 91.04 ± 3.4) (**Figure. 13B**). These effector memory T cells were further characterized as $CD27^+CCR^{neg}$ (33.22% ± 24) similar to our previous reported data for CD19-specific CAR^+ T cells (not shown) [162]. We observed the outgrowth of granzyme-B^+ HERV-K env-specific CAR^+ T cells (98.17% ± 2.3, n = 4) suggesting that these cells should be cytotoxic (**Figure. 13C**). In addition to flow cytometry, we employed a set of 500 bar-coded probes to digitally count mRNA molecules to reveal selected gene expression. Compared to no DNA control T cells (n = 3), the HERV-K env-specific CAR^+ T cells (n = 3) had significantly ($p < 0.5$) increased levels of mRNA species coding for (a) chemokines and receptors (CCR1, CCR5, CCL3 and CCL4) [163], (b) transcriptional regulators (LRP5, PAX5, TCF7) (c) T-cell activators (CD80, RORA, KIR3DL2) and (d) genes participating in lysis (perforin1 and granzyme H) suggesting that the HERV-K env-specific CAR^+ T cells are capable of producing an effective response against the target TAA (**Figure. 14**). In aggregate, these data demonstrate that T cells could be modified with the SB system to express a CAR from 6H5 and propagated on HERV-K env^+ AaPC generating a biologic product with therapeutic potential for melanoma.

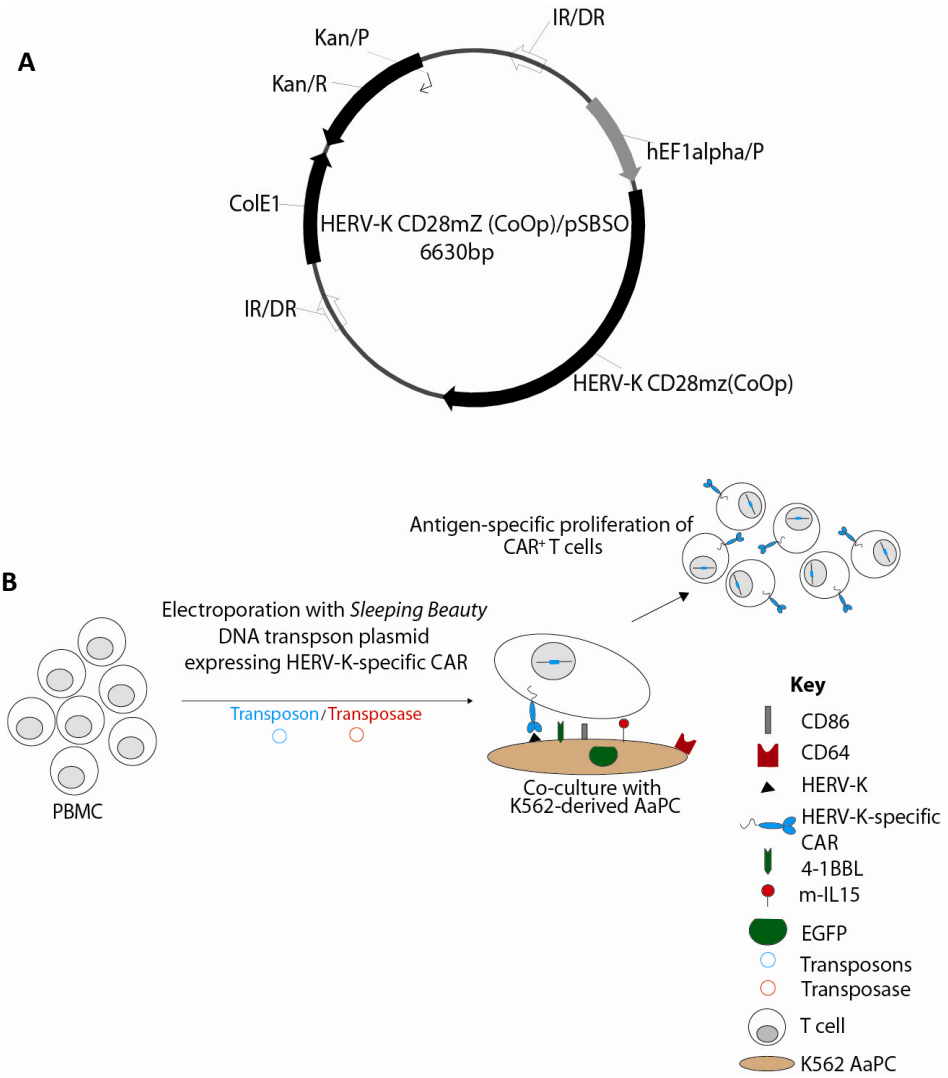

Figure. 11: (A) Generation of HERV-K env-specific CAR$^+$ T cells: (**A**) SB-derived DNA transposon (HERV-K CD28mZ (CoOp)/pSBSO) designed to express HERV-K env-specific CAR. Abbreviations: IR/DR: inverted repeat/direct repeat, hEF-1alpha/p: human elongation factor-1α hybrid promoter, HERV-K CD28mZ (CoOp): codon-optimzed HERV-K envelope scFv, ColE1: *E. coli* origin of replication, Kan/R: kanamycin resistance, Kan/p: kanamycin resistance promoter. PBMCs (n = 4) were electroporated with SB plasmids, HERV-K-specific CAR and SB11 transposase and co-cultured with AaPCs with cytokines. (**B**) Schematic diagram representing propagation of HERV-K env-specific CAR$^+$ T cells.

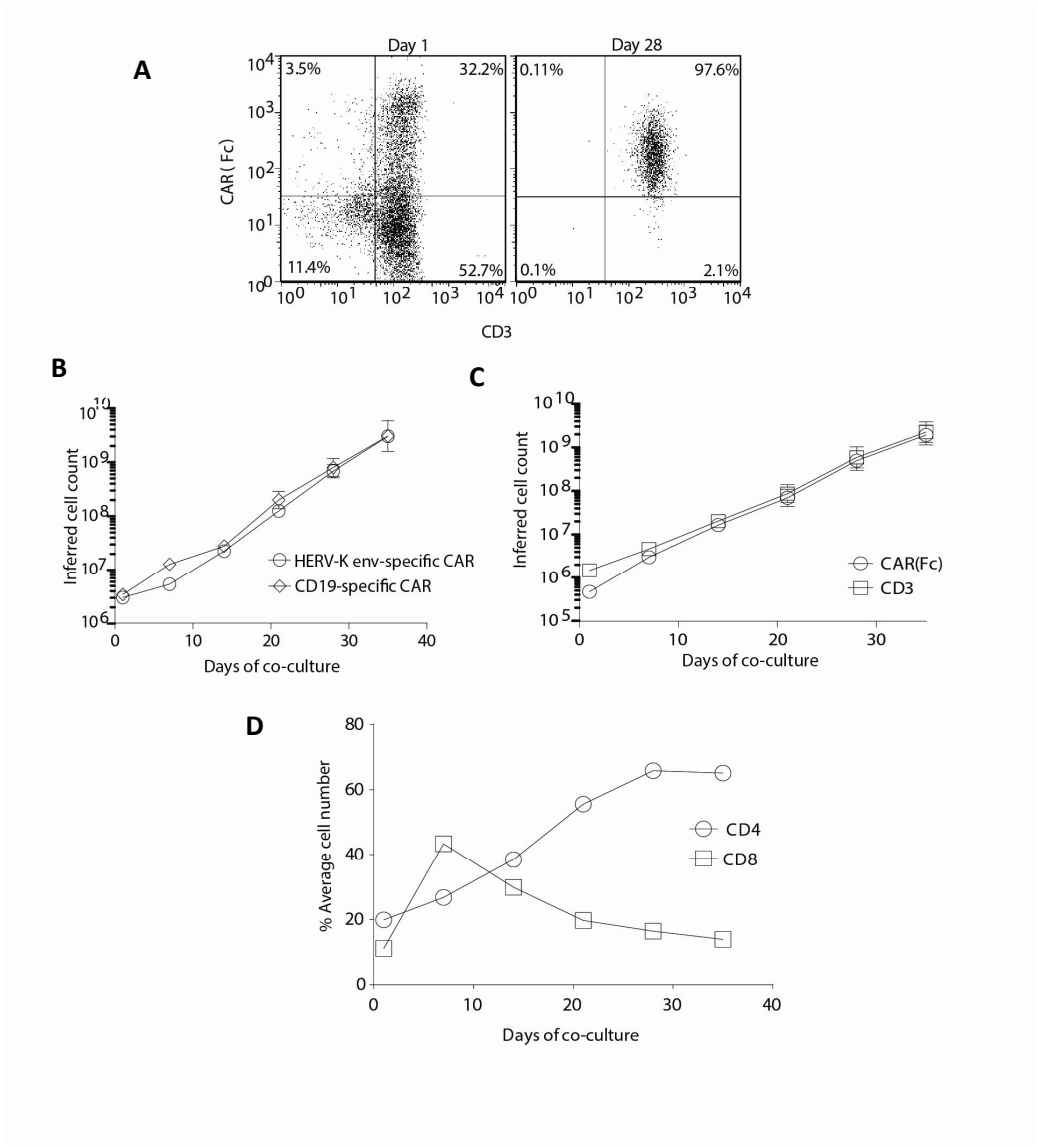

Figure. 12: (**A**) Representative flow plots of transient (day 1) and stable (day 28) CAR (binding of Fc-specific mAb) and CD3 expression on HERV-K env-specific CAR$^+$ T-cell cultures. (**B**) Rate of expansion of total HERV-K env-specific CAR$^+$ T cells and CD19-specific CAR$^+$ T cells propagated on aAPC and cytokines. There was no difference in the kinetics of expansion. (**C**) Rate of expansion of CD3$^+$ and CAR$^+$ HERV-K env-specific T cells propagated on aAPC and cytokines. (**D**) Average growth of CD4$^+$ versus CD8$^+$ HERV-K env-specific CAR$^+$ T cells is shown (n = 4).

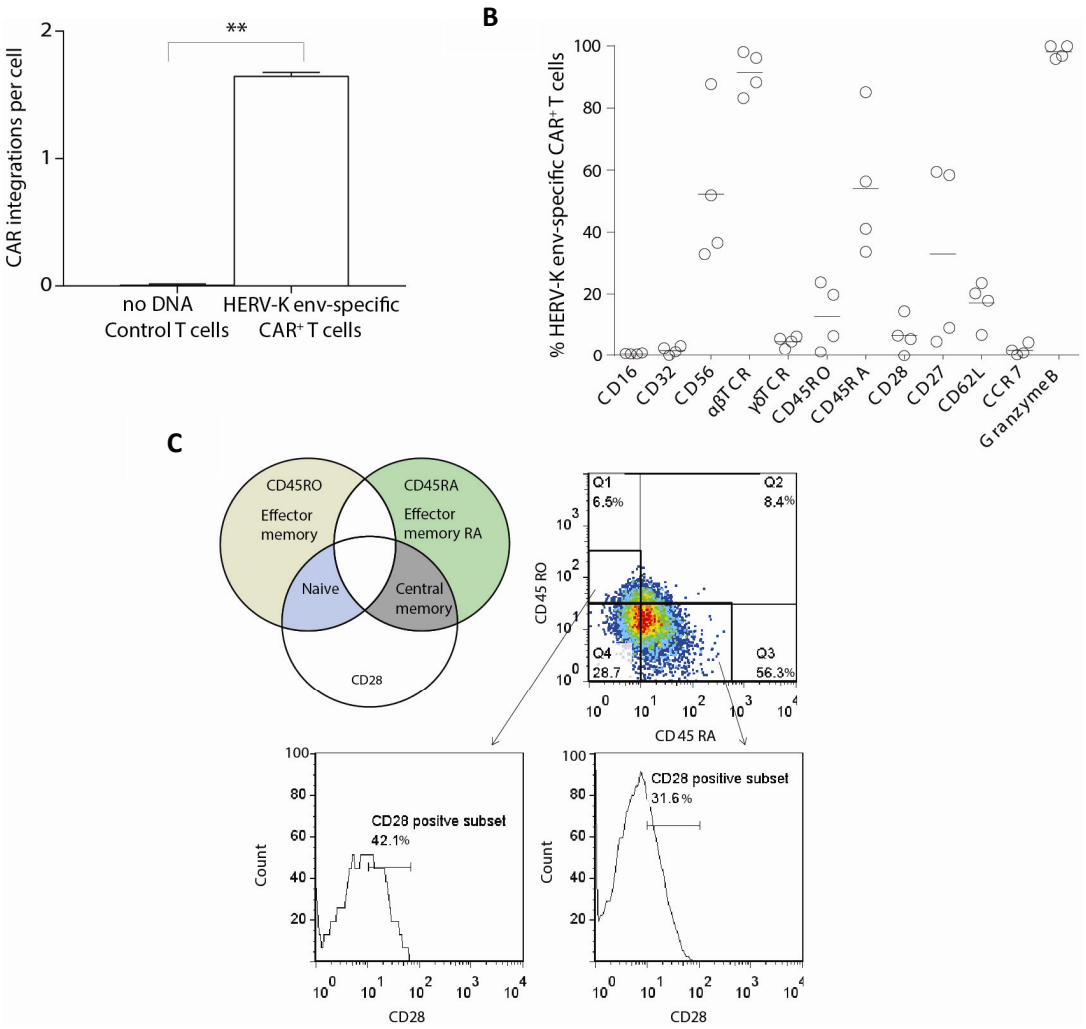

Figure. 13: (**A**) Measurement of the copy number of CAR (transposon) in T-cell genome after electroporation and propagation. (**B**) Multiparameter flow cytometry to evaluate the phenotype of HERV-K env-specific CAR^+ T cells. Each symbol represents an individual donor and the horizontal line represents the mean. (**C**) Venn diagram representing various subtypes of T cells using CD45RA, CD45RO and CD28. Representative flow plot (n = 4) of effector memory phenotype of CAR^+ T cells on day 28 after electroporation and propagation. CAR^+ T cells were co-stained with CD45RA, CD45RO and CD28 markers. Flow plot was analyzed for CD45RA and CD45RO and each subset was further gated and analyzed for CD28 expression. Data represented as mean ± SD (n = 3).

A

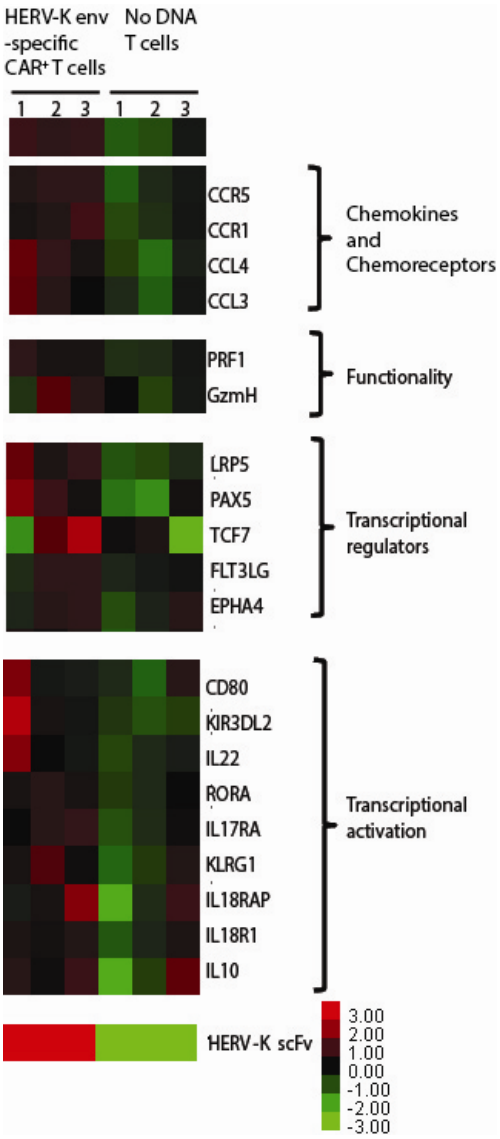

Figure. 14: Digital gene expression analyses of HERV-K env-specific CAR^{+} T cells as compared to no DNA control cells. The intensity of green in the heat map reveals 0-3 fold increased gene expression while intensity of red reveals 0-3 fold reduction in expression of sets of genes ascribed to the cytokine, chemokine, transcriptional regulator and T-cell activator family.

3.3 Generation and characterization of HERV-K env-specific maxibody derived from 6H5 mAb

To help define the specificity of the CAR derived from 6H5, we generated a soluble version of this immunoreceptor as a maxibody (mAx) [164]. The HERV-K env-specific 6H5 mAx consisted of the 6H5 scFv (used to generate the CAR) fused to full-length human IgG4 using the same modified hinge and Fc region employed in the CAR construct (**Figure. 15A-B**). We evaluated cell-surface expression of HERV-K env on EL4, AaPC clone 4, A888, A375-SM and A624 cells using 6H5 mAb (**Figure. 15C**) and 6H5 mAx (**Figure. 15D**). There was a positive trend between the H-indices calculated using 6H5-derived mAb and mAx at three different time points (days 1, 2, and 3 after plating the cells on day 0; spearman correlation coefficient, $\rho = 0.5$, $p = 0.06$) (**Figure. 16A**) indicating that these two soluble species apparently recognize the same TAA. We also performed an ELISA and observed a comparable level of binding of 6H5-derived mAb and mAx to plate-bound purified recombinant HERV-K env antigen (designated K10) [157] (**Figure. 16B**). CD19-specific mAb and plate-bound CD19 antigen were used as a negative control (**Figure. 16C**). As both soluble reagents inhibit the binding of each other, the mAb and mAx thus appear to bind to a shared epitope on K10 (**Figure. 16D**). Taken together, the 6H5-derived mAb and mAx, appear to recognize HERV-K env lending support to the concept that the CAR expressed on T cells will also recognize this TAA in an antigen specific manner.

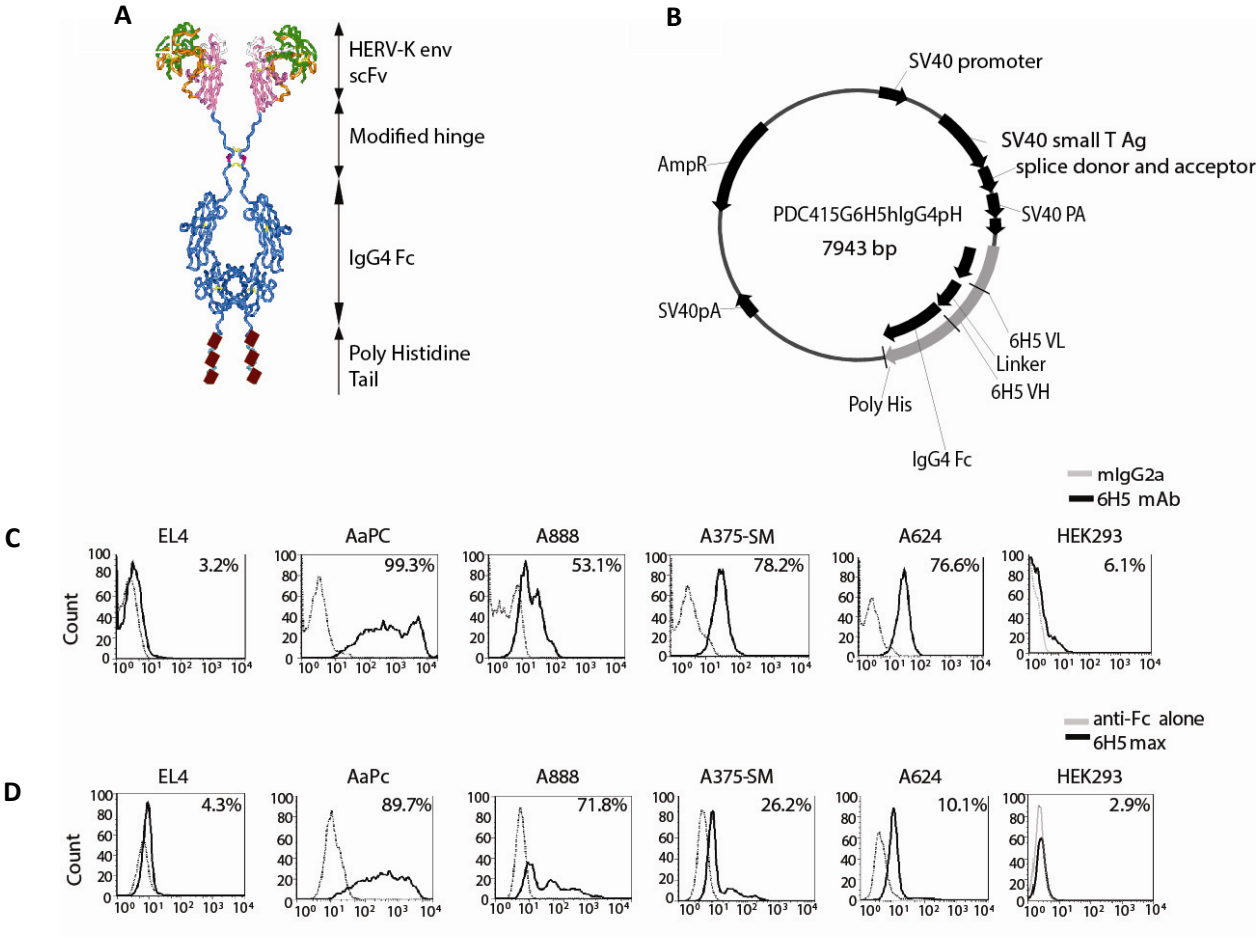

Figure. 15: Comparison of 6H5 mAb versus 6H5 mAx: (**A**) A representation of 6H5 mAx. (**B**) Lentiviral plasmid encoding HERV-K env-specific 6H5 mAx. (PDC4156H5hIgG4pH) to co-express truncated HERV-K scFv and a polyhistidine tag for protein purification. Abbreviations: SV40: simian vacuolating virus 40 promoter, SV40 small T Ag: SV40 small T antigen, SV 40 pA: SV40 polyadenylation signal, 6H5 V_L: 6H5 variable light chain, linker: Whitlow linker, 6H5 V_H: variable heavy chain, Poly His: Polyhistidine, AmpR: ampillicin resistance domain. Histograms representing surface antigen expression of HERV-K env using (**C**) 6H5 mAb (black) and (**D**) 6H5 mAx (black). Isotype (grey) and secondary antibody (grey) were used as controls.

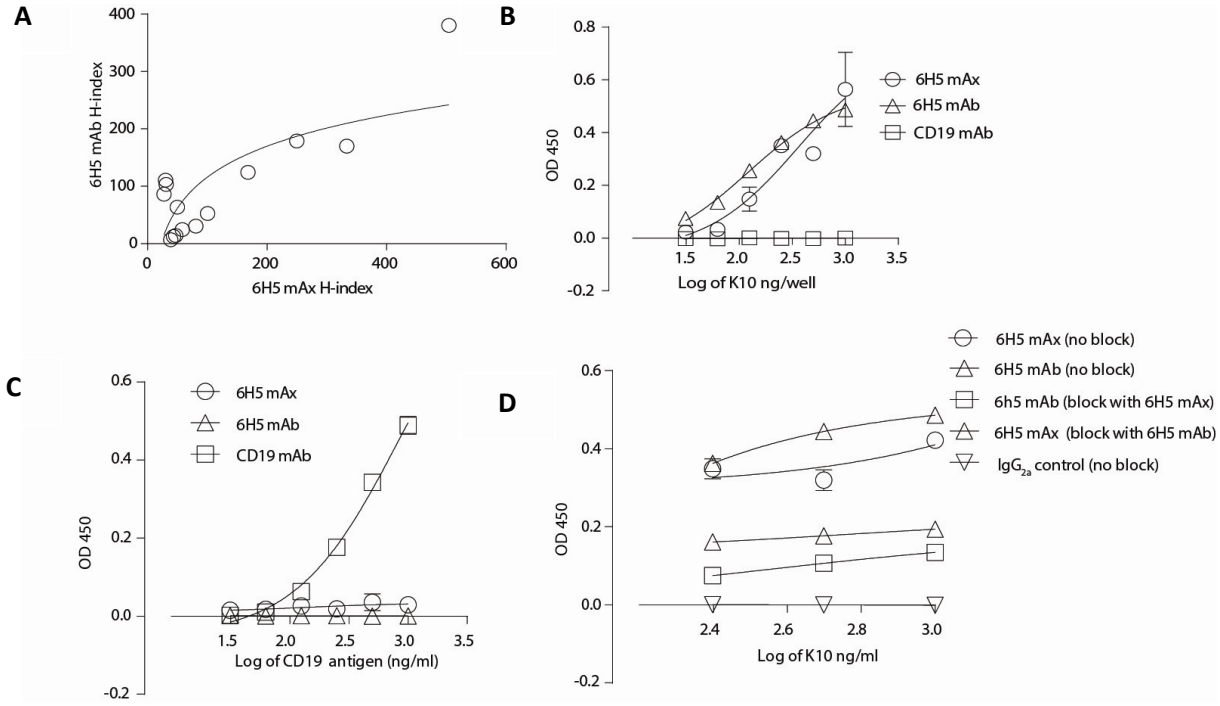

Figure. 16: (**A**) Correlation plot between tumor cell surface (A888, A624, A375, A375-SM, EL4) H-indices of 6H5 mAb or 6H5 mAx staining of tumor cells grown at three different time point with varying cell density (Spearman correlation coefficient ρ = 0.5033, p = 0.067). (**B**) Binding of 6H5 mAx and 6H5 mAb to purified HERV-K env (K10) protein by ELISA. CD19 mAb was used as negative control. H-index was calculated as product of intensity of HERV-K env staining (MFI) on tumor cell surface and percent tumor cells positive for antigen expression. (**C**) ELISA showing the binding of CD19-specific mAb to CD19 and 6H5 mAb and 6H5 mAx not binding to CD19. (**D**) ELISA representing the binding of 6H5 mAx or 6H5 mAb to K10. Pre-incubation of K10 coated plate with 6H5 mAx blocked 6H5 mAb binding and vice versa suggesting the epitope sharing between the two. IgG2a mAb was used as a negative control mAb. ELISA data represents mean ± SD from average of triplicate measurements that were pooled from two independent experiments.

3.4 Specificity of CAR$^+$ T cells for HERV-K env

The redirected effector function of CAR$^+$ T cells was evaluated to establish specificity for HERV-K env. We modified HERV-K env^{neg} EL4 cells to express HERV-K env (**Figure. 17A**) to serve as targets (**Figure. 17B**). HERV-K env-specific CAR$^+$ T cells specifically killed HERV-K env$^+$ EL4, but not parental EL4 cells (**Figure. 17C**). To further test the specificity of the HERV-K-specific CAR, a lentivirus encoding HERV-K env-specific shRNA was transduced into A888 cells (to generate A888 knockdown KD) **(Figure. 18A**) Immunoblot analysis showed a decrease of approximately 50% HERV-K expression compared to a scrambled shRNA control (Fig4B). Using a CRA, we observed a 3 fold and 2.7 fold decrease in killing of A888 and A888 transduced with scrambled shRNA compared to HERV-K transduced with HERV-K-specific shRNA, respectively. ($p < 0.05$; HERV-K-specific CAR$^+$T cell effectors) **(Figure. 18B**).

HERV-K env-specific CAR$^+$ T cells also mediated lysis of melanoma cells expressing endogenous HERV-K env. Compared to control no DNA control T cells, killing of melanoma cell lines A888, A624, A375, A375-SM, which are recognized by 6H5, was significantly greater using HERV-K env-specific CAR$^+$ T cells ($p < 0.001$) (**Figure. 19A**). CD19-specific CAR$^+$ T cells served as an additional negative control and failed to lyse A888 and A624 tumor cells above background (**Figure. 19B)**.

Although the cell surface expression of HERV-K env varied at different time points during cell culture (days 1, 2, and 3 after plating the tumor cells on day 0) as assessed using 6H5mAx by flow cytometry (**Figure. 19C**), we observed a positive correlation between lysis of melanoma cell lines by HERV-K env-specific CAR$^+$ T cells and the density of HERV-K env expression on the tumor cell surfaces as calculated using H-index on ($\rho = 0.68$, p

<0.001) (**Figure. 19D**). We also examined the redirected lysis by HERV-K env-specific CAR^+ T cells by video time-lapse microscopy (VTLM) [165,166]. The genetically modified T cells were co-cultured with HERV-K env^+ A888 or A375 tumor cells or HERV-K env^{neg} HEK293 at an effector to target (E:T) ratio of 1:5. Twenty-five target cells were individually monitored from each cell line for 15 hours and the increase in fluorescence (associated with SYTOX in the media entering damaged tumor cells and intercalating with DNA) was calculated for A888 (mean fluorescent intensity (MFI) = 445, SD = 67.8), A375 (MFI = 434, SD = 20.6) which was significantly greater than HEK293 cells (MFI = 394, SD = 19.1) (p = 0.016) (**Figure. 20A-B).** In addition to killing, we evaluated whether CAR^+ T cells could be activated for IFN-γ production upon co-culture with melanoma cells. These tumor targets were co-cultured with HERV-K env-specific CAR^+ T cells or CAR^{neg} no DNA control T cells at a 10:1 E:T ratio. Compared to control T cells, the percentage of IFN-γ^+ HERV-K env-specific CAR^+ T cells was 2.9, 5.1, 5.9, and 2.6 fold greater when incubated with A888, A375, A375-SM and A624, respectively (**Figure. 21**). These data reveal that CAR^+ T cells are activated for killing and cytokine effector functions by HERV-K env.

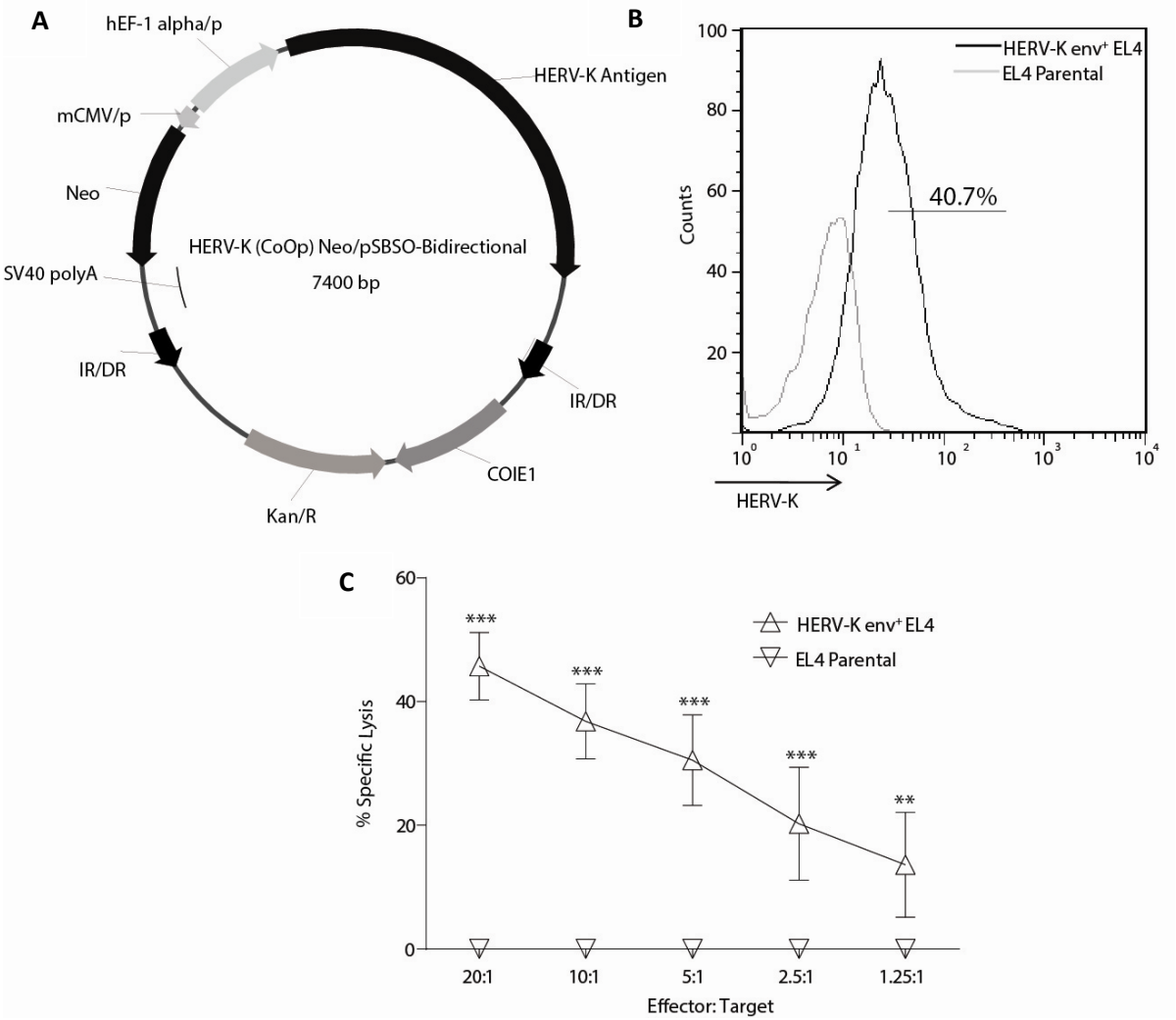

Figure. 17: (**A**) A bidirectional Sleeping Beauty DNA transposon (HERV-K (coOp) Neo/pSBSO-Bidirectional) to co-express HERV-K env full length antigen and neomycin phosphotransferase (neo) for *in vitro* selection. Abbreviations: hEF-1alpha/p: human elongation factor-1α promoter, mCMV/p: mouse cytomegalovirus promoter, Neo/r: neomycin phosphotransferase. B) Representative flow plots (n = 3) of HERV-K env expression on EL4 cells transduced with HERV-K env antigen compared with HERV-K env^{neg} EL4 parental. (**C**) A four hour CRA using HERV-K env-specific CAR^{+} T cells as effectors and either EL4 parental or HERV-K env^{+} EL4 cells as targets.

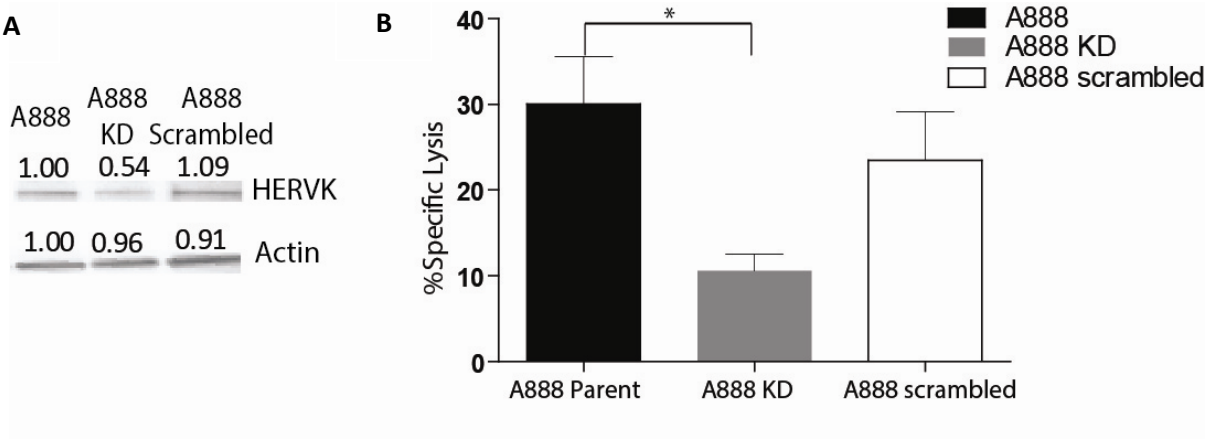

Figure. 18: (A) Immunoblot analysis of HERV-K env from A888 cells treated with HERV-K env specific shRNA (middle lane) or scrambled shRNA (right lane). Actin protein used as a loading control. **(B)** CRA using HERV-K env-specific $CAR^{+}T$ cells as effectors and A888 HERV-K env KD cells, A888 parental (A888P) and A888 scrambled cells as target.

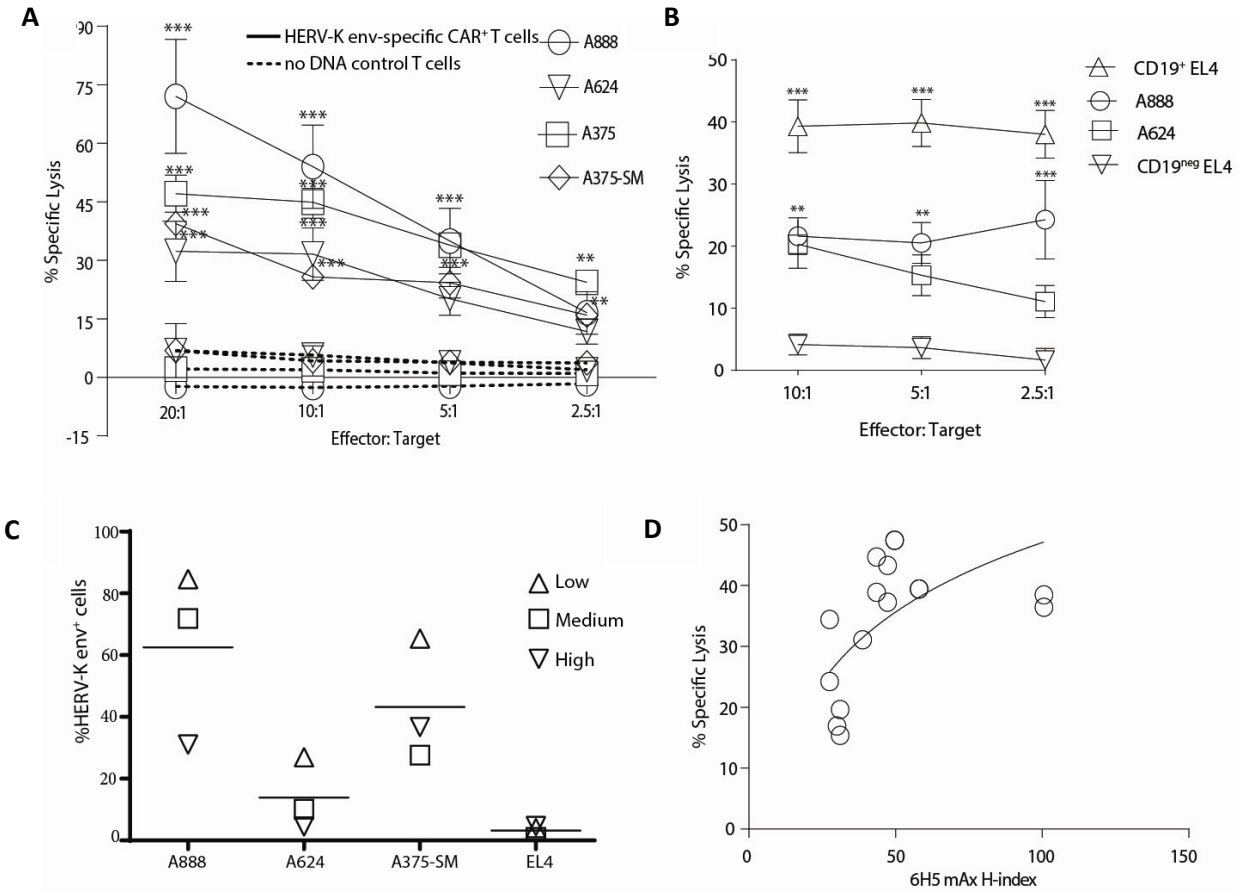

Figure. 19: (**A**) A 4 hour CRA of HERV-K env-specific CAR$^+$ T cells (solid line) compared to no DNA control T cells (dotted lines) using melanoma tumor cells as targets. (**B**) A four hour standard CRA (n = 3) using CD19-specific CAR$^+$ T cells against CD19^{neg} melanoma and CD19$^+$ EL4 tumor targets. (**C**) Percentage expression of HERV-K env protein on tumor cell surface using 6H5 mAx. Each symbol represents a low (20%), medium (50%) and high (70%) confluence in the tissue culture flask (n = 3) and horizontal line the mean. (**D**) Plot of correlation between percent ^{51}Cr release (effector: target ratio is 1:10) and H-index of tumor surface staining (A888, A624, A375) with 6H5 mAx, $\rho = 0.6895$; $p < 0.001$).

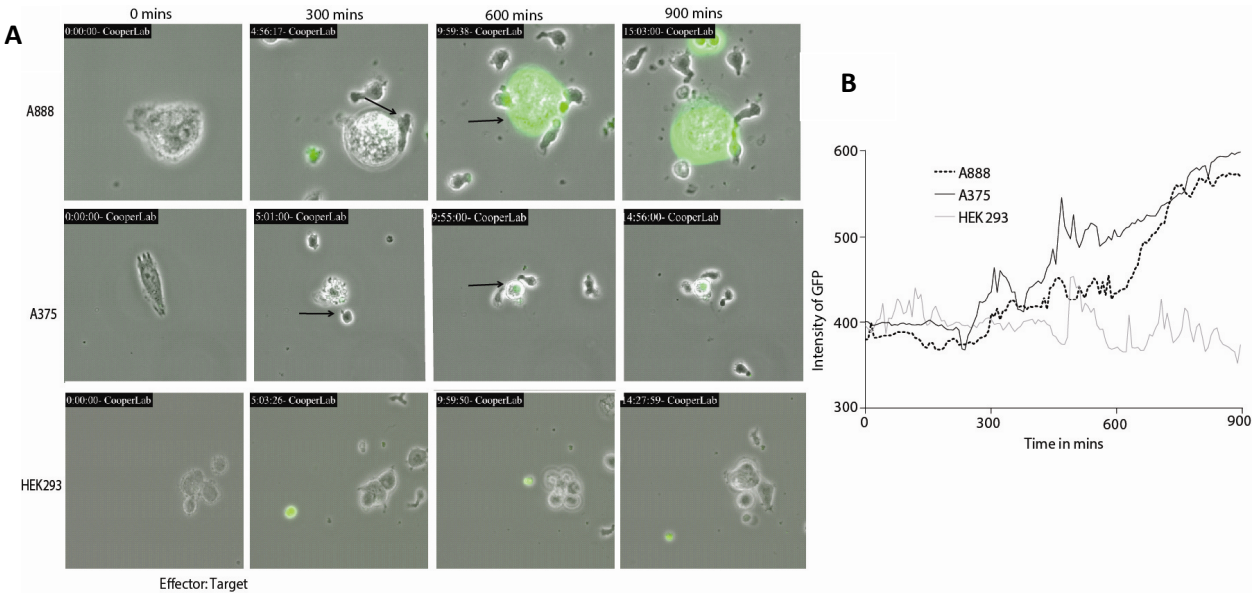

Figure. 20: (**A**) Killing of tumor targets by HERV-K env-specific CAR$^+$ T cells using VTLM. Targets were plated with CAR$^+$ T cells for 15 hours at 1: 5 ratio in the presence of SYTOX. Representative images of 25 tumor cells from two independent experiments of HERV-K env$^+$ cells (A888 and A375) or HERV-K env^{neg} control (HEK293 parent) cells co-cultured with CAR$^+$ T cells at 0, 300, 600, and 900 minutes of VTLM. HERV-K env-specific CAR$^+$ T-cell interaction with HERV-K env$^+$ tumor targets are indicated with two arrows at 300 minutes. Green fluorescence in tumor cells is indicated by two arrows at 600 minutes consistent with cell death. (**B**) VTLM to assess killing by HERV-K env-specific CAR$^+$ T cells and target cells in media with SYTOX. The intensity of the fluorescence was measured. Data represented as mean ± SD from 25 tumor cells pooled from two independent experiments.

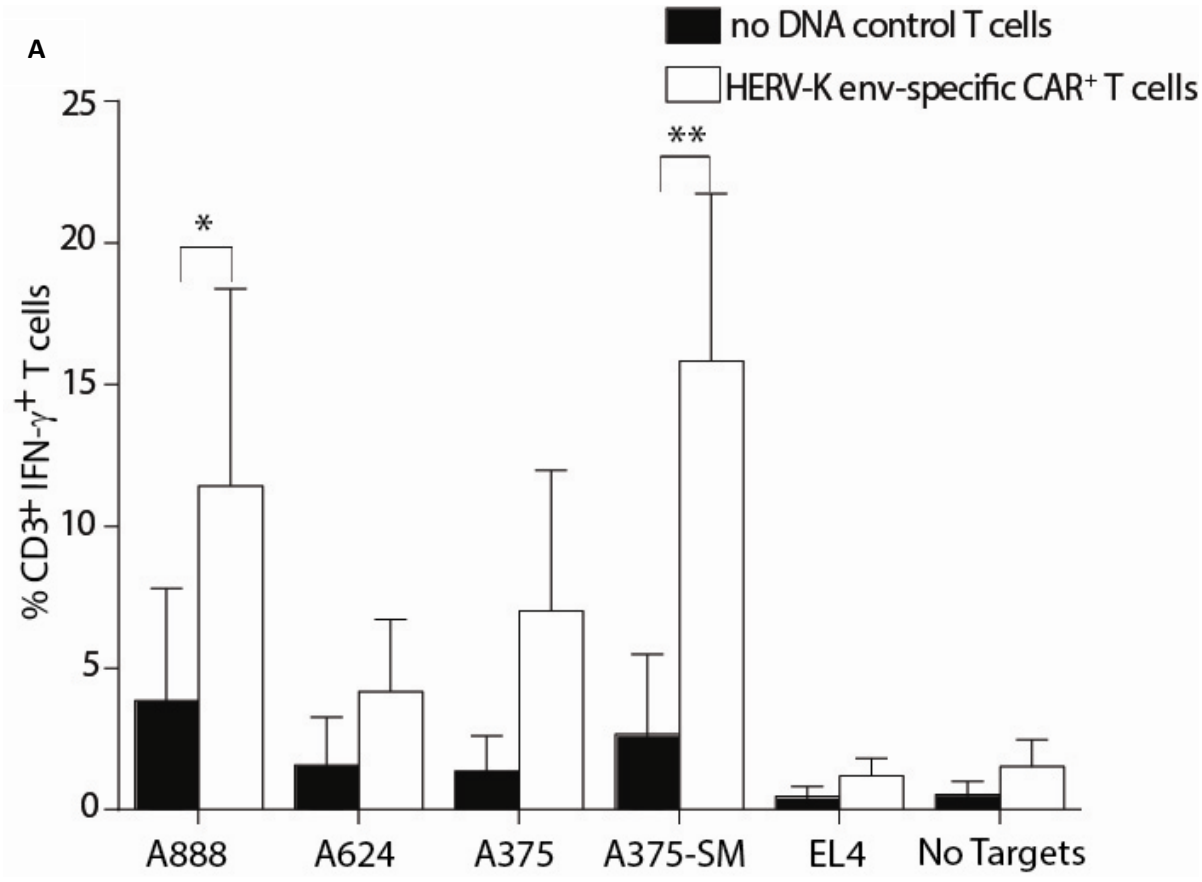

Figure. 21: (A) IFN-γ production by CAR^+ and CAR^{neg} T cells upon incubation with targets. Data represent mean ± SD from three healthy donors (average of triplicate measurements for each donor). Two way ANOVA with Bonferroni post-test was performed on CRA and IFN-γ production assay between the HERV-K env-specific CAR^+ T cells and no DNA control cells *$p < 0.05$, **$p < 0.01$ and ***$p < 0.001$.

3.5 Characterization of HERV-K by structure:

One of the hurdles faced during these specificity determination assays was that we could never stably over express or knock down the HERV-K env. The antigen expression on EL4 HERV-K^+ cells was lost within 10 days though the G418 resistance was retained. Antigen knockdown on A888 was detectable only intracellularly. Antigen expression also varied on the tumor cell surface at various time points. These factors led us to analyze the structure of HERV-K 108 env protein. A typical HERV-K env structure has a 13 amino acid long signal peptide, a surface domain, furin cleavage site and transmembrane domain (**Figure. 22A**) In contrast to previous publication [167], HERV-K seems to have a type II cell membrane protein structure (**Figure. 22B**) and the 13 amino acid long signal peptide does not have properties of a real signal peptide (**Figure. 22C**) when analyzed using the hydrophobic domain prediction and SignalP software. Furthermore, we noticed the presence of a furin cleavage site between the surface and transmembrane unit which might cause unstable expression of HERV-K env antigen. Hence, we developed constructs with various modifications to the antigen which included removal of the furin cleavage site and replacing the transmembrane portion to a known Fc-CD8 transmembrane domain with IgKL as signal peptide (**Figure. 23A-C**) or HERV-K env signal peptide domain flanked by flag M1 and flag M2 tags (**Figure. 23B-C**) in an attempt to stably express them on EL4 cells and understand the structure of the antigen. These changes yielded only transient but not stable expression of the surface envelope protein in contrast to Fc –CD8 transmembrane domain stably expressed intracellularly over a prolonged period of time detected by flow cytometry and mass spectrometry (**Figure. 24A**).

Immunoprecipitation of these cells after transient transfection **(Figure. 25A)** or stable transduction **(Figure. 25B)** of modified HERV-K env plasmids followed by mass spectrometry revealed the presence of the signal peptide and surface unit during transient transfection which is then lost during stable transduction while the Fc-CD8 is detected throughout the period of cell culture.

Previous study has attributed the presence of cryptic cleavage sites for the inability to over-express HERV-K env antigen on any cell surface [168]. Un-biased mass spectrometric analysis performed without using any mAb–based pulled down on AaPCs and A888 cells (every single peptide on the cell membrane was documented) revealed the presence of other HERV-K viral protein (pol and gag) along with other subtypes of HERVs including HERV-F, HERV-H and HERV-R in their total cell extract (**Figure. 26A-B**). These data suggest the presence of more than one type of HERV in a particular tumor cell. Our finding of punctate HERV-K expression on the cell surface of A888 cells is consistent with our hypothesis that HERV-K env is packaged as part of virions associated proteins which are required for stable expression at the cell membrane.

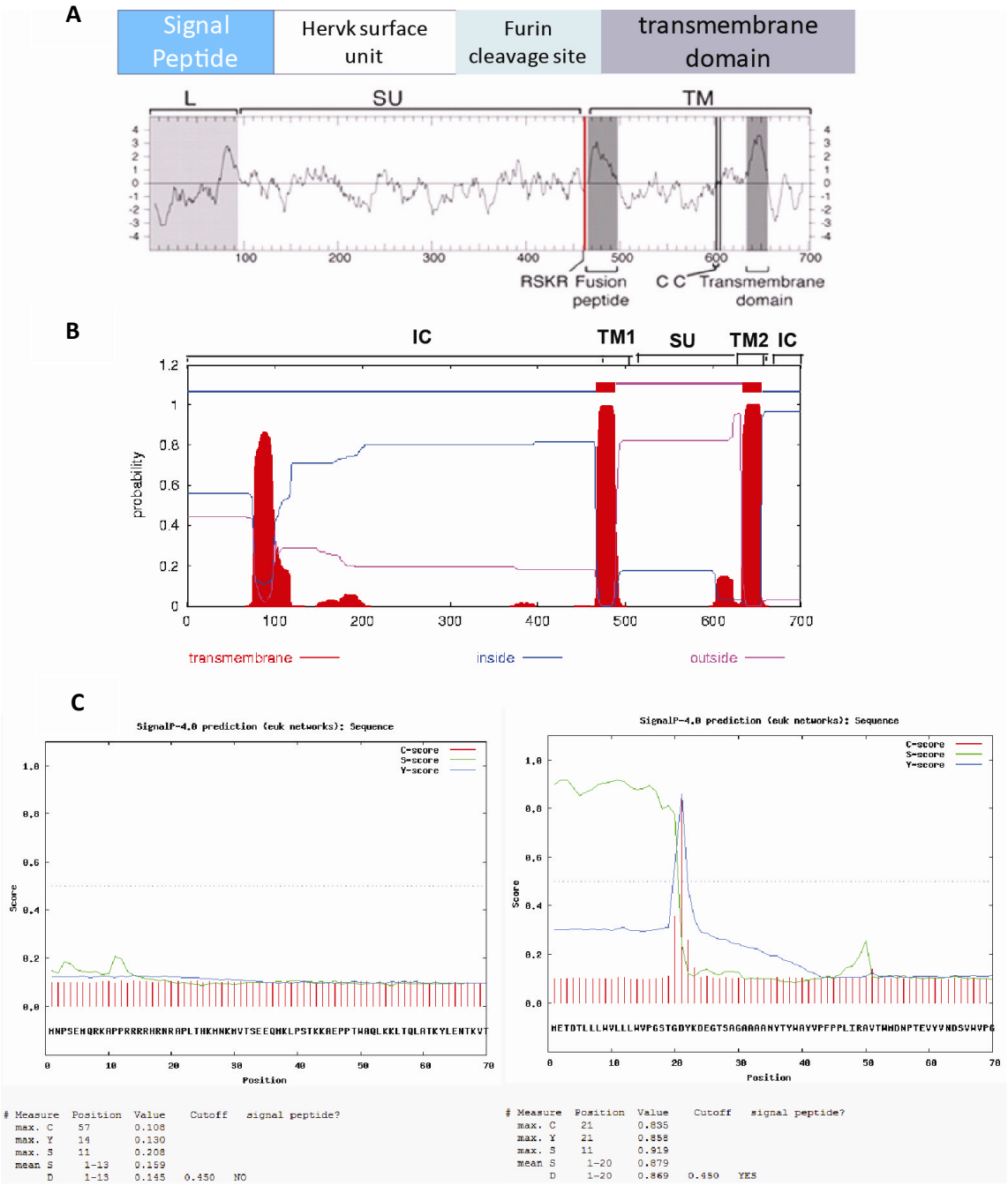

Figure. 22: (**A**) Schematic representation of HERV-K env 108 structure [167]. (**B**) Published and predicted transmembrane hydrophobic domains. Grey bars and red peaks represent hydrophobicity. (**C**) Signal peptide prediction of HERV-K env signal peptide and IgKL signal peptide. Sharp peaks with IgKL represent strong correlation to signal peptide.

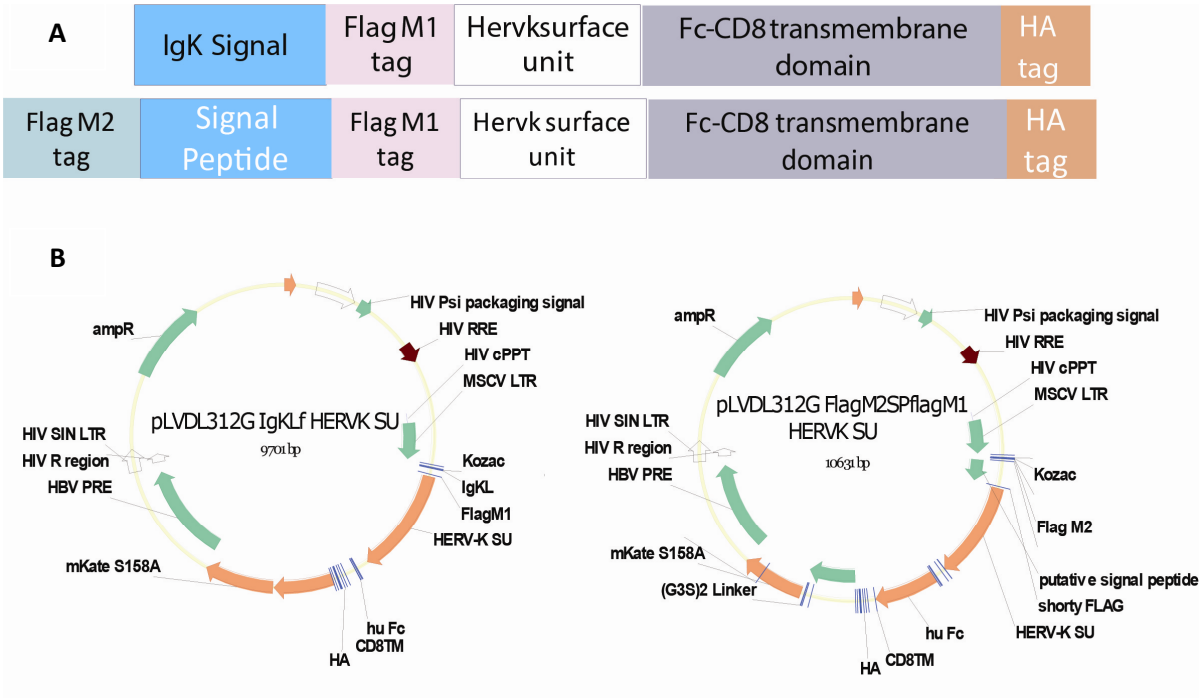

Figure. 23: (**A**) Modifications of HERV-K env signal peptide to IgKL and transmembrane domain to Fc-CD-HA (**B**) Modifications of HERV-K env signal peptide by flanking it with Flag M1 and FlagM2 on either side and switching transmembrane domain to Fc-CD-HA (**C**) Lentiviral plasmids encoding modified IgKl-FlagM1-HERV-K surface unit- Fc-CD8-HA and FlagM2-Signal peptide- Flag M1-HERV-K surface unit- Fc-CD8-HA.

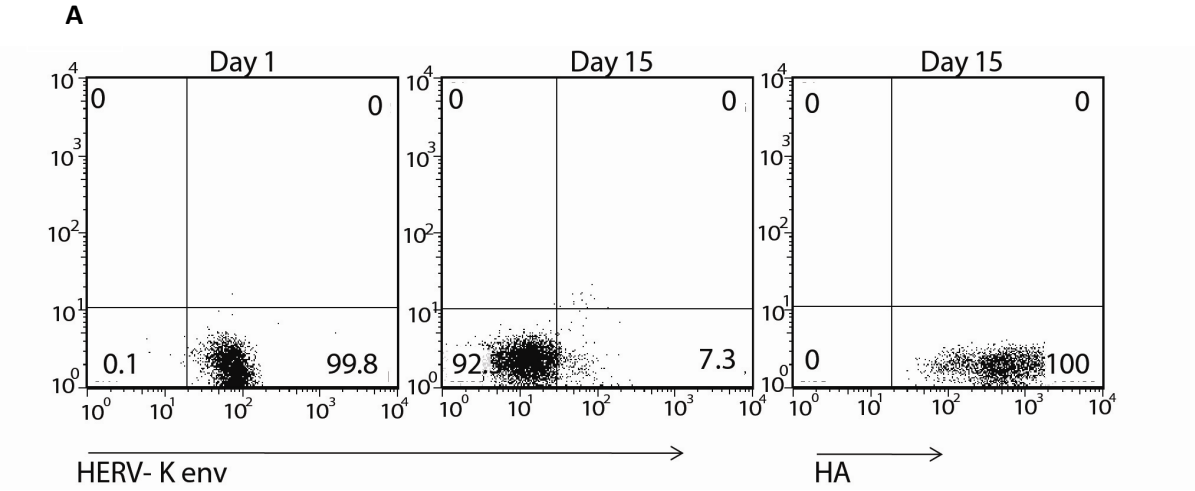

Figure. 24: (A) Representative flowcytometry plots (n=3) of intracellular expression of HERV-K on day 1 and 15 and HA expression on day 15 on IgKL HERV-K SU-Fc $CD8^+$ EL4 cells.

A

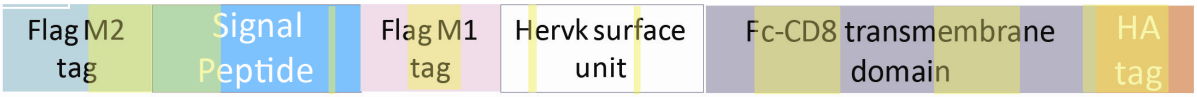

Transient transfection

Confidenc	Sequence	Protein Descrip	Modifications	Activation	DeltaScore	DeltaCn	Rank	Search Engine I	q-Value	PEP	Decoy Peptides I	Peptides Matched	XCorr	Probability
High	FTYHmVSGm		M5(Oxidation);	-3.22	0	0.636		2	1.19	179.43	0	61	3.00E+03	2	552.7263
High	FTYHmVSGmSLRPR		M5(Oxidation);	-1.77	0	0.631	2	2	1	174.13	0	18	6.95E+04	3	571.9439
High	FTYHMVSGmSLRPR		M9(Oxidation)	-2.81	0	0.618	9	6	1.01	230.61	0	47	9.01E+02	3	566.6116
High	VNYLQDFSYQR			2.31	0	0.0503	4	7	3.89	1273.58	0	2	8.31E+04	2	716.8481
High	VNYLQDFSYQR			-1.49	0	0.231	4	8	3.22	689.13	0	50	2.74E+04	3	478.2327
High	VNYLQDFSYQR			0.61	0	0.223	4	7	2.51	787.84	0	43	6.69E+03	2	716.8469
High	KLQSFYPWEWGEK			-0.77	0	0.36	9	6	3.06	589.53	1	43	6.07E+03	3	566.6152
High	LQSFYPWEWGEK			1.81	0	0.233	3	4	3.18	616.19	0	12	4.13E+03	2	785.3737
High	GISTPRPK			-3.96	0	0.493	2	2	1.67	3.39E+02	0	40	6.18E+04	2	428.2543
High	IVSPVSGPEHPELWR			-0.83	0	0.464		5	1.67	252.59	0	18	3.86E+04	3	568.3015
High	IVSPVSGPEHPELWR			0.76	0	0.0624		5	4.64	1104.87	0	2	1.54E+04	2	851.9499
High	LTVASHHIR			-3.34	0	0.23	6	8	3.16	767.49	0	15	1.36E+05	2	517.297
High	TVASHHIR			-2.93	0	0.456	2	4	2.15	390.15	0	19	5.19E+04	2	460.7553
High	GVLNDPAFLYK			0.24	0	0.0918	1	1	3.03	1121.56	0	8	4.89E+04	2	618.835
High	VNTSGSTSGSGKPGSGEGSTSGSR			-3.52	0	0.401	4	1	3.32	494.23	0	1	5.55E+04	3	714.3257
High	VNTSGSTSGSGKPGSGEGSTSGSR			-3.63	0	0.173	4	1	3.84	658.92	0	2	8.70E+03	2	1070.985
High	KVVAAEPK			-3.87	0	0.265		1	2.48	598.32	1	44	5.37E+03	2	421.2591
High	DTLmISR		M4(Oxidation)	-2.14	0	0.279		3	1.84	618.14	0	24	4.70E+04	2	426.2173
High	DTLMISR			-2.13	0	0.433		1	1.74	666.02	0	42	5.35E+04	2	418.2199
High	FNWYVDGVEVHNAK			-0.48	0	0.0691	3	7	3.08	537.64	0	35	5.58E+03	3	559.9386
High	FNWYVDGVEVHNAK			0.81	0	0.0324	5	6	4.71	1497.87	0	8	3.52E+04	2	839.4053
High	FNWYVDGVEVHNAK			-1.02	0	0.427	3	7	2.18	408.12	0	28	1.13E+04	3	559.9383
High	VVSVLTVLHQDWLNGK			0.74	0	0.452	5	6	1.53	142.09	0	61	7.16E+03	3	603.3408
High	EPQVYTLPPSR			0.12	0	0.51	4	2	1.87	230.23	0	8	7.53E+03	2	643.8407
High	EPQVYTLPPSREEmTK		M14(Oxidation)	2.98	0	0.434	2	3	0.8	256.93	1	0	5.47E+03	3	640.9858
High	EPQVYTLPPSREEmTK		M14(Oxidation)	1.69	0	0.468	1	3	3.15	299.97	1	22	1.98E+03	2	960.9739
High	EPQVYTLPPSREEMTK			-0.11	0	0.636	4	6	1.35	292.42	1	71	5.60E+03	3	635.6522
High	EPQVYTLPPSREEmTK		M14(Oxidation)	4.89	0	0.565	2	3	0.63	264.15	1	21	9.68E+02	3	640.9871
High	EPQVYTLPPSREEmTK		M14(Oxidation)	0.5	0	0.528	2	3	1.15	259.52	1	28	4.23E+03	3	640.9843
High	TTPPVLDSDGSFFLYSK			0.8	0	0.22	4	1	3.27	277.7	0	0	7.22E+04	2	937.4653
High	TTPPVLDSDGSFFLYSK			-0.22	0	0.0598	4	1	5.01	1362.57	0	10	3.98E+04	3	625.312
High	SLSLSPGKR			-3.22	0	0.544		2	2.23	311.17	1	75	4.27E+03	2	472.7783
High	PGSGEGSTSGYPYDVPDYA			1.07	0	0.2	1	1	3.34	649.37	0	4	1.26E+04	2	959.9036

B

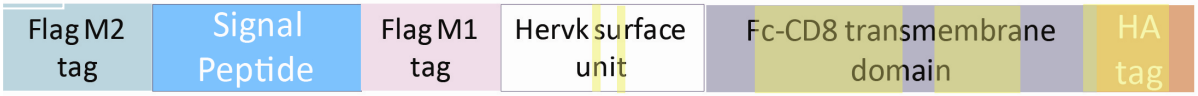

Confidence Level	Sequence	Modifications	q-Value	PEP	XCorr	SpScore	# Missed Cleavages	Intensity
High	VNYLQDFSYQR		0	1.88E-10	3.67	1455.43	0	4.03E+03
High	LWNSQSSIDQK		0	9.66E-11	3.1	1612.56	0	1.01E+04
High	MVTSEEQmKLPSTK	M8(Oxidation)	0	0.229	2.72	372.22	1	1.04E+03
High	LQSFYPWEWGEK		0	0.146	2.6	536.45	0	1.32E+03
High	IVSPVSGPEHPELWR		0	0.0818	2.03	305.15	0	1.04E+04
High	YLENTkVTQTPESmLLAALm	K6(Methyl); M14(Oxidation); M	0	0.229	1.81	249.42	1	1.83E+04
High	VTSEEQmKLPSTK	M7(Oxidation)	0	0.0269	1.75	370.56	1	5.33E+03

Figure. 25: (A) Peptide list from mass spectrometry analysis after transient transfection of FlagM2-Signal peptide- Flag M1-HERV-K surface unit- Fc-CD8-HA in EL4 cells. (B) Peptide list from mass spectrometry analysis after stable transduction of FlagM2-Signal peptide- Flag M1-HERV-K surface unit- Fc-CD8-HA in EL4 cells. Yellow highlights on the schematic HERV-K structure represents the position at which the peptides were retrieved.

A A888 total cell extract:

a) HERV-K GAG polyprotein (GAK5) : VPAGSDVISEYVkAcDGMGGAmHK

b) HERV -K Pol protein (POK2) : QAFINSGAWKIGLANFVGIIDNHYPK

c) HERV -F(c)1 Env polyprotein (EFC1) : LSTVTLATVDcQPHGcQAQVTFNFTSFK

	A	B	C	D	E	F	G	H	I	J
1	Accession	Description	Score	Coverage	# Proteins	# PSMs	Area	# AAs	MW [kDa]	calc. pI
2	P62684	HERV-K_19p13.11 provirus ancestral Gag polyprotein OS	3.83	3.60	2	1	6.862E6	666	74.0	8.73
3		A2	Sequence	# PSMs	# Proteins	Modifications	ΔCn	Area	XCorr	Probability
4		High	VPAGSDVISEYVkAcDGMGGAmHK	1	2	K13(Label:13C(6)); C15(Propionamide);	0.0000	6.862E6	3.83	0.00
5	Q9BXR3	HERV-K_7p22.1 provirus ancestral Pol protein OS=Homo	3.46	2.72	1	1	5.090E6	956	107.6	8.90
6		A2	Sequence	# PSMs	# Proteins	Modifications	ΔCn	Area	XCorr	Probability
7		Medium	QAFINSGAWKIGLANFVGIIDNHYPK	1	1		0.0000	5.090E6	3.46	0.00
8	P60507	HERV-F(c)1_Xq21.33 provirus ancestral Env polyprotein	3.73	4.79	1	1	4.132E6	584	65.2	8.21
9		A2	Sequence	# PSMs	# Proteins	Modifications	ΔCn	Area	XCorr	Probability
10		Medium	LSTVTLATVDcQPHGcQAQVTFNFTSFK	1	1	C11(Propionamide); C16(Propionamide)	0.0000	4.132E6	3.73	0.00

B AaPC total cell extract:

a) HERV-H LTR associated protein 1 (HHLA1) : SQKTLPSTSPGHWTQSTPWASALR , LcmGLAcVLSLWNTVSGIk

b) HERV-K Pol protein (POK6) : DKLIDcYTFLQAEVASAGLAIASDk , HLLScFAVmGVPEK

c) HERV-K Pol protein (POK20) : cPAKPEEEGMMINISIGYR , HLLScFAVmGVPEK

d) HERV-K Pol protein (POK7) : REPLENALTVFTDGSSNGKVAYTGPK , HLLScFAVmGVPEK

e) HERV-K Gag polyprotein (GAK5) : GKVPAGSDVISEYVKAcDGMGGAMHk

	A	B	C	D	E	F	G	H	I	J
1	Accession	Description	Score	Coverage	# Proteins	# PSMs	Area	# AAs	MW [kDa]	calc. pI
2	C9JL84	HERV-H LTR-associating protein 1 OS=Homo sapiens G	10.56	8.10	3	3	7.394E6	531	58.3	8.87
3		A2	Sequence	# PSMs	# Proteins	Modifications	ΔCn	Area	XCorr	Probability
4		Medium	SQKTLPSTSPGHWTQSTPWASALR	1	3		0.0655	9.975E6	3.71	0.00
5		Medium	LcmGLAcVLSLWNTVSGIk	2	2	C2(Propionamide); M3(Oxidation); C7(Pr	0.2840	4.812E6	3.53	0.00
6	P63133	HERV-K_8p23.1 provirus ancestral Pol protein OS=Hon	6.62	4.08	5	2	1.517E7	956	107.6	8.95
7		A2	Sequence	# PSMs	# Proteins	Modifications	ΔCn	Area	XCorr	Probability
8		Medium	DKLIDcYTFLQAEVASAGLAIASDk	1	1	C6(Propionamide); K25(Label:13C(6))	0.0202	2.231E7	3.40	0.00
9		Medium	HLLScFAVmGVPEK	1	9	C5(Propionamide); M9(Oxidation)	0.1202	8.033E6	3.22	0.00
10	Q9UQG0	HERV-K_3q27.3 provirus ancestral Pol protein OS=Hon	6.56	3.41	12	2	8.033E6	969	109.6	9.00
11		A2	Sequence	# PSMs	# Proteins	Modifications	ΔCn	Area	XCorr	Probability
12		Medium	cPAKPEEEGMMINISIGYR	1	8	C1(Propionamide)	0.0000	0.000E0	3.33	0.00
13		Medium	HLLScFAVmGVPEK	1	9	C5(Propionamide); M9(Oxidation)	0.1202	8.033E6	3.22	0.00
14	Q9QC07	HERV-K_1q23.3 provirus ancestral Pol protein OS=Hon	6.43	4.93	5	2	8.033E6	812	91.9	9.09
15		A2	Sequence	# PSMs	# Proteins	Modifications	ΔCn	Area	XCorr	Probability
16		Medium	HLLScFAVmGVPEK	1	9	C5(Propionamide); M9(Oxidation)	0.1202	8.033E6	3.22	0.00
17		Medium	REPLENALTVFTDGSSNGKVAYTGPK	1	1		0.1034	0.000E0	3.21	0.00
18	P62684	HERV-K_19p13.11 provirus ancestral Gag polyprotein (	3.59	3.90	2	1	1.198E7	666	74.0	8.73
19		A2	Sequence	# PSMs	# Proteins	Modifications	ΔCn	Area	XCorr	Probability
20		Medium	GKVPAGSDVISEYVKAcDGMGGAMHk	1	2	C17(Propionamide); K26(Label:13C(6))	0.0000	1.198E7	3.59	0.00

Figure. 26: Unbiased mass spectrometrey analysis without used of mAb mediated immunoprecipitation **(A)** List of peptides retrieved from A888 total cell lysates that aligns to HERV protein **(B)** List of peptides retrieved from AaPC total cell lysates that aligns to HERV proteins.

3.6 Expression of HERV-K on tumor cells:

Since we could not stably express the antigen on HERV-K env^{neg} cells, we wanted to better understand the HERV-K env activity in a tumor cell. We performed an intracellular staining on K-562 parental cells using 6H5 mAx and a FITC-conjugated secondary antibody. Images of the HERV-K env expression in the tumor cells were procured using an Applied Precision OMX deconvolution microscope. These high resolution images revealed five distinct patterns of staining independently seen in each tumor cell including (a) HERV-K env surrounding the nuclear membrane inside the cell, (b) diffuse staining all along the cell membrane and cytoplasm, (c) few punctate dots of HERV-K env mostly on cell membrane, (d) numerous punctate dots of HERV-K env mostly arranged towards one end of the cell and (e) rafts like structure dispersed on the surface of the cells (**Figure 27. A-E**). The punctate and diffuse staining seen here correlates to the staining seen on primary melanoma tumor tissues. These distinct patterns of staining also provide a clue that the HERV-K formed inside the cell moves outwards towards the cell membrane to form clusters that then fuse to form bigger raft-like clusters on the cell surface. These data correlated with the previous studies which predict that HERV-K env can be secreted from the cells from teratocarcinoma cell lines and breast cancer tumors.

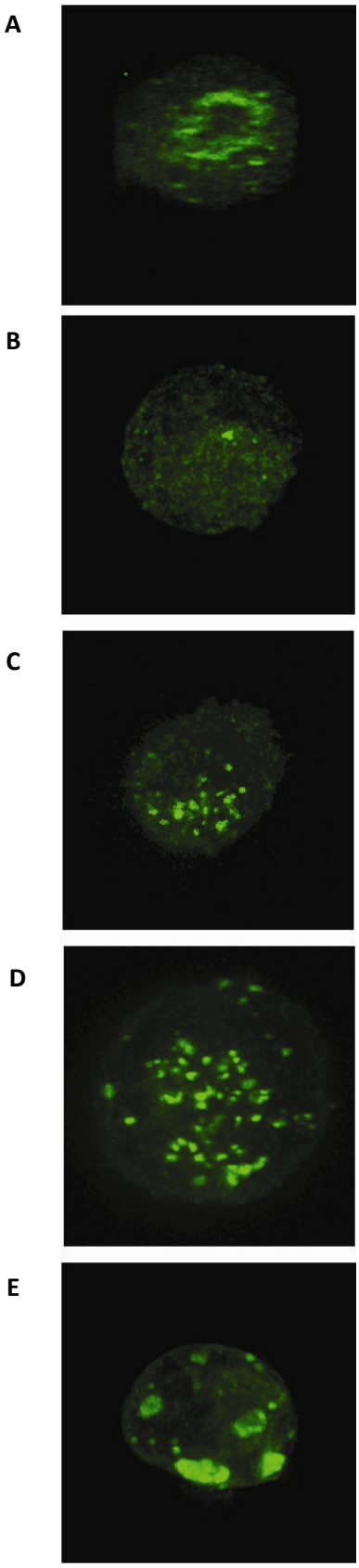

Figure. 27: Volumetric nanoscope images of HERV-K env expression (using 6H5 mAx) on K-562 parental cells **(A)** HERV-K env found surrounding the nuclear membrane forming a ring shaped structure. **(B)** Diffuse staining in the cytoplasm of the cell. **(C)** Few punctate dots of HERV-K env intracellular and on cell surface. **(D)** Dense punctate staining found mostly on one side of the cell. **(E)** Raft-like structures found on tumor cell surface.

3.7 Shed HERV-K env when bound by tumor cells can be targeted by HERV-K env-specific CAR$^+$ T cells

Since the percentage of HERV-K env expression appeared to vary at different time points when cultured tumor cells were analyzed by flow cytometry (**Figure. 19C**), we assessed whether cell-surface expression of this TAA was modulated as a result of shedding and re-attachment over time. Western blot analysis (under reducing condition) of the concentrated supernatant from culture of tumor cells (HERV-K env$^+$ A375-SM, A375, A888, clone 4 and HERV-K env^{neg} EL4 probed with 6H5 mAb revealed a single band at 55 kDa consistent with cleaved HERV-K env lacking the transmembrane domain (in contrast to the 66 kDa band observed from the whole tumor cell lysates which includes the surface and the transmembrane domains) [169,170] (**Figure. 28A**). Pre-incubation of the 6H5 mAb with soluble K10 for one hour at 37 $^{\circ}$C reduced the intensity of staining on the blot, supporting our contention that the band detected in the cultured supernatant was HERK-K env (**Figure. 28B**). A similar band was not was observed in the flow through after concentrating conditioned supernatant through a 100 kDa filter suggesting that shed non-denatured HERV-K env is more than 100 kDa in size (**Figure. 28C**). We next investigated whether shed HERV-K env could be used to introduce this TAA onto tumor cells. We collected conditioned supernatant from AaPC clone 4 since this cell line expressed a high level of HERV-K env by flow cytometry. The concentrated conditioned supernatant was spinfected with EL4 cells for 90 minutes [171]. Negative controls consisted of concentrated tissue culture media in the absence of clone 4. We observed that the expression of transferred HERV-K env decreased over culture time from the cell surface after spinfection (**Figure. 28D**).

Since HERV-K env expression was unstable, shed into the surrounding tumor culture media and can be transferred to tumor cells through spinfection, we analyzed whether the transferred TAA could trigger a T-cell response. IFN-γ production assay performed and HERV-K env-specific CAR^+ T cells specifically produced high (13 fold) levels of IFN-γ when co-cultured with EL4 cells after exposure to concentrated clone 4 supernatant, compared with control EL4 supernatant (media), or when control CD19-specific CAR^+ T cells were used as effectors ($p < 0.001$) (**Figure. 29A**). As a further control for the specificity of binding, we investigated whether concentrated media from A375-SM could block the ability of HERV-K env-specific CAR^+ T cells to target A375-SM tumor cells. This conditioned supernatant, compared with media collected without exposure to tumor cells, resulted in a 20% reduction in tumor lysis ($p < 0.05$) (**Figure. 29B**). These data indicate that HERV-K env protein is apparently present in the tumor cell supernatant and the shedding of the TAA may explain the variability of HERV-K env expression on the tumor cell surface during cell culture period.

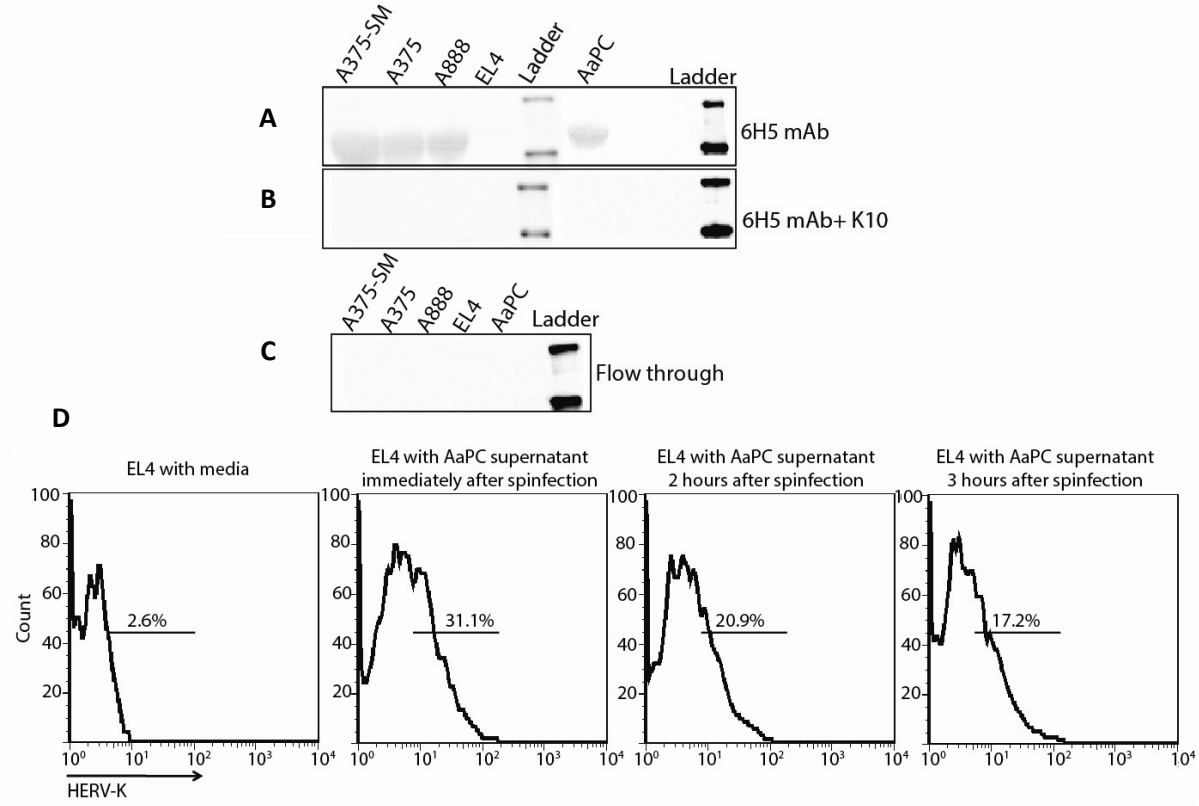

Figure. 28: (**A**) Immunoblot (n = 3) revealing presence of HERV-K env in conditioned culture supernatant harvested from tumor cells. (**B**) Immunoblot assay (n = 3) shows specificity of 6H5 mAb by using recombinant protein (K10) to block binding to shed TAA. Conditioned supernatant from tumor cells containing shed HERV-K env protein was incubated with 6H5 and K10. (**C**) Immunoblot showing the absence of HERV-K env particles in the flow through after conditioned culture media was concentrated through a 100 kDa membrane. (**D**) Representative flow plots (n = 3) using 6H5 mAx showing the ability of shed HERV-K env harvested from supernatant exposed to AaPC clone 4, to bind to cell surface of EL4 parental cells.

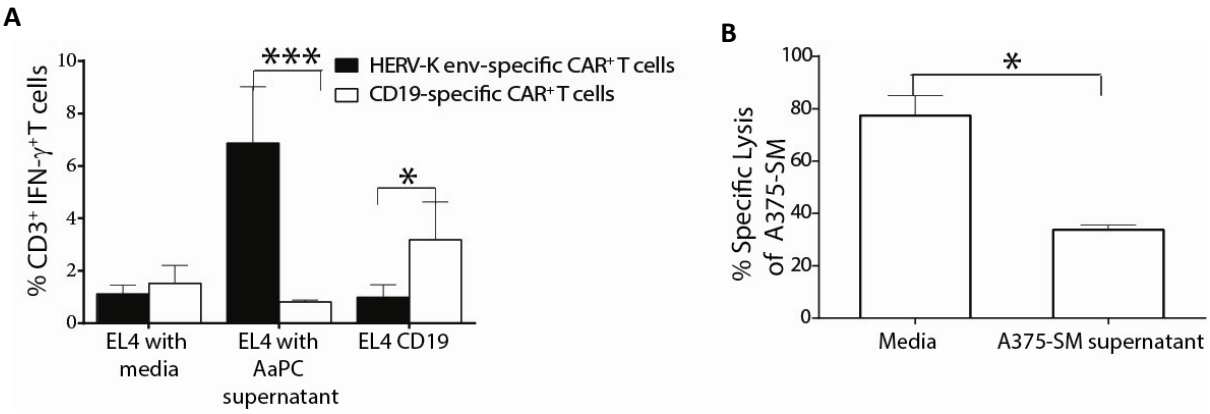

Figure. 29: (**A**) IFN-γ production (n = 3; mean ± SD) by HERV-K env-specific CAR^+ T cells, but not control CD19-specific CAR^+ T cells upon incubation with EL4 parental spinfected with conditioned or control EL4 media. (**B**) A 4 hour CRA (n = 3; effector: target is 1: 10) using HERV-K env-specific CAR^+ T cells as effectors against A375-SM tumor targets incubated with concentrated A375-SM tumor supernatant. Concentrated RPMI media treated were used as control. Two-way ANOVA for IFN-γ production assay and one-way ANOVA for CRA with Turkey's multiple comparison test was used *$p < 0.05$ and ***$p < 0.001$.

3.8 Tumor-killing ability of HERV-K env-specific CAR$^+$ T cells *in vivo*

We investigated whether the anti-melanoma activity observed *in vitro* could be extended to an *in vivo* mouse model. T cells co-expressing Firefly luciferase (ffLuc) and HERV-K env-specific CAR were generated by "double transposition" using the SB system (**Figure. 30A**) [172]. Metastatic melanoma A375-SM tumor cells [155] were genetically modified to co-express Renilla luciferase 8.6535 (rLuc) and mKate S158A fluorescent protein [173] from a bi-cistronic vector (A375-SM-RmK) (**Figure. 30B**). The growth kinetics, cytotoxicity, and specificity of HERV-K env-specific CAR$^+$ffLuc$^+$ T cells and HERV-K env-specific CAR$^+$ T cells were not significantly different ($p > 0.05$) (**Figure. 31A and B**). Next, we developed a xenogenic NSG mouse model of metastatic melanoma where A375-SM-RmK was intravenously (IV) injected (defined as day 0) (**Figure. 32A**). Following tumor cell engraftment in lung and liver, $2x10^7$ HERV-K env-specific CAR$^+$ffLuc$^+$ T cells were IV administered with IL-2 (**Figure. 32B**). Bioluminescent imaging (BLI) was employed to serially measure rLuc-derived tumor burden on days 3, 10, 17 and 25. Localization of HERV-K env-specific CAR$^+$ffLuc$^+$ T cells was assessed the day after each T-cell injection. We observed that HERV-K env-specific CAR$^+$ffLuc$^+$ T cells co-localized with A375-SM-RmK on days 7, 13, and 20 in the lungs (**Figure. 32C**)**.** Twenty-five days after injection of tumor, we observed 4.7-fold increased rLuc activity in untreated tumor bearing mice compared to mice with tumor receiving HERV-K env-specific CAR$^+$ffLuc$^+$ T cells ($p < 0.001$) (**Figure. 32D**). By this time point, the untreated mice had a hunch-back posture and appeared moribund. In contrast, mice treated with HERV-K env-specific CAR$^+$ffLuc$^+$ T cells were active and appeared healthy (**Figure. 32E**). The morphology of the liver in untreated

mice appeared shriveled and necrotic compared to the treated mice (**Figure. 33A**) and using optical imaging at necropsy a 75% reduction in fluorescent tumor colonies was observed in the livers of the T-cell treated group versus the untreated group ($p < 0.05$) (**Figure. 33B**). The tumor cells both at the primary and metastatic sites (lung and liver) had increased HERV-K env expression compared to tumor cells with treatment on day 28 (**Figure. 34A).** Isotype control was used to compare the staining intensity between the tissues analyzed **(Figure. 34B**). These data indicate that genetically modified CAR^+ T cells can be used to treat mice with disseminated HERV-K env^+.

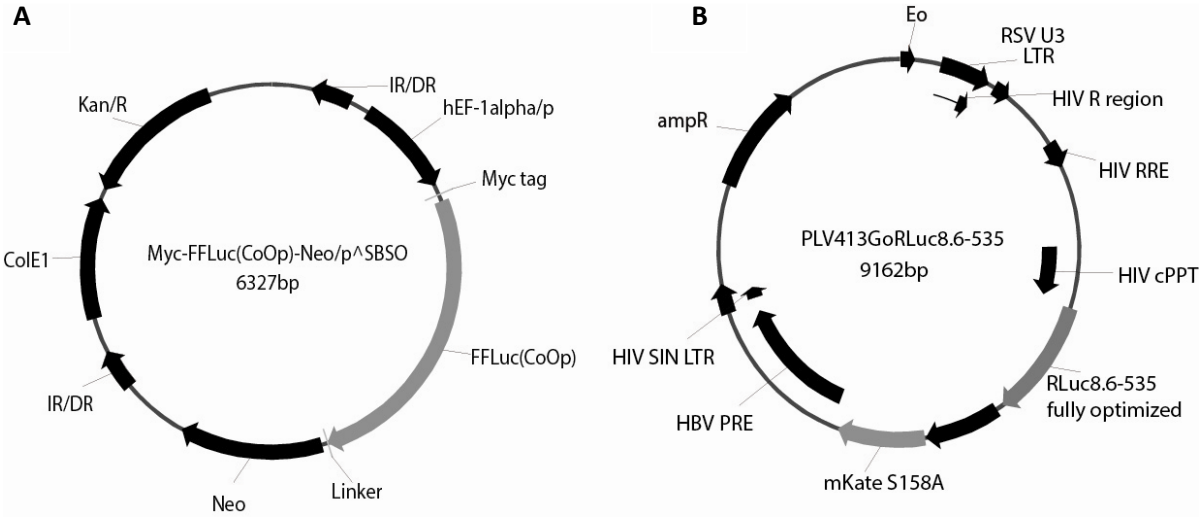

Figure. 30: (**A**) A bidirectional *Sleeping Beauty* DNA transposon (HERV-K (coOp) Neo/pSBSO-Bidirectional) to co-express HERV-K env full length antigen and neomycin phosphotransferase (neo) for *in vitro* selection. Abbreviations: hEF-1alpha/p: human elongation factor-1α promoter, mCMV/p: mouse cytomegalovirus promoter, Neo/r: neomycin phosphotransferase. (**B**) Lentiviral DNA plasmid (PLV413G0RLUC8.6-535) was designed to co-express renilla luciferease 8.6535 and mKate 5158Amarker for *in vivo* and *in vitro* imaging. Abbreviations: Eo: RSV U3: Roes sarcoma virus U3 sequence, HIV R region: human immunodeficiency virus R region, HIV RRE: HIV-1 Rev response element, HIV cPPT: HIV central poly purine tract, RLuc8.6-535: renilla luciferase 8.6-535, mKate S158A: monomeric version of Katusha S158A, HBV PRE: Hepatitis B virus posttranscriptional regulatory element, HIV SIN LTR: HIV self-inactivating LTR.

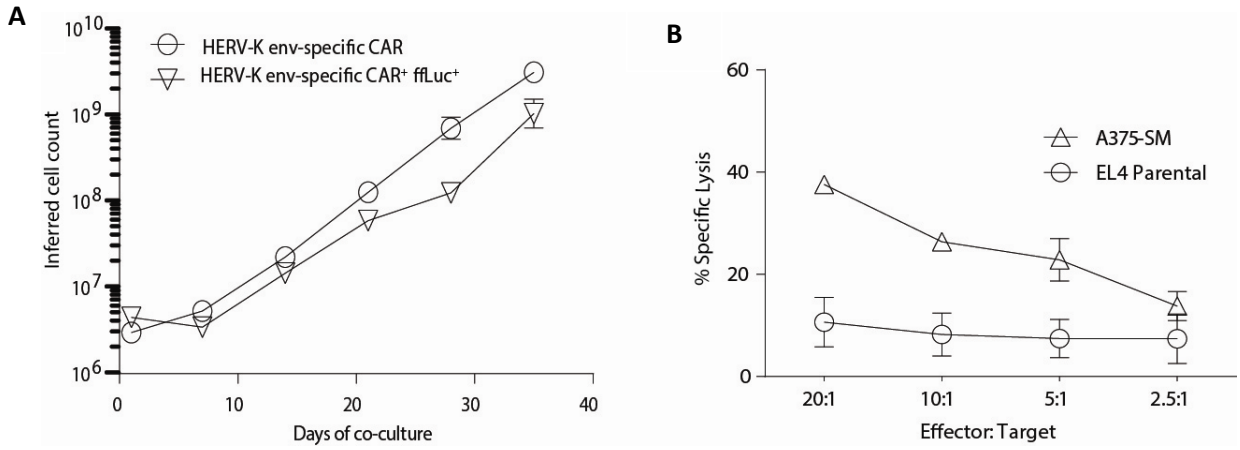

Figure. 31: (**A**) Inferred cell count (n = 3; mean ± SD) was plotted for HERV-K env-specific CAR$^+$ T cells and HERV-K env-specific CAR$^+$ffLuc$^+$ T cells. (**B**) A four hour CRA (n = 3; mean ± SD) revealing lysis of A375-SM versus EL4 parental cells with HERV-K env-specific CAR$^+$ffLuc$^+$ T cells. CRA data using 2-way ANOVA with Bonferroni post-test;

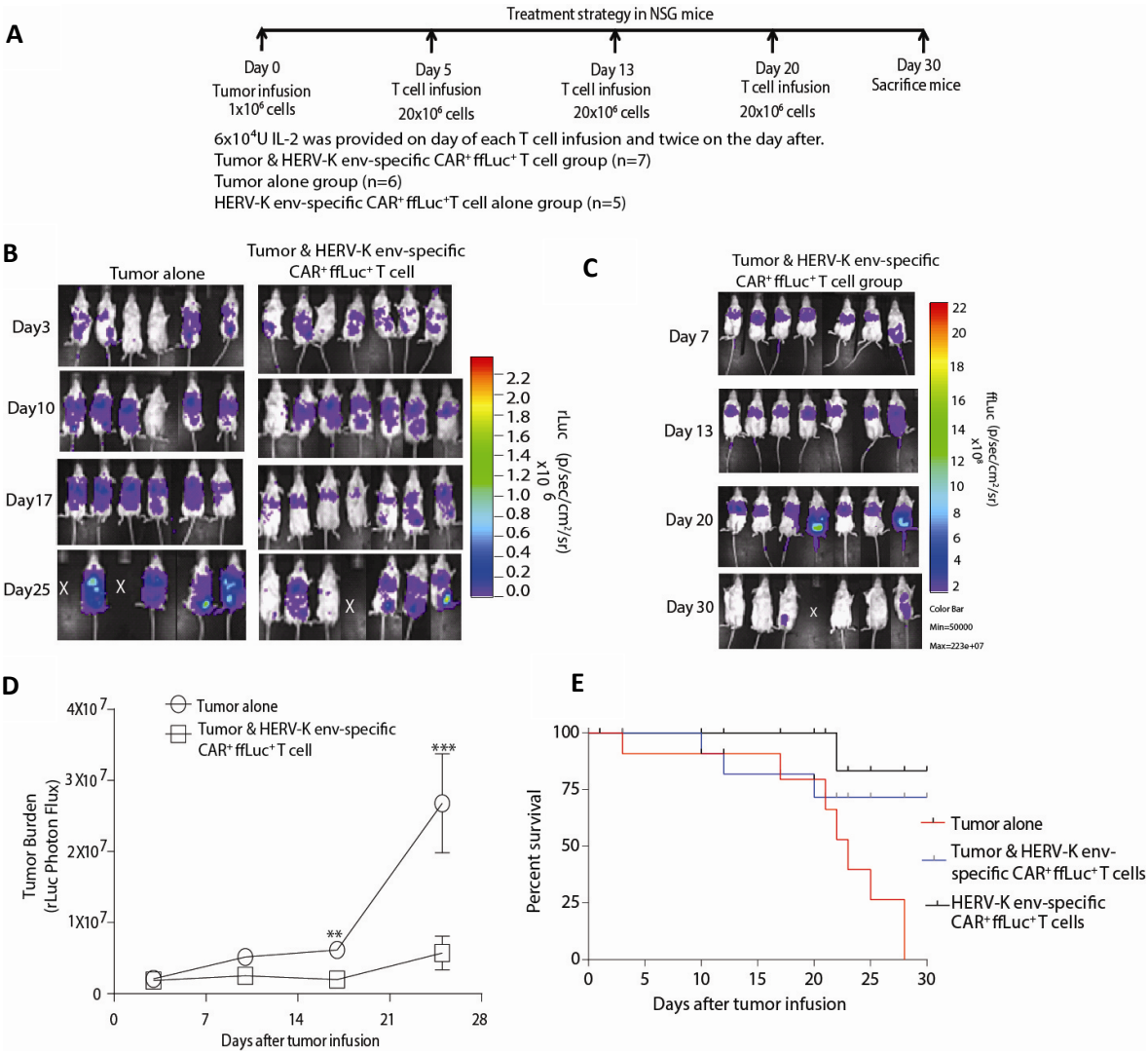

Figure. 32: (**A**) Schematic of *in vivo* experiment. (**B**) BLI images of rLuc-derived tumor cell activity in tumor group (n = 6) and treatment group (n = 7) mice from days 3 to 25. (**C**) Plot of average rLuc flux (mean ± SD) in treated (n = 7) and untreated (n = 6) mouse groups over time. (**D**) BLI images of HERV-K env-specific $CAR^{+}ffLuc^{+}$ T-cell activity in treatment group mice from days 7 to 30. (**E**) Survival plot of tumor (n = 6) and treatment group (n = 7) up to 30 days ($p > 0.05$). Statistics performed with two-way ANOVA with Bonferroni's post-tests to calculate rLuc activity; Log-rank (Mantel-Cox) test for survival plot. **$p < 0.01$ and ***$p < 0.001$.

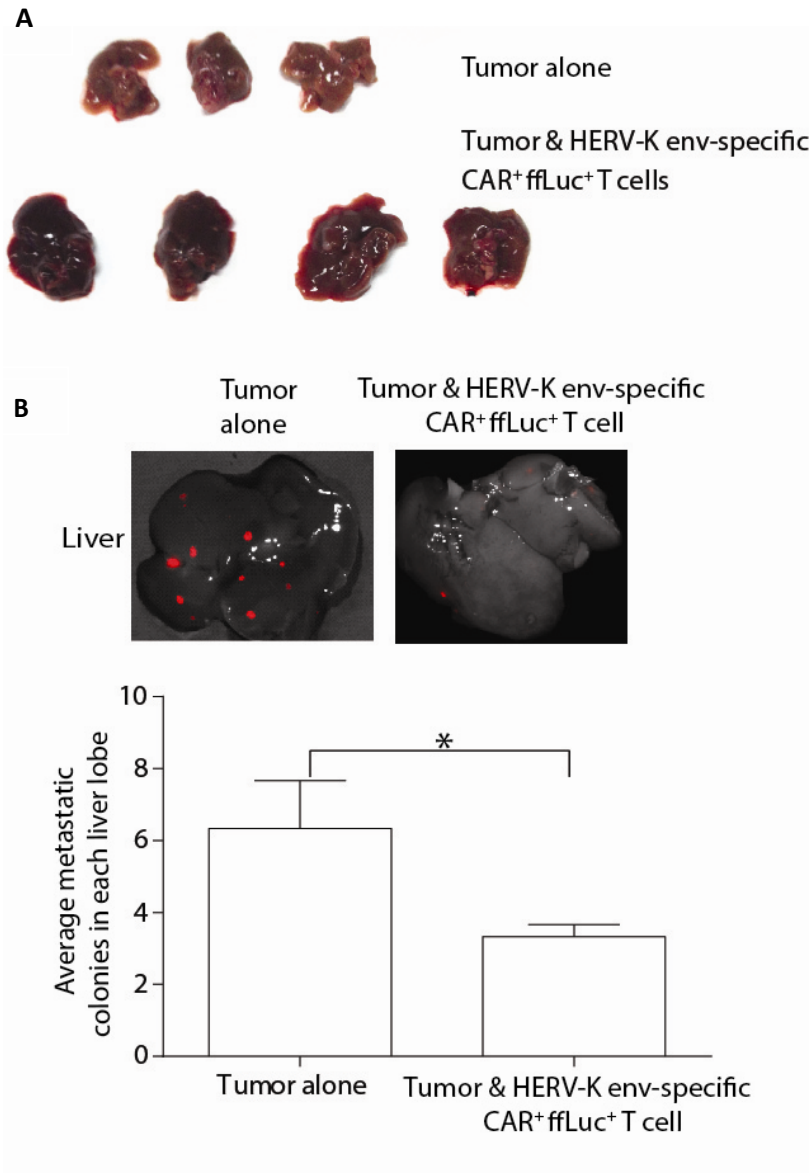

Figure. 33: (**A**) Postmortem imaging of mKate-derived fluorescence representing melanoma metastatic foci in livers of treated and untreated mouse groups. (**B**) Bar graph of average number of tumor metastatic foci on treated and untreated mouse groups. Unpaired Student's t-test was used to calculate significant difference in liver metastatic foci between treated and untreated mice *$p < 0.05$.

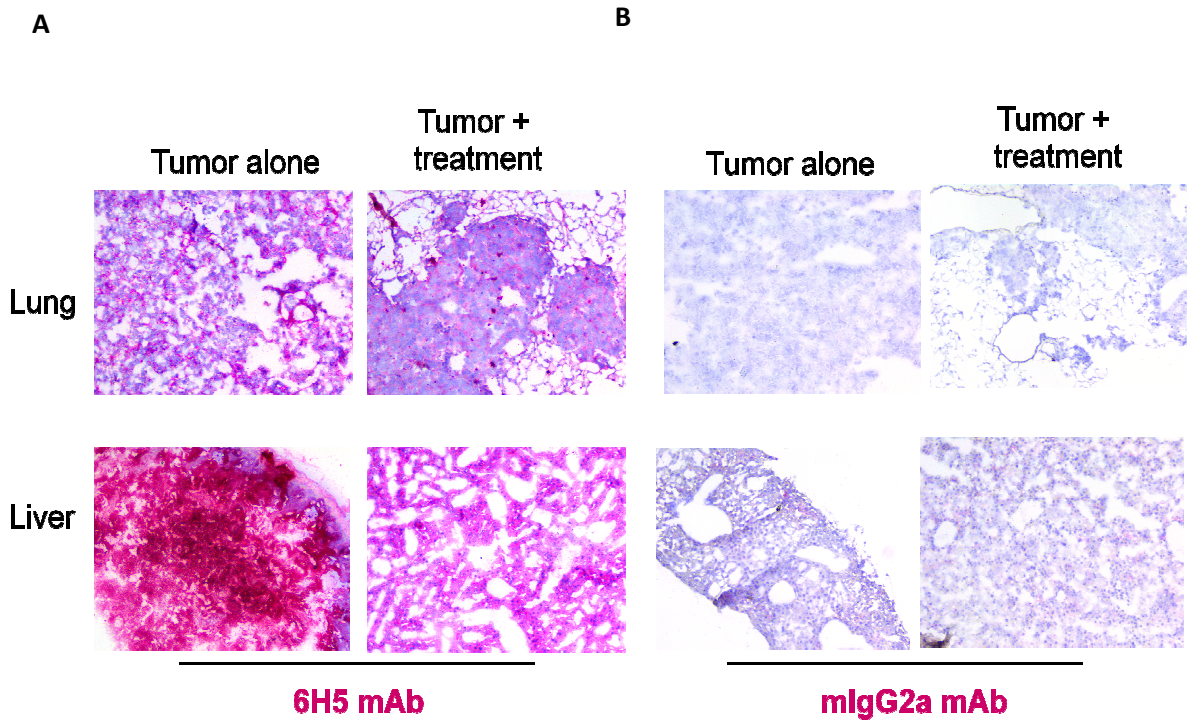

Figure 34: Immunohistological analysis of lung and liver tissues of mice bearing tumor with or without treatment with HERV-K env-specific $CAR^{+}ffLuc^{+}T$ cells on day 28.

(**A**) Increased HERV-K env expression (shown in red) on lung and liver tissues of mice bearing tumor alone compared to treatment group. (**B**) isotype control (IgG2a) expression (shown in red) on tumor on liver and lung tissues.

Chapter 4: Discussion:

HERV-K env has been incorporated in the human genome for millions of years. We have demonstrated its expression on tumor cells and primary patient tissues, including melanoma, but it is not expressed on normal tissues. We engineered a CAR specific for the HERV-K env which could be propagated on HERV-K env$^+$ AaPCs and maintained a preferential effector memory phenotype. We have shown that the viral antigen is shed from tumor cell surface and could modulate the tumor microenvironment. HERV-K env-specific CAR$^+$T cells specifically kill all HERV-K env$^+$ tumor cells in an antigen-specific manner *in vitro* and diminish melanoma tumor growth and metastasis *in vivo*.

HERV-K env has been reported to be expressed on the tumor cell surface of breast cancer, ovarian cancer, renal cell carcinoma, lymphoma, teratocarcinoma, prostate cancer, and infectious diseases such as AIDS [169,170,174-180]. Various studies have been conducted to target HERV-K env antigen to develop novel treatment strategies. Some of the targeted therapy studies include development of 6H5 mAb against HERV-K env present on breast cancer cells which produced a ten-fold tumor volume decrease in a breast cancer mouse model [157]. Renal carcinoma was precluded from formation and metastasis in mice with prophylactic vaccination targeted against HERV-K env [180]. In vitro experiments on HERV-K env-specific CD8$^+$ T cells obtained from patients with HIV responded to HIV infected cells resulting in eliminating these infectious cells in an HERV-K env antigen dependent manner [174]. Anti retroviral drugs such as efavirenze and RNA interference (RNAi) against HERV-K decreased the tumor growth and metastatis of melanoma in a mouse model [181]. HERV-K

env-specific TCR expressed on T cells lysed HERV-K^+ melanoma tumor cells four-fold greater than HERV-K^{neg} melanoma cell line *in vitro* [144].

In this report, we demonstrated that HERV-K env is markedly up-regulated during the transition from melanocytes to primary and metastatic melanoma. Increased mRNA transcript levels of HERVK appear to be involved in melanoma progression resulting in morphological and cellular modifications such as diminished adherence capability and reduced level of HLA class I molecules or tumor cells associated with tumor progression [182,183]. In agreement with a positive correlation between HERV-K env expression and tumorgenicity, tissue-array analysis demonstrated increased levels of HERV-K expression from normal human tissue to tenfold greater in malignant melanoma. Multiple factors regulate HERV-K levels, for example pro-inflammatory cytokines down regulate while steroids such as estradiol and progesterone are known to up regulate HERV-K env expression on tumor cells [184]. Our IHC result has shown two distinct patterns of antigen expression: a diffuse cytoplasmic staining and a cell surface punctate staining. This punctate staining may be associated with recycle of HERV-K env in endosome between the cytoplasm and cell membrane and/or the budding off of exosome [178,185,186]. This is consistent with the variability in cell surface expression for HERV-K env on tumor cell surface. Hence, HERV-K env is a more specific tumor associated antigen (compared to others such as HER2, CD19) that can be targeted on both primary and metastatic melanoma with limited off target toxicity.

In our attempt to understand the structure of the HERV-K viral envelope protein, we observed that with transient transfection, the antigen folds in a type II membrane based structure with the N-, C-terminal and signal peptide being intracellular, and the surface unit of the envelop protein detected partially on the cell surface. The presence of cryptic cleavage sites hinders any attempts to stably overexpress or knockout this antigen on cells [168]. We performed un-biased mass spectrometric analysis on AaPCs and A888 mel cells, where the cell surface and intracellular proteins are biotinylated and every HERV-K protein biotinylated in the cell is detected. We found the presence of HERV-K pol and gag protein on the A888 cell extract along with HERV-F. The AaPCs on the other hand had HERV-K pol along with HERV-H and HERV-R proteins in their total cell extract. These data suggest the presence of more than one type of HERV in a particular tumor cell. The absence of HERV-K env but the presence of pol and gag is complimentary with our data in which we detect the presence of HERV-K env on tumor cell surpernatant. The ability of this viral env protein to be concentrated and infect HERV-K^{neg} EL4 cells temporarily and increase the IFN-γ production by HERV-K env-specific CAR^{+} T cells on exposure to these infected cells shows the potential of our therapy to prevent antigen escape. These mass spectrometry data also suggest that various HERVs could potentially work together but investigating it is out of the scope of this thesis.

Being a highly immunogenic tumor, melanoma is an attractive tumor model for developing potent T cell based therapies. Favorable response was observed while targeting HERV-K antigen on melanoma cells using HERV-K env-specific TCR on cytotoxic T lymphocytes (CTLs) *in vitro* [144]. A major limitation for TCR based T cell immunotherapy is HLA/antigen

restriction[55]. This reduces both antigen selection and the population size (HLA matched) which can be treated. Transgenic expression of scFv based CARs on T cells circumvents this restriction and confers non-HLA based antigen recognition [187]. Genetic modification can be accomplished via viral or non-viral vectors. Our work using the SB system with electroporation is a non-viral approach that utilizes a transposon (encoding CAR) and transposon (responsible for genome integration). The main advantages of the SB system over viral transduction methods include (a) safety, (b) decreased integration into a transcriptionally active site (c) decreased cost and (d) yield of sufficient cells for clinical applications (>1 x10^{10}) [152]. We were able to expand HERV-K env-specific CAR$^+$T cells on AaPCs plus IL-2 and IL-21. Such numbers are known based on our preliminary clinical trial using CD19-specific CAR$^+$T cells for the treatment of B-lineage malignancies[150]. 50% of propagated HERV-K env-specific CAR$^+$ T cells were grown of effector memory phenotype, previously shown to be more effective *in vivo* than other T cell phenotypes such as short lived effector T cells [188].

It is important that the binding characteristics of the mAb from which a CAR is derived are maintained. We wondered, whether this was the case between the 6H5 mAb (mouse IgG2a) and the HERV-K-specific CAR. Thus, we generated a soluble recombinant maxibody version of the CAR consisting of the 6H5 scFv and human IgG4 Fc (6H5 mAx). Although both reagents bound to soluble HERV-K equally, we did observe some differential staining of melanoma tumor cell lines. Importantly, however, we observed a substantial correlation when the H-Index (product of percentage positive cells and MFI) for the mAb was plotted against that for the mAx. Although we only observed a subtle difference, it cannot be

assumed that a CAR engineered from a VH and VL chain of a given mAb will result in a CAR with similar binding characteristics. We strongly recommend that investigators engineer a mAx for each CAR designed and tested. It is conceivable that the HERV-K-specific CAR recognize more than one member of the HERV family. To address this possibility, we performed western blot analysis for the 6H5 antigen using the lysates from several melanoma cell lines. In all cases, we only observed a single band at 66 KDa, the correct size of HERV-K [157], suggesting strongly that HERV-K-specific T cells preferentially and perhaps exclusively recognize HERV-K.

HERV-K shed from spinfected cells over a short time duration describes the difference in the expression of HERV-K env antigen on tumor cell surface during culture period. Spinfection instead of ELISA was used to identify the expression of HERV-K env in the cell culture media of these tumor cells, since the latter technique could not detect the soluble HERV-K env antigen. Initially a 100 kDa filter was used to concentrate the tumor cell culture media, but upon analysis using immunoblot technique a 50kDa band was seen. We predict the shed HERV-K env either appears an oligomer or associated with other proteins which gets dissociated when denatured and run on SDS-page. We could not attest to this prediction since immunoprecipitation of the shed antigen with either 6H5 mAb or 6H5 mAx did not yield any data indicating oligomerization or protein complexes due to high level of background noise. Various previous studies have demonstrated the capability of HERV-K env to extrude or bud from the tumor cell surface as immature provirus [167,189,190]. This shed antigen was also detected in the plasma samples from patients with lymphoma and breast cancer. [169]. Immature provirus can be made to infect normal cells by engineering artificial

mutations to remove the stop codons [191]. The ability of this viral env protein to be concentrated and infect HERV-K^{neg} EL4 cells temporarily and increase the IFN–γ production by HERV-K-specific CAR^+ T cells on exposure to these infected cells shows the potential of our therapy to prevent antigen escape.

Though adoptive T cell therapy has been successful in reducing tumor burden *in vivo,* off-target toxicity remains a primary concern. Other serious side effects include pulmonary therapy of T cells and subsequent cytokine storm that results in multi-organ failure. Such an event has occurred in a trial testing an ERBB2 specific CAR for the treatment of metastatic breast cancer [192]. Liver toxicity can also occur. Five of eleven patients with renal carcinoma treated with carboxy anhydrase IX-specific CAR^+T cells developed liver toxicity [193,194]. Thus, for ACT to be successful the CAR should be specific and pulmonary/liver toxicity must be monitored diligently. We demonstrated that HERV-K env is indeed a highly specific TAA which can be targeted by HERV-K-specific CAR^+T cells in vivo without causing pulmonary or liver toxicity.

Hepatic metastatic melanoma is particularly difficult to treat and is associated with an overall median survival of only four months [195]. The current standard of care includes chemotherapy, surgery, pro-inflammatory cytokine treatment and tumor antigen vaccines [196,197]. All strategies are either ineffective, highly invasive or associated with serious side effects. In contrast, CAR-based T cell immunotherapies are advantageous for targeting tumors in hypervascular organ such as the lungs and liver. Using a mouse model of

metastatic model, a significant reduction in tumor growth and metastasis from lungs to liver was observed without known or observable adverse effects.

Hence, targeting HERV-K env using adoptive T cell therapy may be a treatment option for multiple disease conditions. In conclusion, CAR based HERV-K env specific adoptive immunotherapy represents a promising treatment for multiple malignancies, which may circumvent many of the off-target effects observed in current clinical trials.

4.2 Conclusion:

Advanced and relapsed melanoma is generally considered difficult to treat due to development of tumor resistance to conventional therapies. One way to extend patient survival will be to improve the host immune response to their tumor. To accomplish this, we have developed a strategy to infuse large numbers of tumor-specific T cells. Tumor-specificity is achieved by modifying normal donor-derived T cells to express a receptor specific for a novel tumor molecule, envelope protein of human endogenous retrovirus-K (HERV-K env). This unique viral antigen was found integrated into the human genome and expressed selectively on melanoma cells and not on normal cells.

For tumor-targeting, CAR specific for HERV-K env protein was genetically cloned into the T-cell surface using a non-viral sleeping beauty vector to integrate CAR into the T cells. These HERV-K env-specific CAR^+ T cells were grown in an antigen specific manner to large numbers using our clinical grade AaPCs which endogenously express HERV-K env along with the required co-stimulatory molecules. We developed a solubilized version of the

HERV-K env-specific CAR called the 6H5 mAx and found a positive correlation between 6H5 mAx and 6H5 mAb binding to HERV-K env antigen. HERV-K env-specific CAR^+ T cells were found to target and lyse EL4 artificially engineered to express HERV-K env antigen and did not lyse A888 cells with HERV-K env knockdown using shRNA. These CAR^+ T cells reduce the tumor load significantly by IFN-γ production and CAR-mediated lysis *in vitro* in an antigen dependent manner.

The antigen over expression was never stable possibly due to the presence of cryptic cleavage sites in the HERV-K env sequence. High resolution images of HERV-K env expression on tumor cell surface indicated that the tumor antigen is formed surrounding the nuclear membrane in the cytoplasm of the cell. The antigen then diffused in the cytoplasm or aggregated to form punctate structures which accumulated towards one part of the cell and later formed bigger rafts-like structure on the cell membrane. We later found that the HERV-K env protein was shed from the tumor cell surface using spinfection technique. The shed HERV-K env antigen can be targeted by HERV-K env-specific CAR^+ T cells specifically and elicit an immune response. Thus this therapy has the potential to avoid antigen escape due to shedding or becoming attached to other normal cells. *In vivo*, HERV-K env-specific CAR^+ T cells were successful in reducing the tumor volume and decreasing metastasis of melanoma tumor cells.

Thus, this therapy will benefit patients with aggressive and metastatic melanoma expressing HERV-K env antigen. While we have chosen melanoma as our tumor model, this study has the potential to be applied to other malignancies, including breast cancer, lymphoma and

myeloma due to the restricted expression of HERV-K env protein on these tumor cells. Benefits of this therapy include minimized off-target effects since normal tissue does not express HERV-K env and successful tumor clearance. This therapy can reduce the need for intense chemotherapeutic regimens with their concomitant toxicities.

4.3 Future research:

The mechanism which allows the presence of mRNA of HERV-K env but absence of the viral protein in normal cells needs to be researched. More work is required in understanding the role of these mRNA during normal cell function. Future research work is required to understand the role of other HERVs in tumor cells. Unbiased mass spectrometry showed the presence of other HERV viral proteins and it will be useful to learn the functional interplay between various HERV proteins and between various components of HERV-K virus during tumor progression. To better understand the structure of HERV-K viral env protein on the cell surface and the nature of its signal peptide better strategies of molecular cloning using cDNA library and mass spectrometry will be performed. Transmission electron microscopy will help us visualize the viral shedding dynamics from the tumor cell surface. Since the antigen is known to be shed from the tumor cell surface, tagging the virus with markers such as RFP and following its activity is under progress in order to better understand viral activity in a cell.

Bibliography:

1. Agarwala SS, di Pietro A, Flaherty KT, Garbe C, Grob JJ, Kashani-Sabet M, Kirkwood JM, Leachman S, Messina J, O'Day S, Ribas A, Sondak V 2010. Meeting report from the Third Global Workshop on Melanoma. Pigment Cell Melanoma Res 23(5):e1-7.
2. Siegel R, DeSantis C, Virgo K, Stein K, Mariotto A, Smith T, Cooper D, Gansler T, Lerro C, Fedewa S, Lin C, Leach C, Cannady RS, Cho H, Scoppa S, Hachey M, Kirch R, Jemal A, Ward E 2012. Cancer treatment and survivorship statistics, 2012. CA Cancer J Clin 62(4):220-241.
3. Siegel R, Naishadham D, Jemal A 2012. Cancer statistics, 2012. CA Cancer J Clin 62(1):10-29.
4. Rigel DS 2002. The effect of sunscreen on melanoma risk. Dermatol Clin 20(4):601-606.
5. Cole BF, Gelber RD, Kirkwood JM, Goldhirsch A, Barylak E, Borden E 1996. Quality-of-life-adjusted survival analysis of interferon alfa-2b adjuvant treatment of high-risk resected cutaneous melanoma: an Eastern Cooperative Oncology Group study. J Clin Oncol 14(10):2666-2673.
6. Kirkwood JM, Strawderman MH, Ernstoff MS, Smith TJ, Borden EC, Blum RH 1996. Interferon alfa-2b adjuvant therapy of high-risk resected cutaneous melanoma: the Eastern Cooperative Oncology Group Trial EST 1684. J Clin Oncol 14(1):7-17.
7. Korn EL, Liu PY, Lee SJ, Chapman JA, Niedzwiecki D, Suman VJ, Moon J, Sondak VK, Atkins MB, Eisenhauer EA, Parulekar W, Markovic SN, Saxman S, Kirkwood JM 2008. Meta-analysis of phase II cooperative group trials in metastatic stage IV melanoma to determine progression-free and overall survival benchmarks for future phase II trials. J Clin Oncol 26(4):527-534.
8. Crosby T, Fish R, Coles B, Mason MD 2000. Systemic treatments for metastatic cutaneous melanoma. Cochrane Database Syst Rev (2):CD001215.
9. Atkins MB, Lotze MT, Dutcher JP, Fisher RI, Weiss G, Margolin K, Abrams J, Sznol M, Parkinson D, Hawkins M, Paradise C, Kunkel L, Rosenberg SA 1999. High-dose recombinant interleukin 2 therapy for patients with metastatic melanoma: analysis of 270 patients treated between 1985 and 1993. J Clin Oncol 17(7):2105-2116.
10. Phan GQ, Attia P, Steinberg SM, White DE, Rosenberg SA 2001. Factors associated with response to high-dose interleukin-2 in patients with metastatic melanoma. J Clin Oncol 19(15):3477-3482.
11. Hill GJ, 2nd, Krementz ET, Hill HZ 1984. Dimethyl triazeno imidazole carboxamide and combination therapy for melanoma. IV. Late results after complete response to chemotherapy (Central Oncology Group protocols 7130, 7131, and 7131A). Cancer 53(6):1299-1305.
12. Melero I, Hervas-Stubbs S, Glennie M, Pardoll DM, Chen L 2007. Immunostimulatory monoclonal antibodies for cancer therapy. Nat Rev Cancer 7(2):95-106.
13. Flaherty KT, Puzanov I, Kim KB, Ribas A, McArthur GA, Sosman JA, O'Dwyer PJ, Lee RJ, Grippo JF, Nolop K, Chapman PB 2010. Inhibition of mutated, activated BRAF in metastatic melanoma. N Engl J Med 363(9):809-819.

14. Ribas A, Flaherty KT 2011. BRAF targeted therapy changes the treatment paradigm in melanoma. Nat Rev Clin Oncol 8(7):426-433.
15. Garbe C, Peris K, Hauschild A, Saiag P, Middleton M, Spatz A, Grob JJ, Malvehy J, Newton-Bishop J, Stratigos A, Pehamberger H, Eggermont A 2010. Diagnosis and treatment of melanoma: European consensus-based interdisciplinary guideline. Eur J Cancer 46(2):270-283.
16. Denninghoff VC, Kahn AG, Falco J, Curutchet HP, Elsner B 2004. Sentinel lymph node: detection of micrometastases of melanoma in a molecular study. Mol Diagn 8(4):253-258.
17. Bedikian AY, Wei C, Detry M, Kim KB, Papadopoulos NE, Hwu WJ, Homsi J, Davies M, McIntyre S, Hwu P 2011. Predictive factors for the development of brain metastasis in advanced unresectable metastatic melanoma. Am J Clin Oncol 34(6):603-610.
18. Leiter U, Eigentler TK, Forschner A, Pflugfelder A, Weide B, Held L, Meier F, Garbe C 2010. Excision guidelines and follow-up strategies in cutaneous melanoma: Facts and controversies. Clin Dermatol 28(3):311-315.
19. Bradbury PA, Middleton MR 2004. DNA repair pathways in drug resistance in melanoma. Anticancer Drugs 15(5):421-426.
20. Pak BJ, Chu W, Lu SJ, Kerbel RS, Ben-David Y 2001. Lineage-specific mechanism of drug and radiation resistance in melanoma mediated by tyrosinase-related protein 2. Cancer Metastasis Rev 20(1-2):27-32.
21. Pak BJ, Lee J, Thai BL, Fuchs SY, Shaked Y, Ronai Z, Kerbel RS, Ben-David Y 2004. Radiation resistance of human melanoma analysed by retroviral insertional mutagenesis reveals a possible role for dopachrome tautomerase. Oncogene 23(1):30-38.
22. Faries MB, Morton DL 2003. Melanoma: is immunotherapy of benefit? Adv Surg 37:139-169.
23. Kalialis LV, Drzewiecki KT, Klyver H 2009. Spontaneous regression of metastases from melanoma: review of the literature. Melanoma Res 19(5):275-282.
24. Castelli C, Rivoltini L, Andreola G, Carrabba M, Renkvist N, Parmiani G 2000. T-cell recognition of melanoma-associated antigens. J Cell Physiol 182(3):323-331.
25. Epping MT, Bernards R 2006. A causal role for the human tumor antigen preferentially expressed antigen of melanoma in cancer. Cancer Res 66(22):10639-10642.
26. Fratta E, Coral S, Covre A, Parisi G, Colizzi F, Danielli R, Nicolay HJ, Sigalotti L, Maio M 2011. The biology of cancer testis antigens: putative function, regulation and therapeutic potential. Mol Oncol 5(2):164-182.
27. Kawakami Y, Rosenberg SA 1997. Human tumor antigens recognized by T-cells. Immunol Res 16(4):313-339.
28. Lupetti R, Pisarra P, Verrecchia A, Farina C, Nicolini G, Anichini A, Bordignon C, Sensi M, Parmiani G, Traversari C 1998. Translation of a retained intron in tyrosinase-related protein (TRP) 2 mRNA generates a new cytotoxic T lymphocyte (CTL)-defined and shared human melanoma antigen not expressed in normal cells of the melanocytic lineage. J Exp Med 188(6):1005-1016.
29. Maio M 2012. Melanoma as a model tumour for immuno-oncology. Ann Oncol 23 Suppl 8:viii10-14.
30. Pillay V, Gan HK, Scott AM 2011. Antibodies in oncology. N Biotechnol 28(5):518-529.

31. Riechmann L, Clark M, Waldmann H, Winter G 1988. Reshaping human antibodies for therapy. Nature 332(6162):323-327.
32. Bajorin DF, Chapman PB, Wong GY, Cody BV, Cordon-Cardo C, Dantes L, Templeton MA, Scheinberg D, Oettgen HF, Houghton AN 1992. Treatment with high dose mouse monoclonal (anti-GD3) antibody R24 in patients with metastatic melanoma. Melanoma Res 2(5-6):355-362.
33. Jerne NK 1974. Towards a network theory of the immune system. Ann Immunol (Paris) 125C(1-2):373-389.
34. Rosenberg SA, Dudley ME 2009. Adoptive cell therapy for the treatment of patients with metastatic melanoma. Curr Opin Immunol 21(2):233-240.
35. Balkwill F, Mantovani A 2001. Inflammation and cancer: back to Virchow? Lancet 357(9255):539-545.
36. Moore OS, Jr., Foote FW, Jr. 1949. The relatively favorable prognosis of medullary carcinoma of the breast. Cancer 2(4):635-642.
37. Day CL, Jr., Sober AJ, Kopf AW, Lew RA, Mihm MC, Jr., Hennessey P, Golomb FM, Harris MN, Gumport SL, Raker JW, Malt RA, Cosimi AB, Wood WC, Roses DF, Gorstein F, Postel A, Grier WR, Mintzis MN, Fitzpatrick TB 1981. A prognostic model for clinical stage I melanoma of the upper extremity. The importance of anatomic subsites in predicting recurrent disease. Ann Surg 193(4):436-440.
38. Shilyansky J, Nishimura MI, Yannelli JR, Kawakami Y, Jacknin LS, Charmley P, Rosenberg SA 1994. T-cell receptor usage by melanoma-specific clonal and highly oligoclonal tumor-infiltrating lymphocyte lines. Proc Natl Acad Sci U S A 91(7):2829-2833.
39. Yron I, Wood TA, Jr., Spiess PJ, Rosenberg SA 1980. In vitro growth of murine T cells. V. The isolation and growth of lymphoid cells infiltrating syngeneic solid tumors. J Immunol 125(1):238-245.
40. Muul LM, Spiess PJ, Director EP, Rosenberg SA 1987. Identification of specific cytolytic immune responses against autologous tumor in humans bearing malignant melanoma. J Immunol 138(3):989-995.
41. Chiou SH, Sheu BC, Chang WC, Huang SC, Hong-Nerng H 2005. Current concepts of tumor-infiltrating lymphocytes in human malignancies. J Reprod Immunol 67(1-2):35-50.
42. Forget MA, Malu S, Liu H, Toth C, Maiti S, Kale C, Haymaker C, Bernatchez C, Huls H, Wang E, Marincola FM, Hwu P, Cooper LJ, Radvanyi LG 2014. Activation and Propagation of Tumor-infiltrating Lymphocytes on Clinical-grade Designer Artificial Antigen-presenting Cells for Adoptive Immunotherapy of Melanoma. J Immunother 37(9):448-460.
43. Rivoltini L, Kawakami Y, Sakaguchi K, Southwood S, Sette A, Robbins PF, Marincola FM, Salgaller ML, Yannelli JR, Appella E, et al. 1995. Induction of tumor-reactive CTL from peripheral blood and tumor-infiltrating lymphocytes of melanoma patients by in vitro stimulation with an immunodominant peptide of the human melanoma antigen MART-1. J Immunol 154(5):2257-2265.
44. Reiman JM, Kmieciak M, Manjili MH, Knutson KL 2007. Tumor immunoediting and immunosculpting pathways to cancer progression. Semin Cancer Biol 17(4):275-287.
45. Speeckaert R, van Geel N, Vermaelen KV, Lambert J, Van Gele M, Speeckaert MM, Brochez L 2011. Immune reactions in benign and malignant melanocytic lesions: lessons for immunotherapy. Pigment Cell Melanoma Res 24(2):334-344.

46. Shi H, Liu L, Wang Z 2013. Improving the efficacy and safety of engineered T cell therapy for cancer. Cancer Lett 328(2):191-197.
47. Dembic Z, Haas W, Weiss S, McCubrey J, Kiefer H, von Boehmer H, Steinmetz M 1986. Transfer of specificity by murine alpha and beta T-cell receptor genes. Nature 320(6059):232-238.
48. Zhao Y, Zheng Z, Cohen CJ, Gattinoni L, Palmer DC, Restifo NP, Rosenberg SA, Morgan RA 2006. High-efficiency transfection of primary human and mouse T lymphocytes using RNA electroporation. Mol Ther 13(1):151-159.
49. Robbins PF, Li YF, El-Gamil M, Zhao Y, Wargo JA, Zheng Z, Xu H, Morgan RA, Feldman SA, Johnson LA, Bennett AD, Dunn SM, Mahon TM, Jakobsen BK, Rosenberg SA 2008. Single and dual amino acid substitutions in TCR CDRs can enhance antigen-specific T cell functions. J Immunol 180(9):6116-6131.
50. Schaft N, Willemsen RA, de Vries J, Lankiewicz B, Essers BW, Gratama JW, Figdor CG, Bolhuis RL, Debets R, Adema GJ 2003. Peptide fine specificity of anti-glycoprotein 100 CTL is preserved following transfer of engineered TCR alpha beta genes into primary human T lymphocytes. J Immunol 170(4):2186-2194.
51. de Witte MA, Jorritsma A, Kaiser A, van den Boom MD, Dokter M, Bendle GM, Haanen JB, Schumacher TN 2008. Requirements for effective antitumor responses of TCR transduced T cells. J Immunol 181(7):5128-5136.
52. Cohen CJ, Li YF, El-Gamil M, Robbins PF, Rosenberg SA, Morgan RA 2007. Enhanced antitumor activity of T cells engineered to express T-cell receptors with a second disulfide bond. Cancer Res 67(8):3898-3903.
53. Robbins PF, Morgan RA, Feldman SA, Yang JC, Sherry RM, Dudley ME, Wunderlich JR, Nahvi AV, Helman LJ, Mackall CL, Kammula US, Hughes MS, Restifo NP, Raffeld M, Lee CC, Levy CL, Li YF, El-Gamil M, Schwarz SL, Laurencot C, Rosenberg SA 2011. Tumor regression in patients with metastatic synovial cell sarcoma and melanoma using genetically engineered lymphocytes reactive with NY-ESO-1. J Clin Oncol 29(7):917-924.
54. Parkhurst MR, Yang JC, Langan RC, Dudley ME, Nathan DA, Feldman SA, Davis JL, Morgan RA, Merino MJ, Sherry RM, Hughes MS, Kammula US, Phan GQ, Lim RM, Wank SA, Restifo NP, Robbins PF, Laurencot CM, Rosenberg SA 2011. T cells targeting carcinoembryonic antigen can mediate regression of metastatic colorectal cancer but induce severe transient colitis. Mol Ther 19(3):620-626.
55. Garrido F, Ruiz-Cabello F, Cabrera T, Perez-Villar JJ, Lopez-Botet M, Duggan-Keen M, Stern PL 1997. Implications for immunosurveillance of altered HLA class I phenotypes in human tumours. Immunol Today 18(2):89-95.
56. Kershaw MH, Teng MW, Smyth MJ, Darcy PK 2005. Supernatural T cells: genetic modification of T cells for cancer therapy. Nat Rev Immunol 5(12):928-940.
57. Eshhar Z 1997. Tumor-specific T-bodies: towards clinical application. Cancer Immunol Immunother 45(3-4):131-136.
58. Liu L, Sun M, Wang Z 2012. Adoptive T-cell therapy of B-cell malignancies: conventional and physiological chimeric antigen receptors. Cancer Lett 316(1):1-5.
59. Kuwana Y, Asakura Y, Utsunomiya N, Nakanishi M, Arata Y, Itoh S, Nagase F, Kurosawa Y 1987. Expression of chimeric receptor composed of immunoglobulin-derived V

regions and T-cell receptor-derived C regions. Biochem Biophys Res Commun 149(3):960-968.
60. Willemsen RA, Ronteltap C, Chames P, Debets R, Bolhuis RL 2005. T cell retargeting with MHC class I-restricted antibodies: the CD28 costimulatory domain enhances antigen-specific cytotoxicity and cytokine production. J Immunol 174(12):7853-7858.
61. Stewart-Jones G, Wadle A, Hombach A, Shenderov E, Held G, Fischer E, Kleber S, Nuber N, Stenner-Liewen F, Bauer S, McMichael A, Knuth A, Abken H, Hombach AA, Cerundolo V, Jones EY, Renner C 2009. Rational development of high-affinity T-cell receptor-like antibodies. Proc Natl Acad Sci U S A 106(14):5784-5788.
62. Tassev DV, Cheng M, Cheung NK 2012. Retargeting NK92 cells using an HLA-A2-restricted, EBNA3C-specific chimeric antigen receptor. Cancer Gene Ther 19(2):84-100.
63. Casucci M, Bondanza A 2011. Suicide gene therapy to increase the safety of chimeric antigen receptor-redirected T lymphocytes. J Cancer 2:378-382.
64. Hombach A, Hombach AA, Abken H 2010. Adoptive immunotherapy with genetically engineered T cells: modification of the IgG1 Fc 'spacer' domain in the extracellular moiety of chimeric antigen receptors avoids 'off-target' activation and unintended initiation of an innate immune response. Gene Ther 17(10):1206-1213.
65. Bridgeman JS, Hawkins RE, Bagley S, Blaylock M, Holland M, Gilham DE 2010. The optimal antigen response of chimeric antigen receptors harboring the CD3zeta transmembrane domain is dependent upon incorporation of the receptor into the endogenous TCR/CD3 complex. J Immunol 184(12):6938-6949.
66. Finney HM, Lawson AD, Bebbington CR, Weir AN 1998. Chimeric receptors providing both primary and costimulatory signaling in T cells from a single gene product. J Immunol 161(6):2791-2797.
67. Song DG, Ye Q, Poussin M, Harms GM, Figini M, Powell DJ, Jr. 2012. CD27 costimulation augments the survival and antitumor activity of redirected human T cells in vivo. Blood 119(3):696-706.
68. Altvater B, Landmeier S, Pscherer S, Temme J, Juergens H, Pule M, Rossig C 2009. 2B4 (CD244) signaling via chimeric receptors costimulates tumor-antigen specific proliferation and in vitro expansion of human T cells. Cancer Immunol Immunother 58(12):1991-2001.
69. Savoldo B, Ramos CA, Liu E, Mims MP, Keating MJ, Carrum G, Kamble RT, Bollard CM, Gee AP, Mei Z, Liu H, Grilley B, Rooney CM, Heslop HE, Brenner MK, Dotti G 2011. CD28 costimulation improves expansion and persistence of chimeric antigen receptor-modified T cells in lymphoma patients. J Clin Invest 121(5):1822-1826.
70. Porter DL, Levine BL, Kalos M, Bagg A, June CH 2011. Chimeric antigen receptor-modified T cells in chronic lymphoid leukemia. N Engl J Med 365(8):725-733.
71. Hackett PB, Largaespada DA, Cooper LJ 2010. A transposon and transposase system for human application. Mol Ther 18(4):674-683.
72. Skipper KA, Andersen PR, Sharma N, Mikkelsen JG 2013. DNA transposon-based gene vehicles - scenes from an evolutionary drive. J Biomed Sci 20:92.
73. Ivics Z, Izsvak Z, Minter A, Hackett PB 1996. Identification of functional domains and evolution of Tc1-like transposable elements. Proc Natl Acad Sci U S A 93(10):5008-5013.

74. van Luenen HG, Colloms SD, Plasterk RH 1994. The mechanism of transposition of Tc3 in C. elegans. Cell 79(2):293-301.
75. van Luenen HG, Plasterk RH 1994. Target site choice of the related transposable elements Tc1 and Tc3 of Caenorhabditis elegans. Nucleic Acids Res 22(3):262-269.
76. Horie K, Yusa K, Yae K, Odajima J, Fischer SE, Keng VW, Hayakawa T, Mizuno S, Kondoh G, Ijiri T, Matsuda Y, Plasterk RH, Takeda J 2003. Characterization of Sleeping Beauty transposition and its application to genetic screening in mice. Mol Cell Biol 23(24):9189-9207.
77. Fischer SE, Wienholds E, Plasterk RH 2003. Continuous exchange of sequence information between dispersed Tc1 transposons in the Caenorhabditis elegans genome. Genetics 164(1):127-134.
78. Gao J, Bernatchez C, Sharma P, Radvanyi LG, Hwu P 2013. Advances in the development of cancer immunotherapies. Trends Immunol 34(2):90-98.
79. Yvon E, Del Vecchio M, Savoldo B, Hoyos V, Dutour A, Anichini A, Dotti G, Brenner MK 2009. Immunotherapy of metastatic melanoma using genetically engineered GD2-specific T cells. Clin Cancer Res 15(18):5852-5860.
80. Yun CO, Nolan KF, Beecham EJ, Reisfeld RA, Junghans RP 2000. Targeting of T lymphocytes to melanoma cells through chimeric anti-GD3 immunoglobulin T-cell receptors. Neoplasia 2(5):449-459.
81. Gattinoni L, Klebanoff CA, Palmer DC, Wrzesinski C, Kerstann K, Yu Z, Finkelstein SE, Theoret MR, Rosenberg SA, Restifo NP 2005. Acquisition of full effector function in vitro paradoxically impairs the in vivo antitumor efficacy of adoptively transferred CD8+ T cells. J Clin Invest 115(6):1616-1626.
82. Sadelain M, Brentjens R, Riviere I 2009. The promise and potential pitfalls of chimeric antigen receptors. Curr Opin Immunol 21(2):215-223.
83. McLaughlin-Drubin ME, Munger K 2008. Viruses associated with human cancer. Biochim Biophys Acta 1782(3):127-150.
84. Rosenberg N, Jolicoeur P 1997. Retroviral Pathogenesis.
85. Temin HM, Rubin H 1958. Characteristics of an assay for Rous sarcoma virus and Rous sarcoma cells in tissue culture. Virology 6(3):669-688.
86. Baltimore D 1970. RNA-dependent DNA polymerase in virions of RNA tumour viruses. Nature 226(5252):1209-1211.
87. Ziegler JL, Buonaguro FM 2009. Infectious agents and human malignancies. Front Biosci (Landmark Ed) 14:3455-3464.
88. Maeda N, Fan H, Yoshikai Y 2008. Oncogenesis by retroviruses: old and new paradigms. Rev Med Virol 18(6):387-405.
89. Boeke JD, Stoye JP 1997. Retrotransposons, Endogenous Retroviruses, and the Evolution of Retroelements.
90. Tristem M 2000. Identification and characterization of novel human endogenous retrovirus families by phylogenetic screening of the human genome mapping project database. J Virol 74(8):3715-3730.
91. Hayward JA, Tachedjian M, Cui J, Field H, Holmes EC, Wang LF, Tachedjian G 2013. Identification of diverse full-length endogenous betaretroviruses in megabats and microbats. Retrovirology 10:35.

92. Jern P, Stoye JP, Coffin JM 2007. Role of APOBEC3 in genetic diversity among endogenous murine leukemia viruses. PLoS Genet 3(10):2014-2022.
93. Colmegna I, Garry RF 2006. Role of endogenous retroviruses in autoimmune diseases. Infect Dis Clin North Am 20(4):913-929.
94. Antony JM, Zhu Y, Izad M, Warren KG, Vodjgani M, Mallet F, Power C 2007. Comparative expression of human endogenous retrovirus-W genes in multiple sclerosis. AIDS Res Hum Retroviruses 23(10):1251-1256.
95. Leib-Mosch C, Brack-Werner R, Werner T, Bachmann M, Faff O, Erfle V, Hehlmann R 1990. Endogenous retroviral elements in human DNA. Cancer Res 50(17 Suppl):5636S-5642S.
96. Medstrand P, van de Lagemaat LN, Mager DL 2002. Retroelement distributions in the human genome: variations associated with age and proximity to genes. Genome Res 12(10):1483-1495.
97. van de Lagemaat LN, Medstrand P, Mager DL 2006. Multiple effects govern endogenous retrovirus survival patterns in human gene introns. Genome Biol 7(9):R86.
98. Hughes JF, Coffin JM 2004. Human endogenous retrovirus K solo-LTR formation and insertional polymorphisms: implications for human and viral evolution. Proc Natl Acad Sci U S A 101(6):1668-1672.
99. Jern P, Coffin JM 2008. Effects of retroviruses on host genome function. Annu Rev Genet 42:709-732.
100. Ponferrada VG, Mauck BS, Wooley DP 2003. The envelope glycoprotein of human endogenous retrovirus HERV-W induces cellular resistance to spleen necrosis virus. Arch Virol 148(4):659-675.
101. Mallet F, Bouton O, Prudhomme S, Cheynet V, Oriol G, Bonnaud B, Lucotte G, Duret L, Mandrand B 2004. The endogenous retroviral locus ERVWE1 is a bona fide gene involved in hominoid placental physiology. Proc Natl Acad Sci U S A 101(6):1731-1736.
102. Stoye JP, Coffin JM 2000. A provirus put to work. Nature 403(6771):715, 717.
103. Mangeney M, Renard M, Schlecht-Louf G, Bouallaga I, Heidmann O, Letzelter C, Richaud A, Ducos B, Heidmann T 2007. Placental syncytins: Genetic disjunction between the fusogenic and immunosuppressive activity of retroviral envelope proteins. Proc Natl Acad Sci U S A 104(51):20534-20539.
104. Andersson AC, Venables PJ, Tonjes RR, Scherer J, Eriksson L, Larsson E 2002. Developmental expression of HERV-R (ERV3) and HERV-K in human tissue. Virology 297(2):220-225.
105. Samuelson LC, Wiebauer K, Snow CM, Meisler MH 1990. Retroviral and pseudogene insertion sites reveal the lineage of human salivary and pancreatic amylase genes from a single gene during primate evolution. Mol Cell Biol 10(6):2513-2520.
106. Feuchter A, Mager D 1990. Functional heterogeneity of a large family of human LTR-like promoters and enhancers. Nucleic Acids Res 18(5):1261-1270.
107. Medstrand P, Landry JR, Mager DL 2001. Long terminal repeats are used as alternative promoters for the endothelin B receptor and apolipoprotein C-I genes in humans. J Biol Chem 276(3):1896-1903.
108. Wang T, Zeng J, Lowe CB, Sellers RG, Salama SR, Yang M, Burgess SM, Brachmann RK, Haussler D 2007. Species-specific endogenous retroviruses shape the

transcriptional network of the human tumor suppressor protein p53. Proc Natl Acad Sci U S A 104(47):18613-18618.
109. Takahashi Y, Harashima N, Kajigaya S, Yokoyama H, Cherkasova E, McCoy JP, Hanada K, Mena O, Kurlander R, Tawab A, Srinivasan R, Lundqvist A, Malinzak E, Geller N, Lerman MI, Childs RW 2008. Regression of human kidney cancer following allogeneic stem cell transplantation is associated with recognition of an HERV-E antigen by T cells. J Clin Invest 118(3):1099-1109.
110. Subramanian RP, Wildschutte JH, Russo C, Coffin JM 2011. Identification, characterization, and comparative genomic distribution of the HERV-K (HML-2) group of human endogenous retroviruses. Retrovirology 8:90.
111. Ruprecht K, Mayer J, Sauter M, Roemer K, Mueller-Lantzsch N 2008. Endogenous retroviruses and cancer. Cell Mol Life Sci 65(21):3366-3382.
112. Lower R, Tonjes RR, Korbmacher C, Kurth R, Lower J 1995. Identification of a Rev-related protein by analysis of spliced transcripts of the human endogenous retroviruses HTDV/HERV-K. J Virol 69(1):141-149.
113. Buaas FW, Kirsh AL, Sharma M, McLean DJ, Morris JL, Griswold MD, de Rooij DG, Braun RE 2004. Plzf is required in adult male germ cells for stem cell self-renewal. Nat Genet 36(6):647-652.
114. Boese A, Sauter M, Galli U, Best B, Herbst H, Mayer J, Kremmer E, Roemer K, Mueller-Lantzsch N 2000. Human endogenous retrovirus protein cORF supports cell transformation and associates with the promyelocytic leukemia zinc finger protein. Oncogene 19(38):4328-4336.
115. Hughes JF, Coffin JM 2001. Evidence for genomic rearrangements mediated by human endogenous retroviruses during primate evolution. Nat Genet 29(4):487-489.
116. Waterland RA, Jirtle RL 2003. Transposable elements: targets for early nutritional effects on epigenetic gene regulation. Mol Cell Biol 23(15):5293-5300.
117. Perron H, Lang A 2010. The human endogenous retrovirus link between genes and environment in multiple sclerosis and in multifactorial diseases associating neuroinflammation. Clin Rev Allergy Immunol 39(1):51-61.
118. Contreras-Galindo R, Kaplan MH, Contreras-Galindo AC, Gonzalez-Hernandez MJ, Ferlenghi I, Giusti F, Lorenzo E, Gitlin SD, Dosik MH, Yamamura Y, Markovitz DM 2012. Characterization of human endogenous retroviral elements in the blood of HIV-1-infected individuals. J Virol 86(1):262-276.
119. Kurth R, Bannert N 2010. Beneficial and detrimental effects of human endogenous retroviruses. Int J Cancer 126(2):306-314.
120. Stauffer Y, Marguerat S, Meylan F, Ucla C, Sutkowski N, Huber B, Pelet T, Conrad B 2001. Interferon-alpha-induced endogenous superantigen. a model linking environment and autoimmunity. Immunity 15(4):591-601.
121. Lavie L, Kitova M, Maldener E, Meese E, Mayer J 2005. CpG methylation directly regulates transcriptional activity of the human endogenous retrovirus family HERV-K(HML-2). J Virol 79(2):876-883.
122. Khodosevich K, Lebedev Y, Sverdlov ED 2004. Large-scale determination of the methylation status of retrotransposons in different tissues using a methylation tags approach. Nucleic Acids Res 32(3):e31.

123. Lee YN, Malim MH, Bieniasz PD 2008. Hypermutation of an ancient human retrovirus by APOBEC3G. J Virol 82(17):8762-8770.
124. Philipsen S, Suske G 1999. A tale of three fingers: the family of mammalian Sp/XKLF transcription factors. Nucleic Acids Res 27(15):2991-3000.
125. Knossl M, Lower R, Lower J 1999. Expression of the human endogenous retrovirus HTDV/HERV-K is enhanced by cellular transcription factor YY1. J Virol 73(2):1254-1261.
126. Katoh I, Mirova A, Kurata S, Murakami Y, Horikawa K, Nakakuki N, Sakai T, Hashimoto K, Maruyama A, Yonaga T, Fukunishi N, Moriishi K, Hirai H 2011. Activation of the long terminal repeat of human endogenous retrovirus K by melanoma-specific transcription factor MITF-M. Neoplasia 13(11):1081-1092.
127. Nead MA, Baglia LA, Antinore MJ, Ludlow JW, McCance DJ 1998. Rb binds c-Jun and activates transcription. EMBO J 17(8):2342-2352.
128. Imhof A, Schuierer M, Werner O, Moser M, Roth C, Bauer R, Buettner R 1999. Transcriptional regulation of the AP-2alpha promoter by BTEB-1 and AP-2rep, a novel wt-1/egr-related zinc finger repressor. Mol Cell Biol 19(1):194-204.
129. Laoide BM, Foulkes NS, Schlotter F, Sassone-Corsi P 1993. The functional versatility of CREM is determined by its modular structure. EMBO J 12(3):1179-1191.
130. Tai AK, Luka J, Ablashi D, Huber BT 2009. HHV-6A infection induces expression of HERV-K18-encoded superantigen. J Clin Virol 46(1):47-48.
131. Matsumoto A, Ichikawa T, Nakao K, Miyaaki H, Hirano K, Fujimito M, Akiyama M, Miuma S, Ozawa E, Shibata H, Takeshita S, Yamasaki H, Ikeda M, Kato N, Eguchi K 2009. Interferon-alpha-induced mTOR activation is an anti-hepatitis C virus signal via the phosphatidylinositol 3-kinase-Akt-independent pathway. J Gastroenterol 44(8):856-863.
132. Sicat J, Sutkowski N, Huber BT 2005. Expression of human endogenous retrovirus HERV-K18 superantigen is elevated in juvenile rheumatoid arthritis. J Rheumatol 32(9):1821-1831.
133. Yarilina A, Park-Min KH, Antoniv T, Hu X, Ivashkiv LB 2008. TNF activates an IRF1-dependent autocrine loop leading to sustained expression of chemokines and STAT1-dependent type I interferon-response genes. Nat Immunol 9(4):378-387.
134. Freimanis G, Hooley P, Ejtehadi HD, Ali HA, Veitch A, Rylance PB, Alawi A, Axford J, Nevill A, Murray PG, Nelson PN 2010. A role for human endogenous retrovirus-K (HML-2) in rheumatoid arthritis: investigating mechanisms of pathogenesis. Clin Exp Immunol 160(3):340-347.
135. Chan JK, Greene WC 2012. Dynamic roles for NF-kappaB in HTLV-I and HIV-1 retroviral pathogenesis. Immunol Rev 246(1):286-310.
136. Paces J, Huang YT, Paces V, Ridl J, Chang CM 2013. New insight into transcription of human endogenous retroviral elements. N Biotechnol 30(3):314-318.
137. Lower R, Boller K, Hasenmaier B, Korbmacher C, Muller-Lantzsch N, Lower J, Kurth R 1993. Identification of human endogenous retroviruses with complex mRNA expression and particle formation. Proc Natl Acad Sci U S A 90(10):4480-4484.
138. Mangeney M, Heidmann T 1998. Tumor cells expressing a retroviral envelope escape immune rejection in vivo. Proc Natl Acad Sci U S A 95(25):14920-14925.
139. Blaise S, Mangeney M, Heidmann T 2001. The envelope of Mason-Pfizer monkey virus has immunosuppressive properties. J Gen Virol 82(Pt 7):1597-1600.

140. Kammerer U, Germeyer A, Stengel S, Kapp M, Denner J 2011. Human endogenous retrovirus K (HERV-K) is expressed in villous and extravillous cytotrophoblast cells of the human placenta. J Reprod Immunol 91(1-2):1-8.
141. Larsson E, Andersson AC, Nilsson BO 1994. Expression of an endogenous retrovirus (ERV3 HERV-R) in human reproductive and embryonic tissues--evidence for a function for envelope gene products. Ups J Med Sci 99(2):113-120.
142. Birkmayer GD, Balda BR, Miller F, Braun-Falco O 1972. Virus-like particles in metastases of human malignant melanoma. Naturwissenschaften 59(8):369-370.
143. Muster T, Waltenberger A, Grassauer A, Hirschl S, Caucig P, Romirer I, Fodinger D, Seppele H, Schanab O, Magin-Lachmann C, Lower R, Jansen B, Pehamberger H, Wolff K 2003. An endogenous retrovirus derived from human melanoma cells. Cancer Res 63(24):8735-8741.
144. Schiavetti F, Thonnard J, Colau D, Boon T, Coulie PG 2002. A human endogenous retroviral sequence encoding an antigen recognized on melanoma by cytolytic T lymphocytes. Cancer Res 62(19):5510-5516.
145. Buscher K, Trefzer U, Hofmann M, Sterry W, Kurth R, Denner J 2005. Expression of human endogenous retrovirus K in melanomas and melanoma cell lines. Cancer Res 65(10):4172-4180.
146. Hahn S, Ugurel S, Hanschmann KM, Strobel H, Tondera C, Schadendorf D, Lower J, Lower R 2008. Serological response to human endogenous retrovirus K in melanoma patients correlates with survival probability. AIDS Res Hum Retroviruses 24(5):717-723.
147. Grupp SA, Kalos M, Barrett D, Aplenc R, Porter DL, Rheingold SR, Teachey DT, Chew A, Hauck B, Wright JF, Milone MC, Levine BL, June CH 2013. Chimeric antigen receptor-modified T cells for acute lymphoid leukemia. N Engl J Med 368(16):1509-1518.
148. Cooper LJ, Al-Kadhimi Z, DiGiusto D, Kalos M, Colcher D, Raubitschek A, Forman SJ, Jensen MC 2004. Development and application of CD19-specific T cells for adoptive immunotherapy of B cell malignancies. Blood Cells Mol Dis 33(1):83-89.
149. Singh H, Manuri PR, Olivares S, Dara N, Dawson MJ, Huls H, Hackett PB, Kohn DB, Shpall EJ, Champlin RE, Cooper LJ 2008. Redirecting specificity of T-cell populations for CD19 using the Sleeping Beauty system. Cancer Res 68(8):2961-2971.
150. Jena B, Maiti S, Huls H, Singh H, Lee DA, Champlin RE, Cooper LJ 2013. Chimeric antigen receptor (CAR)-specific monoclonal antibody to detect CD19-specific T cells in clinical trials. PLoS One 8(3):e57838.
151. Davies JK, Singh H, Huls H, Yuk D, Lee DA, Kebriaei P, Champlin RE, Nadler LM, Guinan EC, Cooper LJ 2010. Combining CD19 redirection and alloanergization to generate tumor-specific human T cells for allogeneic cell therapy of B-cell malignancies. Cancer Res 70(10):3915-3924.
152. Maiti SN, Huls H, Singh H, Dawson M, Figliola M, Olivares S, Rao P, Zhao YJ, Multani A, Yang G, Zhang L, Crossland D, Ang S, Torikai H, Rabinovich B, Lee DA, Kebriaei P, Hackett P, Champlin RE, Cooper LJ 2013. Sleeping beauty system to redirect T-cell specificity for human applications. J Immunother 36(2):112-123.
153. Geiss GK, Bumgarner RE, Birditt B, Dahl T, Dowidar N, Dunaway DL, Fell HP, Ferree S, George RD, Grogan T, James JJ, Maysuria M, Mitton JD, Oliveri P, Osborn JL, Peng T, Ratcliffe AL, Webster PJ, Davidson EH, Hood L, Dimitrov K 2008. Direct

multiplexed measurement of gene expression with color-coded probe pairs. Nat Biotechnol 26(3):317-325.
154. Deniger DC, Switzer K, Mi T, Maiti S, Hurton L, Singh H, Huls H, Olivares S, Lee DA, Champlin RE, Cooper LJ 2013. Bispecific T-cells expressing polyclonal repertoire of endogenous gammadelta T-cell receptors and introduced CD19-specific chimeric antigen receptor. Mol Ther 21(3):638-647.
155. Li L, Price JE, Fan D, Zhang RD, Bucana CD, Fidler IJ 1989. Correlation of growth capacity of human tumor cells in hard agarose with their in vivo proliferative capacity at specific metastatic sites. J Natl Cancer Inst 81(18):1406-1412.
156. Singh H, Serrano LM, Pfeiffer T, Olivares S, McNamara G, Smith DD, Al-Kadhimi Z, Forman SJ, Gillies SD, Jensen MC, Colcher D, Raubitschek A, Cooper LJ 2007. Combining adoptive cellular and immunocytokine therapies to improve treatment of B-lineage malignancy. Cancer Res 67(6):2872-2880.
157. Wang-Johanning F, Rycaj K, Plummer JB, Li M, Yin B, Frerich K, Garza JG, Shen J, Lin K, Yan P, Glynn SA, Dorsey TH, Hunt KK, Ambs S, Johanning GL 2012. Immunotherapeutic potential of anti-human endogenous retrovirus-K envelope protein antibodies in targeting breast tumors. J Natl Cancer Inst 104(3):189-210.
158. McDonald JW, Pilgram TK 1999. Nuclear expression of p53, p21 and cyclin D1 is increased in bronchioloalveolar carcinoma. Histopathology 34(5):439-446.
159. Cooper LJ, Topp MS, Serrano LM, Gonzalez S, Chang WC, Naranjo A, Wright C, Popplewell L, Raubitschek A, Forman SJ, Jensen MC 2003. T-cell clones can be rendered specific for CD19: toward the selective augmentation of the graft-versus-B-lineage leukemia effect. Blood 101(4):1637-1644.
160. Manuri PV, Wilson MH, Maiti SN, Mi T, Singh H, Olivares S, Dawson MJ, Huls H, Lee DA, Rao PH, Kaminski JM, Nakazawa Y, Gottschalk S, Kebriaei P, Shpall EJ, Champlin RE, Cooper LJ 2010. piggyBac transposon/transposase system to generate CD19-specific T cells for the treatment of B-lineage malignancies. Hum Gene Ther 21(4):427-437.
161. Daya S, Berns KI 2008. Gene therapy using adeno-associated virus vectors. Clin Microbiol Rev 21(4):583-593.
162. Sallusto F, Lenig D, Forster R, Lipp M, Lanzavecchia A 1999. Two subsets of memory T lymphocytes with distinct homing potentials and effector functions. Nature 401(6754):708-712.
163. Luther SA, Cyster JG 2001. Chemokines as regulators of T cell differentiation. Nat Immunol 2(2):102-107.
164. Holliger P, Hudson PJ 2005. Engineered antibody fragments and the rise of single domains. Nat Biotechnol 23(9):1126-1136.
165. Choi Y, Yuen C, Maiti SN, Olivares S, Gibbons H, Huls H, Raphael R, Killian TC, Stark DJ, Lee DA, Torikai H, Monticello D, Kelly SS, Kebriaei P, Champlin RE, Biswal SL, Cooper LJ 2010. A high throughput microelectroporation device to introduce a chimeric antigen receptor to redirect the specificity of human T cells. Biomed Microdevices 12(5):855-863.
166. Serrano LM, Pfeiffer T, Olivares S, Numbenjapon T, Bennitt J, Kim D, Smith D, McNamara G, Al-Kadhimi Z, Rosenthal J, Forman SJ, Jensen MC, Cooper LJ 2006. Differentiation of naive cord-blood T cells into CD19-specific cytolytic effectors for posttransplantation adoptive immunotherapy. Blood 107(7):2643-2652.

167. Dewannieux M, Harper F, Richaud A, Letzelter C, Ribet D, Pierron G, Heidmann T 2006. Identification of an infectious progenitor for the multiple-copy HERV-K human endogenous retroelements. Genome Res 16(12):1548-1556.
168. Tonjes RR, Limbach C, Lower R, Kurth R 1997. Expression of human endogenous retrovirus type K envelope glycoprotein in insect and mammalian cells. J Virol 71(4):2747-2756.
169. Contreras-Galindo R, Kaplan MH, Leissner P, Verjat T, Ferlenghi I, Bagnoli F, Giusti F, Dosik MH, Hayes DF, Gitlin SD, Markovitz DM 2008. Human endogenous retrovirus K (HML-2) elements in the plasma of people with lymphoma and breast cancer. J Virol 82(19):9329-9336.
170. Lower R, Lower J, Tondera-Koch C, Kurth R 1993. A general method for the identification of transcribed retrovirus sequences (R-U5 PCR) reveals the expression of the human endogenous retrovirus loci HERV-H and HERV-K in teratocarcinoma cells. Virology 192(2):501-511.
171. Geering B, Schmidt-Mende J, Federzoni E, Stoeckle C, Simon HU 2011. Protein overexpression following lentiviral infection of primary mature neutrophils is due to pseudotransduction. J Immunol Methods 373(1-2):209-218.
172. Kumaresan PR, Manuri PR, Albert ND, Maiti S, Singh H, Mi T, Roszik J, Rabinovich B, Olivares S, Krishnamurthy J, Zhang L, Najjar AM, Huls MH, Lee DA, Champlin RE, Kontoyiannis DP, Cooper LJ 2014. Bioengineering T cells to target carbohydrate to treat opportunistic fungal infection. Proc Natl Acad Sci U S A 111(29):10660-10665.
173. Shcherbo D, Merzlyak EM, Chepurnykh TV, Fradkov AF, Ermakova GV, Solovieva EA, Lukyanov KA, Bogdanova EA, Zaraisky AG, Lukyanov S, Chudakov DM 2007. Bright far-red fluorescent protein for whole-body imaging. Nat Methods 4(9):741-746.
174. Jones RB, Garrison KE, Mujib S, Mihajlovic V, Aidarus N, Hunter DV, Martin E, John VM, Zhan W, Faruk NF, Gyenes G, Sheppard NC, Priumboom-Brees IM, Goodwin DA, Chen L, Rieger M, Muscat-King S, Loudon PT, Stanley C, Holditch SJ, Wong JC, Clayton K, Duan E, Song H, Xu Y, SenGupta D, Tandon R, Sacha JB, Brockman MA, Benko E, Kovacs C, Nixon DF, Ostrowski MA 2012. HERV-K-specific T cells eliminate diverse HIV-1/2 and SIV primary isolates. J Clin Invest 122(12):4473-4489.
175. Wang-Johanning F, Radvanyi L, Rycaj K, Plummer JB, Yan P, Sastry KJ, Piyathilake CJ, Hunt KK, Johanning GL 2008. Human endogenous retrovirus K triggers an antigen-specific immune response in breast cancer patients. Cancer Res 68(14):5869-5877.
176. Wang-Johanning F, Frost AR, Jian B, Epp L, Lu DW, Johanning GL 2003. Quantitation of HERV-K env gene expression and splicing in human breast cancer. Oncogene 22(10):1528-1535.
177. Wang-Johanning F, Liu J, Rycaj K, Huang M, Tsai K, Rosen DG, Chen DT, Lu DW, Barnhart KF, Johanning GL 2007. Expression of multiple human endogenous retrovirus surface envelope proteins in ovarian cancer. Int J Cancer 120(1):81-90.
178. Bieda K, Hoffmann A, Boller K 2001. Phenotypic heterogeneity of human endogenous retrovirus particles produced by teratocarcinoma cell lines. J Gen Virol 82(Pt 3):591-596.

179. Seifarth W, Skladny H, Krieg-Schneider F, Reichert A, Hehlmann R, Leib-Mosch C 1995. Retrovirus-like particles released from the human breast cancer cell line T47-D display type B- and C-related endogenous retroviral sequences. J Virol 69(10):6408-6416.
180. Kraus B, Fischer K, Buchner SM, Wels WS, Lower R, Sliva K, Schnierle BS 2013. Vaccination directed against the human endogenous retrovirus-K envelope protein inhibits tumor growth in a murine model system. PLoS One 8(8):e72756.
181. Oricchio E, Sciamanna I, Beraldi R, Tolstonog GV, Schumann GG, Spadafora C 2007. Distinct roles for LINE-1 and HERV-K retroelements in cell proliferation, differentiation and tumor progression. Oncogene 26(29):4226-4233.
182. Serafino A, Balestrieri E, Pierimarchi P, Matteucci C, Moroni G, Oricchio E, Rasi G, Mastino A, Spadafora C, Garaci E, Vallebona PS 2009. The activation of human endogenous retrovirus K (HERV-K) is implicated in melanoma cell malignant transformation. Exp Cell Res 315(5):849-862.
183. Sciamanna I, Landriscina M, Pittoggi C, Quirino M, Mearelli C, Beraldi R, Mattei E, Serafino A, Cassano A, Sinibaldi-Vallebona P, Garaci E, Barone C, Spadafora C 2005. Inhibition of endogenous reverse transcriptase antagonizes human tumor growth. Oncogene 24(24):3923-3931.
184. Taruscio D, Mantovani A 2004. Factors regulating endogenous retroviral sequences in human and mouse. Cytogenet Genome Res 105(2-4):351-362.
185. Tonjes RR, Boller K, Limbach C, Lugert R, Kurth R 1997. Characterization of human endogenous retrovirus type K virus-like particles generated from recombinant baculoviruses. Virology 233(2):280-291.
186. Boller K, Konig H, Sauter M, Mueller-Lantzsch N, Lower R, Lower J, Kurth R 1993. Evidence that HERV-K is the endogenous retrovirus sequence that codes for the human teratocarcinoma-derived retrovirus HTDV. Virology 196(1):349-353.
187. Gross G, Waks T, Eshhar Z 1989. Expression of immunoglobulin-T-cell receptor chimeric molecules as functional receptors with antibody-type specificity. Proc Natl Acad Sci U S A 86(24):10024-10028.
188. Chapuis AG, Thompson JA, Margolin KA, Rodmyre R, Lai IP, Dowdy K, Farrar EA, Bhatia S, Sabath DE, Cao J, Li Y, Yee C 2012. Transferred melanoma-specific CD8+ T cells persist, mediate tumor regression, and acquire central memory phenotype. Proc Natl Acad Sci U S A 109(12):4592-4597.
189. Boller K, Schonfeld K, Lischer S, Fischer N, Hoffmann A, Kurth R, Tonjes RR 2008. Human endogenous retrovirus HERV-K113 is capable of producing intact viral particles. J Gen Virol 89(Pt 2):567-572.
190. Lee YN, Bieniasz PD 2007. Reconstitution of an infectious human endogenous retrovirus. PLoS Pathog 3(1):e10.
191. Laderoute MP, Giulivi A, Larocque L, Bellfoy D, Hou Y, Wu HX, Fowke K, Wu J, Diaz-Mitoma F 2007. The replicative activity of human endogenous retrovirus K102 (HERV-K102) with HIV viremia. AIDS 21(18):2417-2424.
192. Morgan RA, Yang JC, Kitano M, Dudley ME, Laurencot CM, Rosenberg SA 2010. Case report of a serious adverse event following the administration of T cells transduced with a chimeric antigen receptor recognizing ERBB2. Mol Ther 18(4):843-851.
193. Lamers CH, Willemsen R, van Elzakker P, van Steenbergen-Langeveld S, Broertjes M, Oosterwijk-Wakka J, Oosterwijk E, Sleijfer S, Debets R, Gratama JW 2011. Immune

responses to transgene and retroviral vector in patients treated with ex vivo-engineered T cells. Blood 117(1):72-82.
194. Lamers CH, Sleijfer S, Vulto AG, Kruit WH, Kliffen M, Debets R, Gratama JW, Stoter G, Oosterwijk E 2006. Treatment of metastatic renal cell carcinoma with autologous T-lymphocytes genetically retargeted against carbonic anhydrase IX: first clinical experience. J Clin Oncol 24(13):e20-22.
195. Balch CM, Soong SJ, Murad TM, Smith JW, Maddox WA, Durant JR 1983. A multifactorial analysis of melanoma. IV. Prognostic factors in 200 melanoma patients with distant metastases (stage III). J Clin Oncol 1(2):126-134.
196. Creagan ET, Ahmann DL, Green SJ, Long HJ, Rubin J, Schutt AJ, Dziewanowski ZE 1984. Phase II study of recombinant leukocyte A interferon (rIFN-alpha A) in disseminated malignant melanoma. Cancer 54(12):2844-2849.
197. Rosenberg SA, Lotze MT, Muul LM, Leitman S, Chang AE, Ettinghausen SE, Matory YL, Skibber JM, Shiloni E, Vetto JT, et al. 1985. Observations on the systemic administration of autologous lymphokine-activated killer cells and recombinant interleukin-2 to patients with metastatic cancer. N Engl J Med 313(23):1485-1492.

Appendix:

Antibody	Specificity	Catalogue number	Vendor	Amount used for upto 1 million cells
anti–CD3 FITC	CD3	349201	B.D. Pharmingen	5µL
anti–CD3 PerCPCy5.5	CD3	340949	B.D. Pharmingen	2.5µL
anti-CD3 PE	CD3	347347	B.D. Pharmingen	2µL
anti-CD4 APC	CD4	340443	B.D. Pharmingen	2.5µL
anti–CD8 PerCPCy5.5	CD8	341051	B.D. Pharmingen	2.5µL
anti-CD56 APC	CD56	555518	B.D. Pharmingen	2.5µL
AnnexinV-FITC	AnnexinV	556420	B.D. Pharmingen	5µL
anti-CD32 FITC	CD32	555448	B.D. Pharmingen	5µL
anti-CD45RO APC	CD45RO	559865	B.D. Pharmingen	2.5µL
anti-CD45RA FITC	CD45RA	555488	B.D. Pharmingen	5µL
anti–GranzymeB FITC	GranzymeB	560211	B.D. Pharmingen	5µL
anti–CD62L APC	CD62L	559772	B.D. Pharmingen	2.5µL
anti-IFN-γ APC	IFN-γ	554702	B.D. Pharmingen	5.5µL
anti-CD27 PE	CD27	555441	B.D. Pharmingen	2µL
anti-αβTCR FITC	αβTCR	347773	B.D. Pharmingen	5µL
anti-γδTCR PE	γδTCR	555717	B.D. Pharmingen	2µL
anti–CCR7 PerCPCy5.5	CCR7	335605	BioLegend	2.5µL
(ab')² fragment of goat anti-human Fcγ FITC	Fc portion of HERV-K env-specific CAR	115-096-071	Jackson Immunoresearch	5µL
(ab')² fragment of goat anti-human F-cγPE	Fc portion of HERV-K env-specific CAR	115-116-072	Jackson Immunoresearch	2µL
Anti-HERV-K 6H5 APC (6H5 mAb)	HERV-K env		Dr. Wang-Johanning, MDACC	2.5µL
Goat IgG	Fc blocker	005-000-003	Jackson Immunoresearch	1µL
6H5 mAx	HERV-K env		Cooper Lab	5ul

Table 1: List of antibodies used in this study.

Gene	Accession	Target Region	Target Sequence
CCR1	NM_001295.2	536-635	CATCATTTGGGCCCTGGCCATCTTGGCTTCCATGCCAGGCTTATACTTTTCCAAGACCCAATGGGAATTCACTCACCACACCTGCAGCCTTCACTTTCCT
CCR5	NM_000579.1	2731-2830	TAGGAACATACTTCAGCTCACACATGAGATCTAGGTGAGGATTGATTACCTAGTAGTCATTTCATGGGTTGTTGGGAGGATTCTATGAGGCAACCACAGG
CCL4	NM_002984.2	36-135	TTCTGCAGCCTCACCTCTGAGAAAACCTCTTTGCCACCAATACCATGAAGCTCTGCGTGACTGTCCTGTCTCTCCTCATGCTAGTAGCTGCCTTCTGCTC
CCL3	NM_002983.2	160-259	CAGTTCTCTGCATCACTTGCTGCTGACACGCCGACCGCCTGCTGCTTCAGCTACACCTCCCGGCAGATTCCACAGAATTTCATAGCTGACTACTTTGAGA
PRF1	NM_005041.3	2121-2220	ACTGTTTTTCAGGGAGGTGGCTGGGTTTACACGCTAATCCCGATTCACCCTGTCCAAACTGCCTAAGCCCTCCGCCATTCTCAAGCCCTGCAGTCACAGC
GZMH	NM_033423.3	706-805	AAAAAAGGGACACCTCCAGGAGTCTACATCAAGGTCTCACACTTCCTGCCCTGGATAAAGAGAACAATGAAGCGCCTCTAACAGCAGGCATGAGACTAAC
LRP5	NM_002335.1	2516-2615	TGGACACCAACATGATCGAGTCGTCCAACATGCTGGGTCAGGAGCGGGTCGTGATTGCCGACGATCTCCCGCACCCGTTCGGTCTGACGCAGTACAGCGA
PAX5	NM_016734.1	2289-2388	CTCCAAGAGGAGCACACTTTGGGGAGATGTCCTGGTTTCCTGCCTCCATTTCTCTGGGACCGATGCAGTATCAGCAGCTCTTTTCCAGATCAAAGAACTC
TCF7	NM_003202.2	2421-2520	ATTCCATTTCCAGTTCATCTATGGCAGTCCAGCCAGCTCCTGGGCAGCTTGAGAGGGCAAACCCAAAACCTCATGACAGCCAGAGCCTGTCTTTCAGCAT
FLT3LG	NM_001459.3	361-460	AGCGGCTCAAGACTGTCGCTGGGTCCAAGATGCAAGGCTTGCTGGAGCGCGTGAACACGGAGATACACTTTGTCACCAAATGTGCCTTTCAGCCCCCCCC
EPHA4	NM_004438.3	21-120	GCAGCGTTGGCACCGGCGAACCATGGCTGGGATTTTCTATTTCGCCCTATTTTCGTGTCTCTTCGGGATTTGCGACGCTGTCACAGGTTCCAGGGTATAC
CD80	NM_005191.3	1289-1388	AAAGATCTGAAGGTCCCACCTCCATTTGCAATTGACCTCTTCTGGGAACTTCCTCAGATGGACAAGATTACCCCACCTTGCCCTTTACGTATCTGCTCTT
KIR3DL2	NM_006737.2	885-984	TGCCACCCACGGAGGGACCTACAGATGCTTCGGCTCTTTCCGTGCCCTGCCCTGCGTGTGGTCAAACTCAAGTGACCCACTGCTTGTTTCTGTCACAGGA
IL22	NM_020525.4	320-419	CTATCTGATGAAGCAGGTGCTGAACTTCACCCTTGAAGAAGTGCTGTTCCCTCAATCTGATAGGTTCCAGCCTTATATGCAGGAGGTGGTGCCCTTCCTG
RORA	NM_134261.2	1716-1815	AAAATTAACCGAGACACTTTATATGGCCCTGCACAGACCTGGAGCGCCACACACTGCACATCTTTTGGTGATCGGGGTCAGGCAAAGGAGGGGAAACAAT
IL17RA	NM_014339.4	3021-3120	CTACTATGTGGCGGGCATTTGGGATACCAAGATAAATTGCATGCGGCATGGCCCCAGCCATGAAGGAACTTAACCGCTAGTGCCGAGGACACGTTAAACG
KLRG1	NM_005810.3	66-165	CAGAATGACTATGGACCACAGCAAAAATCTTCCTCTTCCAGGCCTTCTTGTTCTTGCCTTGTGGCAATAGCTTTGGGGCTTCTGACTGCAGTTCTTCTGA
IL18RAP	NM_003853.2	2413-2512	GCTTGATGGACAATGGAGTGGGATTGAGACTGTGGTTTAGAGCCTTTGATTTCCTGGACTGGACTGACGGCGAGTGAATTCTCTAGACCTTGGGTACTTT
IL18R1	NM_003855.2	2026-2125	GAATGAGGGGATTTTAAGTGTCTGAAGAGGCATTTTCTAGGGACCAGTGGGTGACTGAGTAACTGAAATGCTGCTTTCACTCCCTAACACCATGGATCTG
IL10	NM_000572.2	231-330	AAGGATCAGCTGGACAACTTGTTGTTAAAGGAGTCCTTGCTGGAGGACTTTAAGGGTTACCTGGGTTGCCAAGCCTTGTCTGAGATGATCCAGTTTTACC
HERV-K_6H5_s	SCFV012.1	138-237	CGGCGGCACCAGCTACAACCAGAAGTTCAAGGACAAGGCCATCCTGACCGTGGACAAGAGCAGCAGCACCGCCTACATGGAACTGCGGAGCCTGACCAGC

Table 2: List of target sequence used during mRNA analysis of HERV-K env-specific CAR^+ T cells.

VITA

Janani Krishnamurthy was born in Chennai, India on January 29, 1984, the daughter of Jaya Krishnamurthy and Krishnamurthy Rangarajan. After completing her work at Fatima High School, Chennai, India in 2001, she entered Sri Ramachandra Medical College (SRMC), Chennai, India. She received the degree of Bachelor of Pharmacy with a major in clinical Pharmacology and Pharmaceutics May, 2005. She then continued her education at University of Texas at San Antonio for next 2 years where she pursued her Master's in Biotechonology with her thesis work on neuroimmunology. In May of 2008 she entered The University of Texas Health Science Center at Houston Graduate School of Biomedical Sciences.

Permanent address :

7900 Cambridge street, Apt 2-2F,

Houston Texas- 77054